STUDIES OF SOME (^{3}He,d) AND (t,p) REACTIONS

A THESIS SUBMITTED

BY

HAMIDA BANU

FOR THE DEGREE OF DOCTOR OF PHILOSOPHY

OF THE UNIVERSITY OF DACCA, DACCA

JULY 1982 DACCA

A B S T R A C T

The present work discusses the (τ,d) reaction on ^{56}Fe and ^{45}Sc and the (t,p) reaction on ^{59}Co and ^{102}Ru.

The level properties of ^{57}Co and ^{46}Ti were studied respectively from the ^{56}Fe(τ,d) reaction at E_τ = 18 MeV and ^{45}Sc(τ,d) reaction at E_τ = 16 MeV. These experiments were carried out using the Tandem accelerator and multichannel magnetic spectrograph of the Nuclear Physics Laboratory, Oxford. The energy levels on ^{57}Co and ^{46}Ti are measured upto E_x = 7.8 MeV and 9.89 MeV respectively with an energy resolution of$\sim$22 keV (FWHM) in both the cases. The angular distributions are measured for most of the levels and are analyzed in terms of the DWBA theory of direct stripping reaction. The DWBA calculations were carried by Prof.H.M.Sen Gupta with the IBM 360/195 computer of Rutherford High Energy Laboratory. More ℓ_p transfer for both ^{57}Co and ^{46}Ti have been made than in previous ones. Special care was taken for the measurement of the absolute cross sections ; this was particularly important in view of the rather large systematic differences in the spectroscopic factors given by previous (τ,d) studies. The spectroscopic strengths have been obtained for 2p, $1f_{5/2}$ and $1f_{7/2}$ transition in the case of ^{56}Fe(τ,d)^{57}Co reaction. The summed 2p $T_<$ strength in the present work is fairly in agreement with the shell model limit and the $1f_{7/2}$ $T_<$ strength

is appreciably smaller than the expected one. The spectroscopic strengths in the case of $^{45}Sc(\tau,d)^{46}Ti$ reaction were calculated for 2p and 1f. The $T_<$ component of the total 1f strength for the $^{45}Sc(\tau,d)$ reaction comes to be 6.3 as against the single particle limit 10.5 for $1f_{7/2}+1f_{5/2}$ shells. For 2p transitions the observed strength is found to be 3.7 being fairly close to the expected $T_<$ component of the total $2p_{3/2}+2p_{1/2}$ strength of 4.5.

The experiments on $^{59}Co(t,p)$ and $^{102}Ru(t,p)$ were performed at E_t = 15 MeV with Tandem accelerator and multi-channel magnetic spectrograph of the University of Pennsylvania, Philadelphia. The energy levels in ^{61}Co and ^{104}Ru are obtained upto E_x = 5.23 and 5.08 MeV with energy resolution (FWHM)$\sim$18 keV and$\sim$ 20 keV respectively. The relative values of the angular distribution have been measured for most of the transitions (target thickness being not known) and are fitted by DWBA calculations. The DWBA calculations were performed with the IBM 370/115 Computer of the Bangladesh University of Engineering and Technology, Dacca and L-values were obtained. These gave the J^π limits/values for ^{61}Co and ^{104}Ru. The level scheme of ^{61}Co in the present work is studied upto E_x = 5.23 MeV as against E_x = 3.97 MeV by Hudson et al.(Hu 71). The present study also gives evidences for

the existence of the high spin states predicted by theoretical calculations in a region not studied before. The spectroscopic information of the level structure of ^{104}Ru is studied for the first time by the (t,p) reaction.

The level properties of ^{57}Co and ^{61}Co have been compared with the theoretical calculations based on the shell model and unified model for ^{57}Co and by unified model for ^{61}Co.

The low lying level spectra of ^{46}Ti are satisfactorily explained by MBZ theory.

CONTENTS

CHAPTER 1

INTRODUCTION

A nuclear reaction is a complicated process and different models have been put forward to describe these different processes based on evidences of experimental results. The functions associated with the theories depend upon observed nuclear properties. The information on nuclear properties usually is obtained in the form of cross section, shape of angular distribution, relative intensities etc. The success of these models therefore depends on the way these quantities are measured and correspond to the observed ones.

Direct reaction is one of such processes to consider as a source of information about nuclear structure. It is a single step process in which few internal degrees of freedom are involved. Plane wave method was at the beginning used to describe the nuclear process, which neglects the effect due to absorption, refraction, diffraction, polarization and Coulomb repulsion (important for heavier element). This theory overestimates the magnitude of peak cross section and underestimates the elastic scattering cross section and fails to predict absolute cross section.

The DWBA theory takes account of all these effects

by assuming a correct nature of potential, the optical potential. This potential generates the distorted waves in place of plane waves in the initial and final channels for elastic scattering in them. This distortion considerably influences both the shapes and magnitude of differential cross sections.

The DWBA theory is used both for single and multi-bucleon transfer processes. The essence of the DWBA theory of single particle transfer is that the reaction amplitude can be factored into spectroscopic and kinematic part. The spectroscopic part carries the structure information and the kinematic part is essentially independent of the properties of nuclear states.

For two-nucleon transfer reactions such factorization is not in general possible. Several configurations are responsible in a given transition and each configuration is characterized by a radial wave function representing the c.m. motion of the pair of particles (for the S state). The reaction amplitude consists of a coherent sum of terms, each composed of factors containing details of nuclear structure information and probability transition amplitude for transferring a structureless nuclide into the orbital state N,L in a structureless nucleus.

The shapes of the angular distribution of direct

reaction are similar in the both single and two-nucleon transfers. Only difference is that in the single-particle transfer reaction angular momentum is carried by a single particle and the intensity of reaction is proportional to the probability that the nucleon has the angular momentum transferred in the nuclear state. For two-nucleon transfer, on the other hand, the angular momentum is carried by a pair of nucleons and many different configurations of the two nucleons are involved in the angular momentum transfer. So coherence can lead to a very strong transition to the level for which it is constructed. The reaction is highly selective favouring in stripping reaction those states that have a large percentage based on the target in its ground state. The structure factor contains information regarding the relative contribution of different radial functions, correlation due to angular momentum coupling, residual interaction, and configuration mixing. So two-nucleon transfer reaction like (t,p) provides a means of studying the nuclear functions in detail not accessible to a single-nucleon transfer reaction. The (t,p) reactions are also useful for an investigation of the levels of neutron-rich nuclei and deal with the levels of more complicated nature. Studies of single-proton transfer reactions have been found to be useful in obtaining information regarding the ground state wave function of target nuclei and single particle/hole proton state in the final nuclei ; in the case of an odd-odd final

nucleus such reactions also provide information regarding the residual n-p interaction. The (τ,d) reaction has an obvious advantage over other single proton stripping reactions like (α,t) and (d,n) from experimental point of view.

In analysing the reaction mechanism it is assumed that projectile consists of two structureless lumps of nuclear matter bound together, one of which is stripped off as a unit and captured by the nucleus and the other emerges.

The reactions studied in the present work are (τ,d) reaction on ^{56}Fe and ^{45}Sc at 18 MeV and 16 MeV respectively and (t,p) reaction of ^{59}Co and ^{102}Ru at 15 MeV.

CHAPTER 2

EXPERIMENTAL PROCEDURE

2.1. Multichannel Magnetic Spectrograph

The present experiments were performed at two different places, one at the University of Oxford and the other at the University of Pennsylvania. The multichannel magnetic spectrograph used in those places are of type described by Middelton and Hinds (Mi 62). This spectrograph is actually twenty four instruments in one large vacuum enclosure having common magnetic circuit, each spectrograph recording a broad range of spectrum of particles emitted at a given angle with respect to the incident beam. The range of angles is 3.75^{o} to 176.25^{o} in steps of 7.5^{o}. The exciting coils are wound on the iron segments between the gaps. By changing current in the exciting coils the magnetic field can be adjusted according to the requirement of a particular exposure. To minimize the effects of stray fields, the coils have been placed so as to achieve balance between reluctance and the magnetomotive force throughout the magnetic circuit. The target is kept at the centre of the toroid. The incident beam from the accelerator enters the magnet through a hole bored at one of the iron segments. The beam enters the chamber through energy defining slit of rectangular shape. It then passes through the

electrostatic quadrupole lens. Before hitting the target, the beam is passed through two sets of slits which are adjusted so as not to intercept any part of the main beam. After passing through the target the beam is collected by a Faraday cup at the opposite end of the target, just inside the magnet fringing field. Reaction products enamating from the target are restricted to a divergence of a few degrees measured in the vertical plane, by a series of appertures placed close to the entrances of the various magnet gaps. In the field region (inside the toroid) the particles are deflected through a mean angle of 90^{o} and brought to focus according to their energy somewhere along the plates mounted in rigid holders above each gap. The entire enclosure is kept cold by cooling arrangement. After the exposure, the plates are developed.

2.2. Emulsion Plate

Photographic emulsion plate consists of photosensitive layer of silver bromide dispersed on gelatine coated on glass backings. The nature of ionizing particle can be deduced from the appearance of its track which depends upon the number of ionization caused per unit length. The chance that silver halide grain is made developable depends on the number of ionization it receives.

Two types of emulsion plate were used for the purpose of recording the data in the present experiments. The plates used in Oxford for (τ,d) reactions were Ilford L4 and in Pennsylvania for (t,p) reactions were Ilford K-minus. Emulsion thickness for both plates was 25 μm. The Oxford plates were of dimension 18"X2". Two such plates together were placed end to end in a particular angle (i.e. channel) at the time of exposure. For the purpose of scanning as well as for ready determination of the position of a group with respect to the nearest index line, six index marks on the combined plate were used from A to F ; relative distances between two adjacent index marks are 15 cm. Active regions which the reaction products occupied are 10 mm at both edges.

The Pennsylvania plates were of size 21"X1.5". Again two such plates placed end to end were used for a particular loading in the experiments. Thus photographically active length is 42". Each plate was marked with four black index lines. Eight such marks all on the combined plate were given a letter from A to H.

All scannings were done with reference to these marks whose relative distances from one another remains fixed. Active regions occupy the space from 5 mm to 9.5 mm at both edges. Tables show position of index lines. These index

lines are then converted into scans. There are four scans per mm.

Table 2.1

Index position of Oxford experimental plate

Index	A	B	C	D	E	F
(Scan)	600	1200	1800	2400	3000	3600
(cm)	15	30	45	60	75	90

Table 2.2

Index position of Pennsylvania experimental plate

Index	A	B	C	D	E	F	G	H
(Scan)	533	1033	1565.8	2099.1	2632.5	3165.5	3699.4	4231.4
(cm)	12.500	25.825	39.145	52.478	65.813	79.138	92.485	105.785

2.3. Target preparation

Four targets were used in the present experiments. ^{56}Fe and ^{45}Sc were used in the University of Oxford and ^{59}Co and

^{102}Ru were used in the University of Pennsylvania.

The ^{56}Fe target was prepared by vacuum deposition of Fe_2O_3 (isotopically enriched to 99.5% of ^{56}Fe) onto thin carbon backing.

Target ^{45}Sc (natural Sc) was prepared by evaporation technique from Scandium metal onto a thin carbon backing. The target was continuously monitored during the experiment against any deterioration.

The targets ^{59}Co and ^{102}Ru were both prepared by evaporation technique.

2.4. Scanning Procedure

For the analysis of the plates, a Vickers binocular microscopes with an overall magnification of X400 was used in the present work. The mechanical stage over which the plates were placed was mounted on ball bearing spring.

At first one of the plates was placed on the microscope stage with emulsion side up and approximate position of swatch was set properly so that the Y control was moved until limits of group were determined in the Y directions. Now the X control of the stage was moved until the index mark from which the scan was to be started, was just at the middle of

the large graticule of the eye-piece and was made to coincide with the Y-axis of the cross wire.

In scanning, the X control was to be moved so that the plate was scanned from high energy side to the low energy side. In a typical scan all tracks in a particular swatch were to be counted at intervals of 0.25 mm. All tracks which fell between the vertical lines of the graticule were to be counted i.e. when the point of entry of a certain track was inside the graticule for that strip. Those tracks whose tails were inside the square graticule and had points of entry outside the graticule were not counted for that specific strip.

2.5 Experiments on different targets

2.5.1 Oxford Plates

$^{56}Fe(\tau,d)$ reaction

The ^{3}He beam of energy 18 MeV was used to induce the reaction $^{56}Fe(\tau,d)$. The reaction products after momentum analysis in a magnetic spectrograph were detected in Ilford L4 nuclear emulsion placed at the focal plane of the spectrograph. The deuteron spectra were taken from 11.25^{o} to 78.75^{o} in steps of 7.5^{o}. The exposure time was 18 hr. The reaction products were momentum analysed in a magnetic field of strength 12.79 K-gauss.

$^{45}Sc(\tau,d)$ reaction

$^{45}Sc(\tau,d)$ reaction was performed using 16 MeV ^{3}He ions and a magnetic field of strength 13.57 K-gauss for 24 hours. Deuterons were recorded from 11.25^{o} to 48.75^{o} in intervals of 7.5^{o} on Ilford L4 plates.

To reduce the yields of deuterons at 11.25^{o} and 18.75^{o} the slits in the exit were narrowed down. So yields at these angles for both the reactions were corrected by multiplying with appropriate slit factors (2 for 11.25^{o} and 1.33 for 18.75^{o}) with respect to the rest of the angles.

2.5.2 Pennsylvania Plates

A triton beam of energy 15 MeV from University of Pennsylvania Tandem accelerator was used for the (t,p) reactions on ^{59}Co and ^{102}Ru.

Protons from the reactions coming out at different angles were allowed to pass through the magnetic field to suffer magnetic deflection. As a result the protons at each angle were divided into groups according to their momenta and the groups ultimately reached the emulsion plates forming different radii of curvature on their paths. Ilford K minus plates were placed in the focal plane of the magnetic spectrograph. The spectra were taken in 7.5^{o} steps from 3.75^{o} to

86.25^{o} on 12 sets of plates. Both the reactions $^{59}Co(t,p)$ and $^{102}Ru(t,p)$ were recorded on the same plate, the former on the strip one (or lower edge) and the latter on the strip two (or upper edge).

2.6 Energy Calibration

Energy levels of the final nuclei for all the reactions were obtained from the spectra at four angles, namely 11.25^{o}, 18.75^{o}, 26.25^{o} and 33.75^{o}. For this purpose each channel (i.e. angle) was calibrated internally in energy using the least squares fit of the parabolic equation $Y = a_o + a_1 x + a_2 x^2$ for several well established and accurately known levels. Here x represents the peak position of the group in terms of scan number (arbitrarily) divided by 1000 and Y the energy of the group (in MeV). The levels used for calibration and the least squares values of a_o, a_1 and a_2 for each channel for all the reactions are given in the respective chapters. The criteria used for the identification of the levels were that the excitation energies of the levels in residual nucleus obtained at different angles were consistent to within 10 KeV and that the groups due to emitted particles at different angles belonging to the same levels had similar widths.

2.7 Target Thickness

To measure the target thickness the formula used is

$$t = \frac{N_{Scatt}}{N\ \sigma_{Lab}(\theta_L)\ n_i\ \Delta\ \Omega} \qquad 2.1$$

N = Avogadro number

n_i = Total number of particles in the incident beam.

N_{Scatt} = Number of counts in a given group at a laboratory angle θ_L

$\Delta\ \Omega$ = Solid angle

$\sigma_{Lab}(\theta_L)$ = Scattering cross section

Target	Beam	Energy (MeV)	Field strength K-gauss	Exposure current μc	Effective thickness of the target μgm / cm^2
^{56}Fe	$^{3}He^{++}$	6	4.7	0.0504	90
^{45}Sc	deuteron	3	5.04	0.92	53

Yields of the elastic groups for target ^{56}Fe at an angle 26.25^{o}

and 33.75° were obtained from a short exposure of 6 MeV $^{3}He^{++}$ particles ; for ^{45}Sc target yield of 3 MeV deuteron elastically scattered at 26.25° from the same target was similarly used. These yields were then normalized to the Rutherfold scattering for respective target at respective angles to get the target thickness (equation 2.1).

2.8 Absolute Cross Section

The differential cross section $\sigma(\theta_L)$ for a reaction in the lab system is proportional to number of particles $N(\theta_L)$ scattered at an angle θ_L. The cross section $\sigma(\theta_L)$ in the lab system is converted to c.m. value $\sigma(\theta)$ through the relation $\sigma(\theta) = f(\theta_L)\sigma(\theta_L)$. The $\sigma(\theta_L)$ is known from equation (2.1) of section (2.7) and

$$f(\theta_L) = \frac{\sin^2\theta_L}{\sin^2\theta}\cos(\theta-\theta_L)$$

where
$$\frac{\sin(\theta-\theta_L)}{\sin\theta_L} = \frac{m_1 m_2}{m_o m_3}\cdot\frac{1}{1+\frac{(m_o+m_1)Q}{E_{Lab}\, m_o}} \qquad 2.8.1$$

m_o = mass of the target nucleus

m_1 = mass of the incident particle

m_2 = mass of the emitted particle

m_3 = mass of the residual nucleus

Q = Q-value of the reaction

When target thickness is not known as in the case of $^{59}Co(t,p)$ and $^{102}Ru(t,p)$ reaction, the relative cross section, were obtained from the relation

$$\sigma (\theta) = f (\theta_L) N_{Scatt} (\theta_L) \qquad 2.8.2$$

CHAPTER 3

DWBA Analysis

3.1 Introduction

The direct nuclear reaction processes in the fifties were treated by plane wave approximation in which i) Coulomb force, and ii) nuclear interaction were ignored. Although this theory was successful in some respect for light nuclei, it failed to predict the absolute cross section and to give correct amount of relative cross section and their dependence on energy and Q-value. The elastic scattering is also assumed to be small.

The DWBA theory has been developed to give a more accurate and realistic description of reaction process. It is assumed that interaction responsible for the reaction is a single-step process in which the relative motion of the pair of nuclei before and after collision is described by distorted waves in place of plane waves. These waves are generated by a complex potential called optical potential by which the nucleons are scattered by nuclei. This theory has provided a means to describe nuclear reactions through parameters which have fundamental relationship with the properties of the many body problem.

These parameters are found to vary considerably with energy and to certain extent on mass number.

3.2 DWBA Theory

In the description of a nuclear reaction $a + A \rightarrow b + B$ Hamiltonian used for it is

$$H = H_a + K + V \qquad 3.2.1$$

where H_a is the internal Hamiltonian, K the K.E of their relative motion and V the interaction potential. In the course of above reaction the projectile is assumed as made up of emitted particle b and another particle x which is captured by the target forming the final nucleus B. The particle b escapes with momentum $\hbar\underline{k}_b$,

$$\underline{k}_b = \underline{k}_i + \tfrac{1}{2}\underline{k}_a \qquad 3.2.2$$

where $\hbar\underline{k}_a$ is the initial momentum of the incident particle a and $\hbar\underline{k}_i$ is the momentum of b relative to center of mass motion of a (internal momentum). The particle x about to be captured approaches with momentum $\hbar\underline{k}$ (Fig. 3.1),

$$\underline{k} = \underline{k}_a - \underline{k}_b \qquad 3.2.3$$

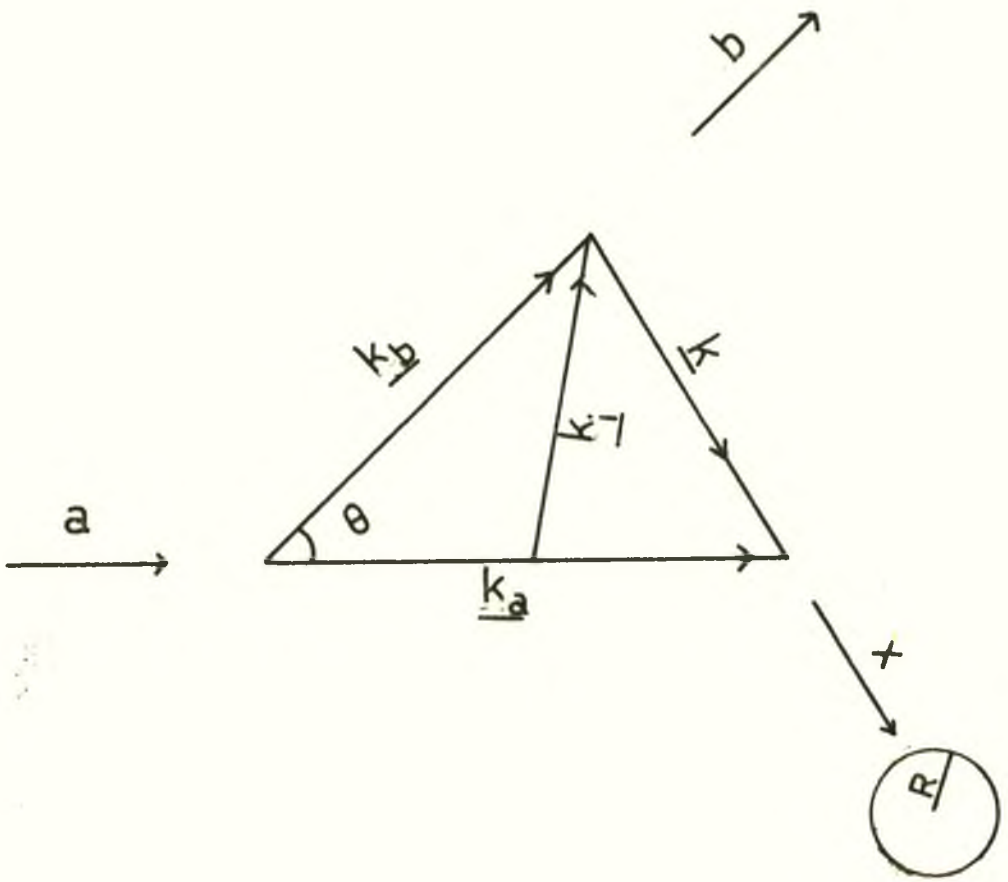

FIG. 3.1: Conservation of momentum of the reaction A(a,b)B.

x is assumed to be captured at the surface of the nucleus, A and B is formed in the ground state of excited state. If it is captured with quantized angular momentum $\hbar\ell$, the impact parameter R (the nuclear radius) is related with,

$$\underline{k}R \approx \sqrt{\ell(\ell+1)} \qquad 3.2.4$$

The energy with which x enters the target A is E_x

$$E_x = -[E_b - E_a + \varepsilon_a] \qquad 3.2.5$$

ε_a → binding energy of a

E_a → initial energy of a

E_b → energy associated with b

Both the initial and final wave functions will be eigen-function of Hamiltonian H.

The method following to compute the transition T_{ab} (Sa 64) is the method of distorted waves. The transition amplitude for the reaction A(a,b)B is given by

$$T_{ab} = \int \int d\underline{r}_a \int d\underline{r}_b \; \psi_f^{(-)*}(\underline{k}_b, \underline{r}_b) \; \langle bB|V|aA\rangle \; \psi_i^{(+)}(\underline{k}_a, \underline{r}_a) \qquad 3.2.6$$

$\mathcal{J}$ is the Jacobian of the transformation to the relative coordinates $\underline{r}_a$, $\underline{r}_b$ (Fig. 3.2). The quantity $\langle bB|V|aA\rangle$ is the form factor for the reaction and must contain the delta function for the coordinates $\underline{r}_a$ and $\underline{r}_b$.

The function $\psi_f^{(-)}$ is time reversal scattering wave function for the potential U and is related to the out-going wave as

$$\psi^{(-)*}(\underline{k}, \underline{r}) = \psi^{(+)}(-\underline{k}, \underline{r}) \qquad 3.2.7$$

When the particles a and b have spin, the functions $\psi^{\pm}$ become matrices in spin space $\psi_{m',m}$ where m is the Z-component of spin. Terms $m' \neq m$ allow the possibility of spin flip during the elastic scattering.

For $\underline{L}.\underline{S}$ coupling, the expansion of distorted waves into partial waves may be written as

$$\psi^{(+)}_{m'm}(\underline{k},\underline{r}) = \frac{4\pi}{kr} \sum_{JLM} \langle LsMm|JM+m\rangle\langle LsM+m-m',m'|JM+m\rangle$$

$$\times\, i^L\, \psi_{JL}(k,r)\; Y_L^{M*}(\theta_k,\phi_k)\; Y_L^{M+m-m'}(\theta_r,\phi_r) \qquad 3.2.8$$

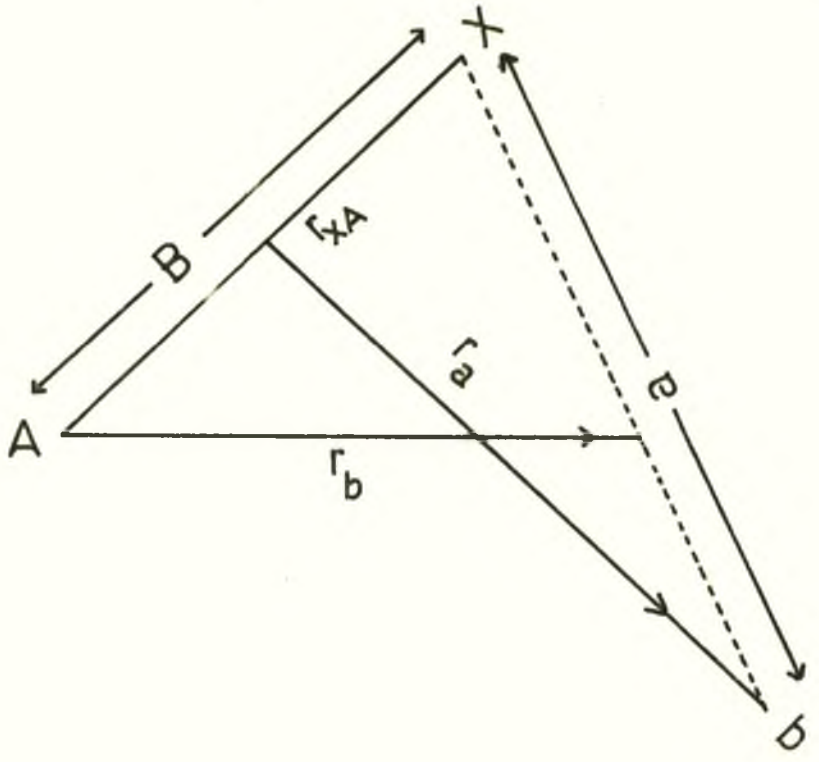

FIG. 3.2. Co-ordinate system for the reaction A(a,b)B.

θ_k, ϕ_k indicate the direction $\underline{k_b}$ with respect to the coordinate axes.

The partial waves are the solutions of Schrödinger equation

$$\left[\frac{d^2}{dr^2} + k^2 - \frac{L(L+1)}{r^2} - \frac{2\mu}{\hbar^2} (U+U_C+U_L^J) \right] \psi_{LJ}(k,r) = 0 \qquad 3.2.9$$

The radial wave functions ψ_{LJ} are required to vanish at $r_b = 0$ and for large r, where $U + U_L^J$ may be neglected and also satisfy the boundary condition

$$\psi_{LJ}(k,r) = \left[\frac{H^*(k,r) - \eta_L^J(k,r)}{2i} \right] \exp(i\sigma_L) \qquad 3.2.10$$

where η_L^J is the reflection coefficient for the ℓ th partial wave and $H_L(k,r)$ in terms of the regular and irregular radial Coulomb functions is

$$H_L(k,r) = G_L + iF_L \qquad 3.2.11$$

The σ_L is the Coulomb phase shift. The η_L^J's are computed by

matching ψ_{JL} to the Coulomb functions G_L and F_L at last two integration points and the over all normalization constants.

The form factor $\langle b\ B|V|a\ A\rangle$ contains the nuclear structure information and is expanded into a series of multipoles, each of which corresponds to the transfer to the target nucleus of a definite angular momentum j composed of an orbital part ℓ and a spin part s. If the particles a and b have spin s_a and s_b and the target and residual nuclear spins are J_A and J_B,

$$\underline{j} = \underline{J_B} - \underline{J_A} \quad , \quad \underline{s} = \underline{s_a} - \underline{s_b}, \quad \underline{\ell} = \underline{j} - \underline{s} \qquad 3.2.12$$

This multipole series may be written with Clebsch-Gordan coefficient corresponding to the vector coupling, the nuclear matrix elements of the form factor becomes

$$\oint \langle J_B M_B,\ s_b m_b|V|J_A M_A,\ s_a m_a\rangle = \sum_{\ell s j} i^{-\ell} G_{\ell s j, m}(\underline{r_b}, \underline{r_a}; bB, aA)$$

$$\times (-)^{s_b - m_b} \langle J_A\ j;\ M_A,\ M_B - M_A | J_B M_B\rangle \langle s_a s_b; m_a, -m_b | s, m_a - m_b\rangle$$

$$\times \langle \ell s;\ m, m_a - m_b | j,\ M_B - M_A\rangle \qquad 3.2.13$$

where $m = M_B + m_b - M_A - m_a$. 3.2.14

The multipole operator $G_{\ell sjm}$ depends on various nuclear quantum numbers. The function G may be defined by inverted form of expansion of (3.2.13). The factor i^{ℓ} is included to ensure convenient time reversal properties $G_{\ell sj,m}$ can be transformed under rotation of the coordinate system like the spherical harmonic Y_{ℓ}^{m*} . The parity change of G in the nuclear transition is given by $(-1)^{\ell}$ in the zero range approximation.

$G_{\ell sj,m}$ can be expressed as a product of two factors

$$G_{\ell sj,m}(\underline{r}_b, \underline{r}_a) = A_{\ell sj} \; f_{\ell sj,m}(\underline{r}_b, \underline{r}_a) \qquad 3.2.15$$

$f_{\ell sj,m}$ is the form factor and $A_{\ell sj}$ is the spectroscopic coefficient which includes fractional parentage coefficients for the initial or final nuclear states and interaction strength.

The transition amplitude reduces to a sum over multipole contributions

$$T_{ab} = \sum_{\ell sj} (2\ell+1)^{\frac{1}{2}} A_{\ell sj} (-)^{s_b - m_b} \langle J_A j; M_A, M_B - M_A \mid J_B M_B \rangle$$

$$\times \langle \ell s; m, m_a - m_b \mid j, m - m_b + m_a \rangle \langle s_a s_b; m_a - m_b \mid s, m_a - m_b \rangle \beta_{sj}^{\ell m}$$

3.2.16

Here the reduced amplitude $\beta_{sj}^{\ell m}$ is defined by

$$(2\ell+1)^{\frac{1}{2}}\ \beta_{sj}^{\ell m}\ i^{\ell} = \int d^3\underline{r}_a \int d^3\underline{r}_b\ \psi_b^{(-)*}(\underline{k}_b,\underline{r}_b)\ f_{\ell sj,m}(\underline{r}_b,\underline{r}_a)\psi_a^{(+)}(\underline{k}_a,\underline{r}_a)$$

3.2.17

The unpolarized differential cross section for a reaction A(a,b)B is defined in terms of T_{ab}, sum over final spin projections and average over initial projections

$$\sigma(\theta) = \frac{\mu_a\ \mu_b}{(2\pi\hbar^2)^2}\ \frac{k_b}{k_a}\ (2J_A+1)^{-1}(2s_a+1)^{-1} \sum_{\substack{M_a,M_b,\\ m_a,m_b}} |T_{ab}|^2$$

3.2.18

In terms of reduced amplitude

$$\sigma(\theta) = \frac{\mu_a\mu_b}{(2\pi\hbar^2)^2}\ \frac{k_b}{k_a}\ \frac{2J_B+1}{(2J_A+1)\ (2s_a+1)} \sum_{\ell sj} |A_{\ell sj}|^2 \sum_m |\beta_{sj}^{\ell m}|^2$$

3.2.19

The sum over ℓ,s,j is incoherent.

If only one value each of s and ℓ are allowed

$$\sigma(\theta) = \frac{2J_B+1}{2J_A+1} \sum_j \frac{|A_{\ell sj}|^2}{2s_a+1}\ \sigma_{\ell sj}(\theta)$$

3.2.20

$$\text{where } \sigma_{\ell si}(\theta) = \frac{\mu_a \mu_b}{(2\pi\hbar^2)^2} \frac{k_b}{k_a} \sum_m |\beta_{sj}^{\ell m}|^2$$

3.3 Zero range approximation

The reduced amplitude $\beta_{sj}^{\ell m}$ is of the form of six dimensional integration over the space of both vectors $\underline{r}_a$ and $\underline{r}_b$. The numerical evaluation of such a six dimensional integral is quite difficult. The above difficulty is removed on the assumption that the form factor is of very small range perhaps because V has a short range or perhaps because the internal wave functions have a small range. The zero range approximation is therefore introduced. It has the physical meaning that the particle b is emitted at the same point at which particle a is absobed so that $\underline{r}_b = \frac{M_A}{M_B} \underline{r}_a$ where M_A and M_B are the masses of nuclei A and B. The form factor can be written as

$$f^{(zero)}_{\ell sj,m}(\underline{r}_b, \underline{r}_a) = \delta(\underline{r}_b - \frac{M_A}{M_B}\underline{r}_a) \int f_{\ell sj,m}(s + \frac{M_A}{M_B}\underline{r}_a, \underline{r}_a) d^3s$$

$$= F_{\ell sj}(r_a)\, Y_\ell^{m*}(\theta_a \phi_a)\, \delta(\underline{r}_b - \frac{M_A}{M_B}\underline{r}_a) \qquad 3.3.1$$

The reduced amplitude becomes in the zero range approximation

may be written as

$$(2\ell+1)^{\frac{1}{2}}\, i^{\ell}\beta_{sj}^{\ell m} \approx \int d^3r\ \psi_b^{(-)*}\left(k_b, \frac{M_A}{M_B}\,\underline{r}\right) F_{\ell sj}(r) Y_{\ell}^{m*}(\hat{r})\psi_a^{(+)}(k_a, \underline{r})$$

3.2.2

which is easier to evaluate.

The distorted waves are inserted into above equation in the form of the partial wave expansion and then the angular integration of it are done analytically. Then $\beta_{sj}^{\ell m}$ can be written in a more compact form as

$$\beta_{sj}^{\ell m} = \sum_{L_a L_b} i^{L_a - L_b - l} e^{i\sigma_{aL_a} + i\sigma_{bL_b}} \sqrt{2L_b+1}\ I_{L_a L_b}^{\ell sj} \langle L_b \ell; 00 | L_a 0\rangle$$

$$\times \langle L_b\ \ell;\ -m, m | L_a\ 0\rangle\ Y_{L_b}^{-m}(\Theta,\ 0) \qquad 3.2.3.$$

where Θ is the scattering angle, the angle between $\underline{k}_a$ and $\underline{k}_b$

The Clebsch Gordan coefficient $\langle L_b\ \ell;\ 00 | L_a 0\rangle$ vanishes unless $(l + L_a + L_b)$ is an even number. As a result parity of reaction is given uniquely in terms of multipole index ℓ and has the value $(-1)^{\ell}$.

3.4 Two-nucleon transfer

The angular distribution for a two-nucleon transfer reaction is characterized by the transferred angular momentum in much the same way as for a single-nucleon transfer reaction. Many different configurations from the two individual nucleons may contribute coherently for the total orbital angular momentum L carried by the two nucleons. In general thus the cross section for a two-nucleon transfer cannot be factorized into a part containing kinematic information and other nuclear structure information like a single-nucleon transfer reaction.

The differential cross section (Gl 65) is found to be incoherent sum over L,S,J and T given by

$$\frac{d\sigma}{d\Omega} = \frac{2J_B+1}{2J_A+1} \frac{k_b}{k_a} \frac{\mu_a \mu_b}{(2\pi\hbar^2)^2} \sum_{LSJTM} C_T^2 \, b_{ST}^2 \left| \Sigma G_{NLSJT} \, B_{NL}^M \right|^2 \qquad 3.4.1$$

where $C_T = \langle T_1 \; T_{Z_1} | T \; T_Z \; T_2 \; T_{Z_2} \rangle$ is the Clebsch Gordan coefficient for the isospins where the transferred pair carries T T_Z. The quantity b_{ST}^2 arise from the spin-isospin overlap of particles a and a-2. The several radial states characterized by N, contribute coherently to the cross section. In this

expression all nuclear structure information is contained in G_{NLSJT} which is in turn sum over the many configuration.

3.5 Optical potential

The optical model potential used to generate the distorted waves is phenomological in origin. To it is added Coulomb potential, usually assumed of a uniform charge distribution for protons. The optical model potential contains a central term of the Woods-Saxon type, a spin orbit term of opposite sign to that of the well known spin-orbit term of atomic spectra, usually of Thomas type. The optical model potential includes in addition an imaginary potential (Surface and / or Volume absorption) which takes into account of the absorption of the particles from the incident beam. All these potentials are characterized by a well depth and the geometrical (the radius and diffuseness) parameters. The values of these parameters are given in respective chapters.

The optical potential is assumed energy dependent and local i.e.

$V(\underline{r}',\underline{r}) = V(r)\ \delta(\underline{r}'-\underline{r})$ in the limit the non locality

a phenomological parameter $b \rightarrow 0$.

In the reaction amplitude calculation, the contributions from nuclear interior are also considered.

CHAPTER 4

REACTION $^{56}Fe(\tau,d)$

4.1 Introduction

The level structure of ^{57}Co has been the subject of a number of experimental investigations through several nuclear reaction processes like $^{58}Ni(d,\tau)$, $^{58}Ni(t,\alpha)$, $^{57}Fe(p,n)$, $^{54}Fe(\alpha,p)$, $^{56}Fe(p,\gamma)$, $^{60}Ni(p,\alpha)$, $^{56}Fe(d,n)$, $^{56}Fe(\tau,d)$ and β-decay studies from ^{57}Ni as has been summarized by Auble (Au 77). The subject of the present investigation is to study the single proton states in ^{57}Co by means of the (τ,d) reaction on ^{56}Fe ; such information is a desirable supplement to the existing data.

Several theoretical calculations have been made in order to understand the structure of ^{57}Co based on the shell model and unified model. The unified model gives good description of the levels upto E_x = 2.5 MeV, the shell model results have in general not been that successful.

The ^{58}Ni (d,τ) reaction was studied by Cujec et. al.(Cu 62) at 15 MeV and Mairle et al.(Ma 69) at 52 MeV ; ℓ_p- values and spectroscopic factors were measured from DWBA calculation for transitions to several low-lying levels in ^{57}Co.

Blair et al. (Bl 66) studied the (t,α) reaction on ^{58}Ni at E_t = 15 MeV covering an excitation energy of 3.259 MeV and measured ℓ_p-transfer from DW calculation. They also measured transition strengths.

The ^{57}Fe(p,n) reaction was studied by Cookson et al. (Co 67) at 13 MeV. The analogue of target ground state was seen and the Coulomb displacement energy was obtained.

Bouchard et al. (Bo 68) investigated the ^{54}Fe(α,p) reaction at 11 MeV covering the levels upto an excitation of 4.08 MeV.

The properties of a few low lying levels of ^{57}Co upto $E_x \sim 3.2$ MeV have been studied through β-decay (At 68, Li 67, Ga 69).

The level structure of ^{57}Co has also been studied by (p,γ) reaction on ^{56}Fe (O'B 70, Le 71, Sa 75). O'Brien et al. identified analog of the ground state of ^{57}Fe and Saleh et al. (Sa 75) found analog states corresponding to low-lying levels of ^{57}Fe. Leslie et al. (Le 71) observed several new levels and J^{π}-assignments were made to some of them.

The ^{60}Ni(p,α) reaction was investigated by Coop et al.

(Co 69) at 10 MeV and Mateja et al. (Ma 76) at ∿13-16 MeV upto an excitation energies 3.271 and 4.971 with resolution 20-30 keV and 10-14 keV. Mateja et al. observed several levels within this region. Coop et al. made J^{π} assignment for first few levels.

The $^{56}Fe(d,n)$ reaction has been recently studied by Adam et al. (Ad 76) upto an excitation energy of 4.8 MeV. They measured ℓ_p-values and spectroscopic factors from DWBA calculation which are in disagreement with those of Blair et al. (Bl 66). Earlier (d,n) reactions as quoted in Adam et al. (Ad 76) were concerned with a few low-lying levels. The $^{56}Fe(\tau,d)$ reaction was previously studied by Rosner and Holbrow (Ro 67) at E_t=16.5 MeV and later by Hardie et al. (Ha 72) at E_T=22 MeV covering levels upto E_x ∿7.982 MeV and 7.265 MeV respectively. The orbital angular momentum transfers in the two experiments, with a few exceptions are in general agreement to each other ; but there is a systematically large variation in the spectroscopic factors between two measurements, some times by a factor of 3 or more, even for strong transitions. Different conclusions were consequently drawn in the two works. A more recent (τ,d) investigation due to Baghdadi (Ba 75) at E_T= 6 MeV was concerned only with the lowest 2p transitions, two of which carry the major parts of the $p_{3/2}$ and $p_{1/2}$ single particle-strengths. The

spectroscopic factors were found to be closer to those by Rosner and Holbrow (Ro 67) than to Hardie et al. (Ha 72). The spectroscopic factors by Adam (Ad 76) are close to those given by Rosner and Holbrow for some levels and close to Hardie et al.(Ha 72) for some others.

The present work was therefore undertaken to reexamine the level properties of ^{57}Co through the ^{56}Fe(τ,d) reaction at E_τ= 18 MeV and special care taken for the measurement of the absolute cross section.

4.2 Experimental Procedure

The plates were exposed with the products of the ^{56}Fe(τ,d) reaction and were scanned at the Nuclear Physics Laboratory, University of Dacca. A typical spectrum at 18.75^{o} is shown in fig. 4.1. Peaks of the levels have been shown with numbers which refer to the numbering of table 4.4. Contaminant groups resulting from different reactions like (τ,d) and (τ,p) on impurities ^{12}C and ^{16}O present in the target are also lebeled using the corresponding level energy in residual nuclei. The energy resolution (FWHM) was $\sim$22 keV. Several levels have been identified upto $E_x \sim$ 7.8 MeV and the angular distributions are measured for most of them. Because of

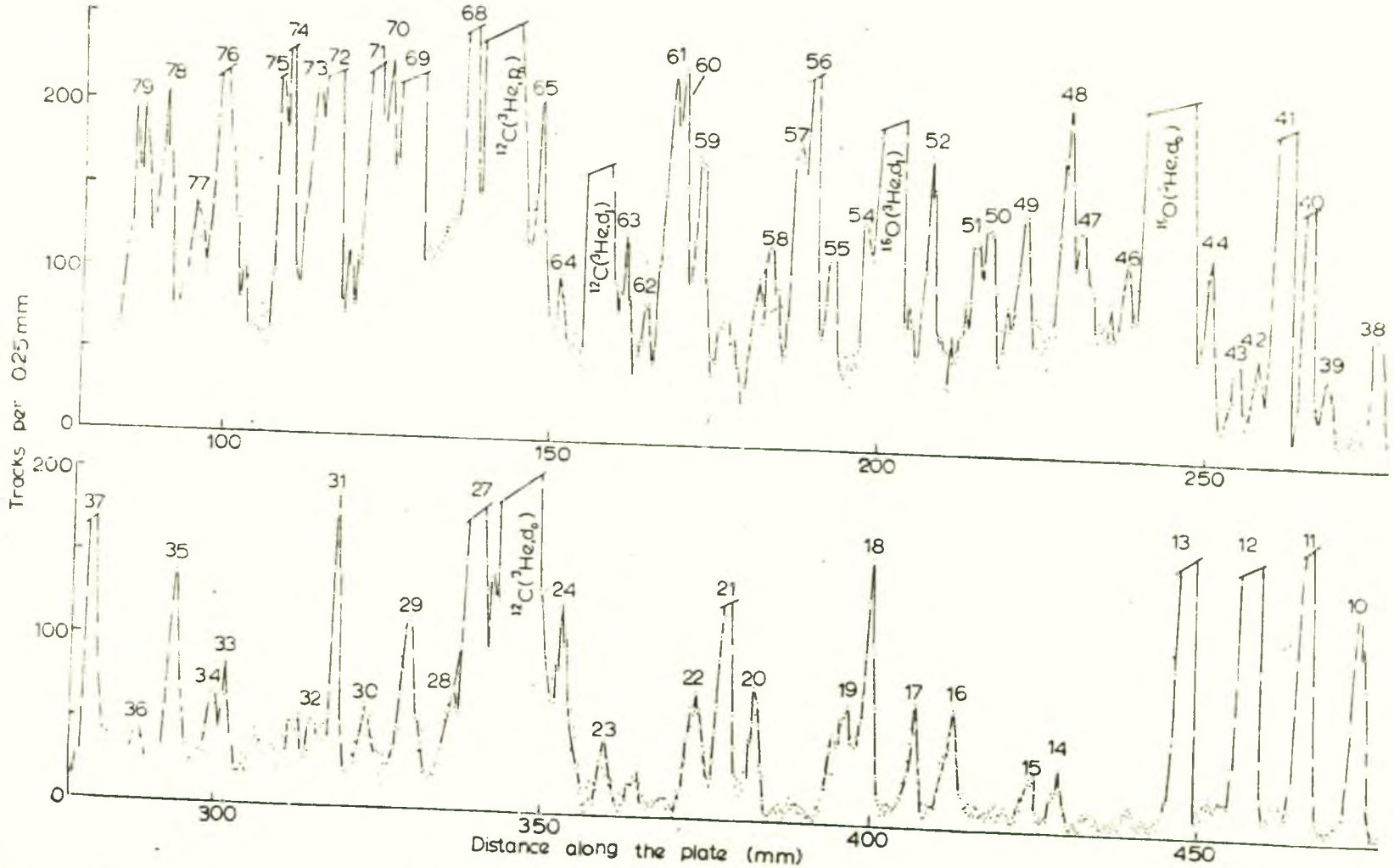

FIG. 4.1. Part of the energy spectrum of deuterons arising from the $^{56}Fe(\tau,d)$ reaction at 18.75° showing the region of high group density.

uncertainty in the spectrograph calibration at the high field used (B ∿12.8K-gauss) an internal calibration was performed by using some well established levels, namely, gs, 1.501, 2.134, 2.878, 3.177, 3.459, 4.001, 5.228, 5.532 MeV. These levels are shown underlined in table 4.4. The method followed for the calibration is the least squares fit mentioned in Chapter 2(Section 2.6). The values of constants a_o, a_1, a_2 for each channel are listed in table 4.1. The target thickness was measured and found to be $90\mu gm.cm^{-2}$. The uncertainty in the absolute value of the (τ,d) reaction cross section (resulting mainly from the errors in the target thickness, scanning and background subtraction) is less than 15%.

4.3 DWBA Analysis

The optical model potential used has the form :

$$V(r) = V_C(r) - V\left(1+\exp\frac{r-r_o A^{1/3}}{a}\right)^{-1} - W\left(1+\exp\frac{r-r_o' A^{1/3}}{a_I}\right)^{-1}$$

$$+ 4i W_D \frac{d}{dr}\left(1+\exp\frac{r-r_o' A^{1/3}}{a_I}\right)^{-1} + \frac{V\lambda}{45.2}\frac{1}{r}\frac{d}{dr}\left(1+\exp\frac{r-r_o A^{1/3}}{a}\right)^{-1}\underline{\ell}.\underline{s} \qquad -4.3.1$$

The symbols carry their usual meaning. The Coulomb potential $V_C(r)$ is taken as due to a uniformly charged sphere

Table 4.1

Constants of least squares fit for

^{56}Fe (τ,d) reaction

Channel	a_o	a_1	a_2
2	11.182	-36.386	18.926
3	11.171	-36.897	19.854
4	11.055	-36.584	19.192
5	11.151	-38.044	21.934

of radius $r_c A^{1/3}$ with r_c = 1.25 fm.

The optical model potential (table 4.2) was of the standard Woods-Saxon form for the ^{3}He - potential and the real part of the deuteron potential, while Woods-Saxon derivative was used for the imaginary part of the deuteron potential. The bound state potential well was taken as the (real) Woods-Saxon form with the geometrical parameters given by r_o = 1.25 fm and a = 0.65 fm including a Thomas-Fermi spin orbital term with λ = 25 and Woods-Saxon form factor. The strength of the potential was adjusted so as to give the transferred proton binding energy $E_B = Q(^3He,d) + 5.49$ MeV.

The DWBA cross sections in local zero range approximation were computed using the code due to Kunz. The calculations were carried out by Professor H. M. Sen Gupta with the IBM 360/195 Computer of Rutherford High Energy Laboratory.

To start with, the DWBA analysis were carried out for four strong transitions leading to the g.s. and the 1.376, 1.501 and 2.134 MeV levels having $J^\pi = 7/2^-$, $3/2^-$, $1/2^-$ and $5/2^-$ respectively. The transition strengths are summarized in table 4.3. Of the different combinations of ^{3}He and

Table 4.2

Optical model parameters

Particle	Notation	V_o (Mev)	r_o (fm)	a (fm)	W_o (MeV)	$4W_D$ (MeV)	r_l (fm)	a_l (fm)	$V_{s,o.}$ (MeV)	$r_{s,o.}$ (fm)	$a_{s,o.}$ (fm)	r_c (fm)	Ref
τ	A	139.0	1.08	0.80	12.3		1.743	0.721				1.4	a,b)
	B	165.0	1.43	0.613	30.3		1.50	0.71	8.0	1.43	0.613	1.4	c)
d	A	94.8	1.12	0.79		61.2	1.32	0.74	6.6	0.90	1.16	1.3	d)
	B	90.0	1.15	0.81		84.0	1.34	0.68				1.15	e)
p		f)	1.25	0.65					λ=25			1.3	

Form factor : for τ-potential, Woods-Saxon for both the real and imaginary parts; for d-potential, Woods-Saxon for the real part and Woods-Saxon derivative for the imaginary part.

a) (Ba 66) R.H.Bassel, Phys.Rev.149(1966)791

b) (Oh 68) H.Ohmura et al. J.Phys.Soc. Japan 25(1968)953

c) (St 67) R.Stock et al. Nucl.Phys.A104(1967)136

d) (Ch 74) J.D.Childs et al. Phys.Rev.C10(1974)217

e) (Pe 63) C.M.Perey and F.G.Perey, Phys.Rev.132(1963)755

f) adjusted to reproduce the binding energy.

Table 4.3

Transition strengths for different combinations of potential parameters

Excitation (Mev)	$n\ell_j$	$(2J_f+1)C^2S$		
		τ_A-d_A	τ_B-d_A	τ_B-d_B
g.s.	$1f_{7/2}$	1.50	1.93	2.07
1.376	$2p_{3/2}$	1.29	1.50	1.59
1.501	$2p_{1/2}$	0.49	0.58	0.61
2.134	$1f_{5/2}$	0.98	1.25	1.21

deuteron potential parameters, the set τA-dA gives the best fit to the data and also satisfies the condition

$$V_\tau \approx V_d + V_p \qquad 4.3.2$$

for the real depths. All the DWBA calculations used in the present work were performed with this set.

The spectroscopic transition strengths $(2J_f+1)C^2S/(2J_i+1)$ were obtained by normalizing the computed cross section $\sigma_{DW}(\theta)$ to the measured value $\sigma_{Exp}(\theta)$ through the relation

$$\sigma_{Exp}(\theta) = N \frac{2J_f+1}{2J_i+1} C^2S \frac{\sigma_{DW}(\theta)}{2j+1} \qquad 4.3.3$$

as suggested in the DWUCK code, where J_i and J_f are respectively the angular momentum of the initial and final nuclear levels and j is the angular momentum of the transferred proton.

4.4 Results and Discussion

The results of the present work are summarized in table 4.4. The energy levels in column 3 are from the compilation

by Auble (Au 77) upto $E_x \sim 4.3$ MeV ; beyond this, the levels are taken from the compilation by Hardie (Ha 72). Information given by the previous (τ,d) and (d,n) studies (Ro 67, Ha 72, Ad 76) is also included in the table for a comparison. The transition strengths $(2J_f+1)C^2S$ in the present as well as in the previous (τ,d) works were extracted for the normalization constant N=4.42, relevant to the Gunn-Irving wave function for ^{3}He and Hulthen for deuteron (Pe 63).

For Q(τ,d) values more negative than -5.5 MeV, corresponding to the breakup of ^{3}He particles, the DWBA cross sections, hence the transition stregths, are not reliable. Such strengths as shown in parenthesis in table 4.4 are extracted from the extrapolation of the DWBA cross sections to that excitation. The spin-parities in column 13 are from all previous measurements as considered to be the best assignments by the present work.

The (τ,d) reaction excites both normal ($T_<$) and analogue ($T_>$) states and the summed transition strengths according to the shell model $G_j (=\Sigma(2J_f+1)C^2S/(2J_i+1))$ related to the shell vacancies as given by

$$G_j = \begin{cases} \langle \text{neutron holes} \rangle / (N-Z+1), & T_> \text{ state} \\ \langle \text{proton holes} \rangle - \langle \text{neutron holes} \rangle / (N-Z+1), & T_< \text{ state} \end{cases} \qquad 4.4.1$$

Table 4.4

Summary of the level properties of ^{57}Co

Group	Excitation (MeV)		$\sigma_{max}(\theta)$	ℓ_p transfer				$(2J_f+1)C^2S$				J^π	
	a)	b)	(mb/sr) [a)]	a)	c)	d)	e)	a)	c)	d)	e)	f)	a)
0	0	0	0.80	3	3	3	3	1.50	0.89	1.80	1.90	$7/2^-$	g)
	1.224											$9/2^-$	
1	1.376	1.378	12.75	1	1	1	1	1.29	0.52	1.80	1.07	$3/2^-$	g)
2	1.501	1.505	5.70	1	1	1	1	0.49	0.35	0.72	0.45	$1/2^-$	g)
		1.689										$11/2^-$	
3	1.758	1.757	2.34	1	1	1	1	0.23	0.13	0.30	0.20	$3/2^-$	g)
4	1.898	1.897	0.056	n.s								$7/2^-$	
		1.919										$5/2^-$	
5	2.134	2.133	1.05	3	3	3	3	0.98	1.20	2.00	1.18	$5/2^-$	
6	2.314	2.311	0.25	3	3	3	3	0.35	0.20	0.70	0.35	$7/2^-$	
		2.486										$11/2^-$	
		2.524										$\geq 13/2^-$	

Table 4.4 (continued)

Group	Excitation (MeV)		$\sigma_{max}(\theta)$	ℓ_p transfer				$(2J_f+1)C^2S$				J^π	
	a)	b)	(mb/sr) a)	a)	c)	d)	e)	a)	c)	d)	e)	f)	a)
		2.560										≥11/2⁻	
		2.611										7/2⁻	
		2.723										7/2⁻	
		2.731										3/2⁻,5/2⁻	
		2.743											
		2.804										3/2⁻,5/2⁻	
7	2.878	2.879	1.87	1	1	1	1	0.21	0.11	0.39	0.14	3/2⁻	g)
8	2.985	2.981	0.13	0	0			0.026				1/2	g)
9	3.112	3.108	0.32	1	1		1	0.028,0.019 0.035			0.09, 0.09	1/2⁻,1/2⁻	g)
		3.121											
		3.165											
10	3.177	3.177	0.42	3	3	3	3	0.31	0.55	0.84	0.84	5/2⁻	g)
		3.184											
		3.246											

Table 4.4 (continued)

Group	Excitation (MeV)		$\sigma_{max}(\theta)$	ℓ_p transfer				$(2J_f+1)C^2S$				J^π	
	a)	b)	(mb/sr) a)	a)	c)	d)	e)	a)	c)	d)	e)	f)	a)
11	3.267	3.262	0.64	3	3	3	3	0.46, 0.71	0.65, 0.44	1.62	0.94, 0.55	$5/2^-, 7/2^-$	g)
12	3.355	3.357	3.56	1	1	1	1	0.30, 0.39	0.16	0.56	0.30 0.27	$1/2^-, 3/2^-$	g)
		3.394											
		3.431											
13	3.459	3.461	2.84	1	1	1	1	0.26 0.35	0.14	0.38	0.25, 0.23	$1/2^-, 3/2^-$	g)
		3.522											
		3.540										$3/2^+, 5/2^+$	
		3.553											
		3.622											
		3.665											
14	3.681	3.672	0.091	n.s								$7/2^-$	
		3.681											
15	3.727	3.720	0.069	4			(0)	0.16			0.02	$(1/2^+)$	$9/2^+$
		3.834											

Table 4.4 (continued)

Group	Excitation (MeV)		$\sigma_{max}(\theta)$	ℓ_p transfer				$(2J_f+1)C^2S$				J^π	
	a)	b)	(mb/sr) a)	a)	c)	d)	e)	a)	c)	d)	e)	f)	a)
16	3.862	3.854	0.18	2				0.30				$(3/2^+)$	
		3.909										$(3/2^+)$	
17	3.923	3.918	0.38	1			1	0.033, 0.045			0.04, 0.04	$1/2^-,3/2^-$	g)
		3.991										$(5/2^-)$	
18	4.001	3.999	0.51	(1)	(1)		1	0.045,0.029 0.062			0.05, 0.05	$1/2^-,3/2^-$	g)
		4.037											
19	4.067	4.058	0.19	1	(1)			0.019,0.009 0.024				(3/2) $1/2^-,3/2^-$	
		4.111											
20	4.194	4.187	0.38	1	1		1	0.034,0.024 0.044			0.06, 0.04	$1/2^-,3/2^-$	g)
		4.217											
		4.238											
21	4.253	4.251	0.32	3	3	3	3	0.20, 0.26 0.31		0.70	0.56, 0.41	$5/2^-,7/2^-$	g)

Table 4.4 (continued)

Group	Excitation (MeV)		$\sigma_{max}(\theta)$	ℓ_p transfer				$(2J_f+1)C^2S$				J^π	
	a)	b)	(mb/sr) a)	a)	c)	d)	e)	a)	c)	d)	e)	f)	a)
		4.272											
		4.284											
22	4.293	4.297	0.59	1	(1)			0.053,0.020 0.071			0.08, 0.07	$1/2^-,3/2^-$ g)	
		4.308											
		4.379					1				0.03, 0.02	$1/2^-,3/2^-$	
		4.399											
23	4.455	4.454	0.080	n.s			1+3				0.03, 0.23		
24	4.517	4.500	0.082	n.s									
25	4.537	4.525	0.54	1		(1)		0.050, 0.064				$(1/2^-,3/2^-)$	
26	4.590	4.595 4.615	1.53	4		4	2+4	2.60		4.8	0.09, 1.93	$9/2^+$	
27	4.677	4.685	2.60	(1)	(1)	(2)	2	0.26, 0.15 0.33			1.08, 0.30	$(1/2^-,3/2^-)$	

Table 4.4 (continued)

Group	Excitation (MeV)		$\sigma_{max}(\theta)$	ℓ_p transfer				$(2J_f+1)C^2S$				J^π	
	a)	b)	(mb/sr) a)	a)	c)	d)	e)	a)	c)	d)	e)	f)	a)
28	4.737	4.730	0.14	n.s									
29	4.806	4.800	0.32	n.s			3				0.28, 0.23	$5/2^-, 7/2^-$	
30	4.886		0.20	n.s									
31	4.938		0.30	0				0.031				$1/2^-$	
32	4.985	4.981	0.25	n.s									
33	5.138		0.16	n.s									
34	5.167		0.14	n.s									
35	5.228	5.223	0.34	0	0			0.035	0.027			$1/2^-$	
36	5.296		0.14	n.s									
37	5.387	5.370	0.77	1				0.074, 0.086				$1/2^-, 3/2^-$	
38	5.447	5.425	0.35	1				0.038, 0.041				$1/2^-, 3/2^-$	
39	5.532	5.528	0.12	n.s									

Table 4.4 (continued)

Group	Excitation (MeV)		$\sigma_{max}(\theta)$	ℓ_p transfer				$(2J_f+1)C^2S$				J^π	
	a)	b)	(mb/sr) a)	a)	c)	d)	e)	a)	c)	d)	e)	f)	a)
40	5.570	5.559	0.73	1				0.086, 0.098				$1/2^-, 3/2^-$	
41	5.615	5.621	3.70	1	1	(1)		0.39, 0.44				$1/2^-, 3/2^-$ g)	
42	5.664	5.653	0.076	n.s									
43	5.699	5.693	0.14	n.s									
44	5.747	5.743	0.23	1				0.045, 0.050				$1/2^-, 3/2^-$	
45	5.806	5.799	0.55	n.s									
46	5.914	5.91	0.14	n.s								$3/2^+$	
47	5.992	5.976	0.39	n.s								$3/2^+$	
48	6.024	6.013	0.75	n.s									
49	6.098	6.093	0.33	n.s									
50	6.159	6.153	0.41	1				(0.052, 0.056)				$1/2^-, 3/2^-$	

Table 4.4 (continued)

Group	Excitation (MeV)		$\sigma_{max}(\theta)$	ℓ_p transfer				$(2J_f+1)C^2S$				J^π	
	[a]	[b]	(mb/sr)[a]	[a]	[c]	[d]	[e]	[a]	[c]	[d]	[e]	[f]	[a]
51	6.187	6.184	0.45	n.s									
52	6.278	6.268	0.52	1				(0.068, 0.074)				$1/2^-,3/2^-$	
53	6.348	6.344	1.62					(0.14, 0.15)				$1/2^-,3/2^-$	
54	6.391		0.41	1				(0.050, 0.052)				$1/2^-,3/2^-$	
55	6.472		0.20	n.s									
56	6.504	6.492	0.49	n.a		(3)						$(5/2^-,7/2^-)$	
57	6.540		0.28	n.s									
58	6.589	6.594	0.12	n.a									
59	6.712	6.699	0.50	n.a									
60	6.750	6.739	0.46	n.a									
61	6.785	6.786	0.17	n.a									
62	6.846	6.848	0.11	n.s									

Table 4.4 (continued)

Group	Excitation (MeV)		$\sigma_{max}(\theta)$	ℓ_p transfer				$(2J_f+1)C^2S$				J^π	
	a)	b)	(mb/sr) a)	a)	c)	d)	e)	a)	c)	d)	e)	f)	a)
63	6.890	6.885	0.34	(1)		(1)		(0.063, 0.059)				$(1/2^-,3/2^-)$	
64	7.032	7.020	0.30	(1)		(1)		(0.065, 0.060)				$(1/2^-,3/2^-)$	
65	7.066		0.16	n.s									
66	7.115	7.115	0.41	n.s	(1)							$(1/2^-,3/2^-)$	
67	7.150	7.162	0.46	1				(0.073, 0.073)				$1/2^-,3/2^-$	
68	7.187		0.57	1				(0.084, 0.076)				$1/2^-,3/2^-$	
69	7.271	7.265	2.86	1	1	1		(0.34, 0.31)		(0.12)		$1/2^-,3/2^-$ g)	
		7.281											
70	7.322	7.324	0.35	n.s									
71	7.370	7.367	0.32	n.s									

Table 4.4 (continued)

Group	Excitation (MeV)		$\sigma_{max}(\theta)$	ℓ_p transfer				$(2J_f+1)C^2S$				J^π	
	a)	b)	(mb/sr) [a]	a)	c)	d)	e)	a)	c)	d)	e)	f)	a)
72	7.434	7.432	1.17	3	2,3	3		(0.52, 0.75)		(0.80)		$5/2^-,7/2^-$	
73	7.473	7.480	0.56	n.a									
74	7.531	7.528	0.42	n.s									
75	7.559		0.38	n.s									
		7.610											
		7.626											
		7.634											
		7.648											
76	7.665	7.656	0.87	1		1		(0.14, 0.11)		(0.04)		$1/2^-,3/2^-$ g)	
		7.662											
77	7.708		0.27	n.s									

Table 4.4 (continued)

Group	Excitation (MeV)		$\sigma_{max}(\theta)$	ℓ_p transfer				$(2J_f+1)C^2S$				J^π	
	a)	b)	(mb/sr) a)	a)	c)	d)	e)	a)	c)	d)	e)	f)	a)
78	7.809	7.799	0.48	2				(0.047)				$5/2^+$	
79	7.839		0.60	2				(0.072)				$5/2^+$	

a) Present work.

b) Summarized by Auble (Au 77) upto E_x=4.308, beyond which the levels are from the ^{56}Fe(τ,d) work of Hardie et al.(Ha 72)

c) (τ,d) reaction at E_τ=22 MeV, Hardie et al.(Ha 72)

d) (τ,d) work of Rosner and Holbrow (Ro 67) at E_τ=16.5 MeV.

e) (d,n) reaction by Adam et al.(Ad 76)

f) Previous experiments, summarized by the present authors.

g) The J^π-values are consistent with the assignment in column 13.

n.s. - Nonstripping angular distribution.

n.a. - Data not analysed.

The estimated errors in energies in present experiment are $\pm$ 15 keV.

where N and Z are the neutron and proton numbers of the target nucleus. The results of the sum rule analysis are summarized in table 4.5 ; also included are those from previous (τ,d) and (d,n) measurements (Ro 67, Ha 72, Ad 76) as well as the theoretical limits given by the single-particle shell model. Typical examples of the DWBA fits to the measured angular distributions are shown in figs. 4.2 - 4.5. The single-particle strengths are fragmented over levels as displayed in fig. 4.6.

The results are discussed below.

4.4.1. The Angular distribution and Transition Strength

4.4.1.1. The ℓ = 1 transitions.

The 2p transition strengths are distributed over a large number of levels (fig 4.6). The spectroscopic factor for ℓ =1 transitions, level by level, found in the present work lies between that given by Rosner and Holbrow (Ro 67) and Hardie et al. (Ha 72). The higher value of $\Sigma(2J_f+1)C^2S$ for the 2p states given by the present work than that by Rosner and Holbrow is due to the fact that more ℓ=1 transitions are observed by us than by them. The measured 2p, $T_<$ strength in the present work is 4.53, being almost identical to the expected single-particle value of 5.20 within the limits of uncertainty. The value obtained by Adam et al. (Ad 76), from the (d,n)

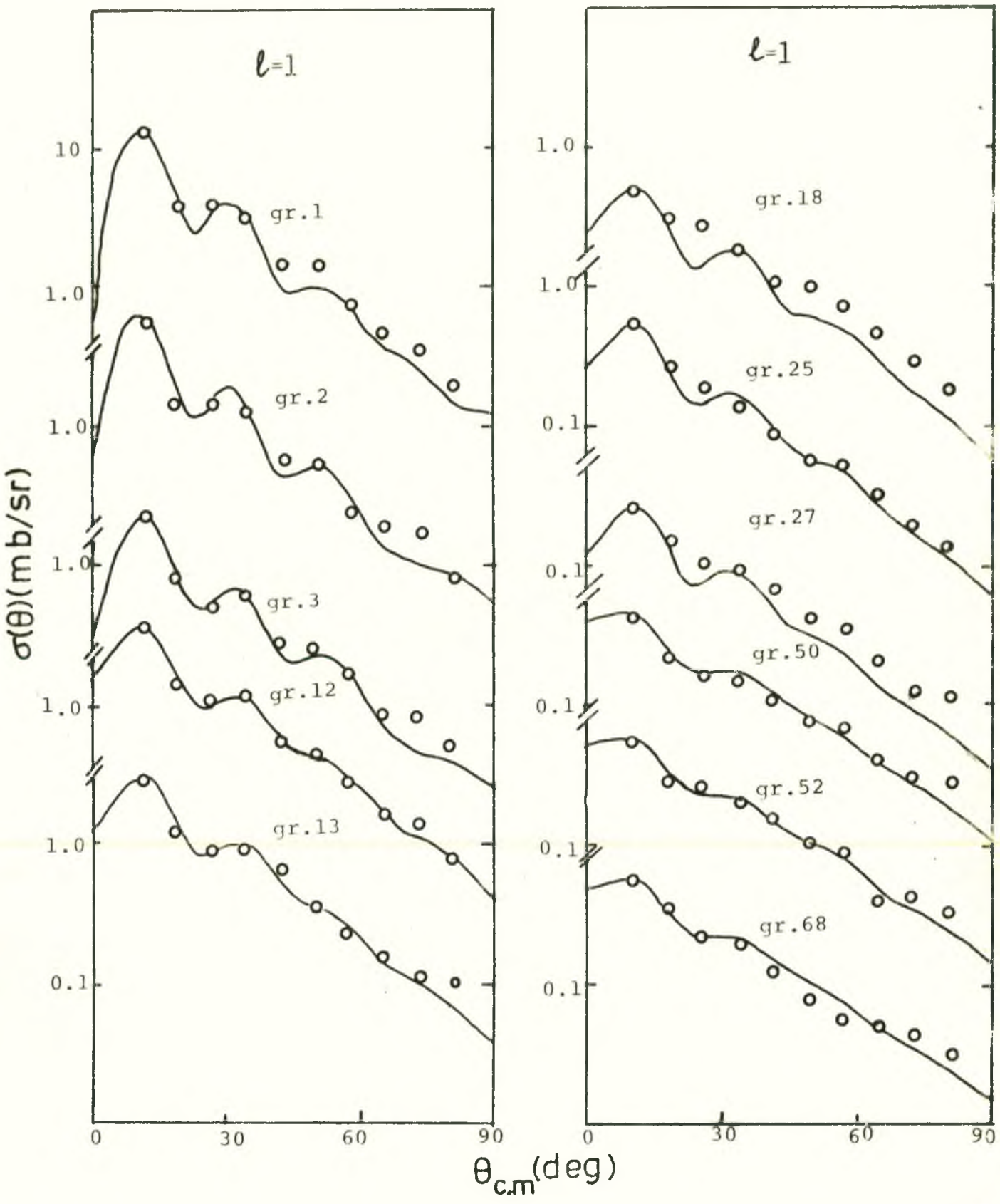

FIG. 4.2. Measured angular distributions fitted with ℓ=1 DWBA curves.

reaction is about 50% of the expected strength. Splitting of the observed strength into $p_{3/2}$ and $p_{1/2}$ components is difficult, since of all the ℓ=1 transitions, the J-values are known for only a few low-lying levels (table 4.4) and further the angular distribution data do not display a J-dependence. The transition strengths of the remaining levels were calculated for both $3/2^-$ and $1/2^-$ states. The known $J^\pi=3/2^-$ levels, namely 1.376, 1.758 and 2.878 MeV, together carry about 50% of the expected $T_<$ strength (table 4.5). The levels at 7.271 and 7.655 MeV are considered to be analogues, as discussed in section 4.4.2. The summed transition strength for the remaining levels assumed as $1/2^-$ levels is 2.80 as against the single particle limit of 1.60. The J^π-value of the 3.355, 3.459 and 4.067 MeV levels has been found to be $3/2^-$ by Esat et al. (Es 74) in the $^{56}Fe(p,\gamma)$ reaction. With this assignment, the $\Sigma(2J_f+1)C^2S$ value for the $2p_{3/2}$ and $2p_{1/2}$ states becomes 2.49 and 2.22 respectively, still far from the single particle limits. A different choice of the τ and d potentials increases the values by $\sim$20% (table 4.3), the $p_{3/2}$ strength thus comes closer to the expected value than above, but at the same time the $p_{1/2}$ value differs further from the shell model value. Summing up, the observed $2p_{1/2}, T_<$ strength is higher than that predicted and the $2p_{3/2}, T_<$ measured value is less than the sum rule limit. It is thus possible that

Table 4.5

Results of the sum rule analysis for proton $T_<$ states in ^{57}Co

Single-particle state [a]	$\Sigma(2J_f + 1)C^2S$					$E_{n\ell j}$ (MeV)			
	theory	b]	c]	d]	e]	b]	c]	d]	e]
$1f_{7/2}$	2.00	1.85	1.80	1.09	2.25	0.44	0.0	0.42	0.36
$2p_{3/2}$	3.60	1.73[f], 2.49[g]	2.10	1.06	2.00	1.61	1.43	1.19	2.11
$1f_{5/2}$	4.80	1.95	5.86	2.66	4.32	2.78	2.87	2.83	3.28
$2p_{1/2}$	1.60	2.80[f], 2.22[g]	2.05	0.65	0.69	4.44	2.63	2.39	2.44

[a] Data for other states being incomplete are not included

[b] Present work

[c] The $^{56}Fe(\tau,d)$ reaction (Ro 67)

[d] The $^{56}Fe(\tau,d)$ reaction (Ha 72)

[e] The $^{56}Fe(\tau,n)$ reaction (Ad 76)

[f] Assuming $J^\pi = \frac{1}{2}^-$ for the levels 3.357, 3.459 and 4.067 MeV, as discussed in the text.

[g] Assuming $J^\pi = \frac{3}{2}^-$ for the levels 3.357, 3.459 and 4.067 MeV, as discussed in the text.

some of the assumed $2p_{1/2}$ levels really belong to the $2p_{3/2}$ state. It is also possible that the $2p_{3/2}$ proton orbit is not completely vacant as assumed in shell model ; the observed $lf_{7/2}, T_<$ strength however does not support the latter suggestion. Further comments should await a determination of the J-values of at least the strong $\ell_p = 1$ transitions.

The angular distribution leading to the 3.355 MeV level is characterized by the $\ell=1$ transition (Fig.4.2) in agreement with previous (τ,d) and (d,n) reactions, but in disagreement with the $\ell=3$ assignment in the $^{58}Ni(t,\alpha)$ reaction by Blair and Armstrong (Bl 66). The transition to the 4.677 MeV level has contradictory ℓ_p-assignments in proton stripping reactions (table 4.4); in agreement with Hardie et al.(Ha 72) the present work favours $\ell_p=1$ assignment made to the levels at 4.067, 4.293 and 4.537 MeV in one or the other (τ,d) reaction (table 4.4).

4.4.1.2 The $\ell=3$ transitions

The measured angular distributions are shown in fig. 4.3. The J-values of the ground state (g.s.) and the lowest three levels (E_x=2.134, 2.314 and 3.177 MeV) belonging to the $\ell=3$ transitions are known (table 4.4). The g.s. and 2.314 MeV level together exhaust the $lf_{7/2}$, $T_<$ strength (table 4.5). The 7.434 MeV level is presumably a $5/2^-$, $T_>$ level as discussed later

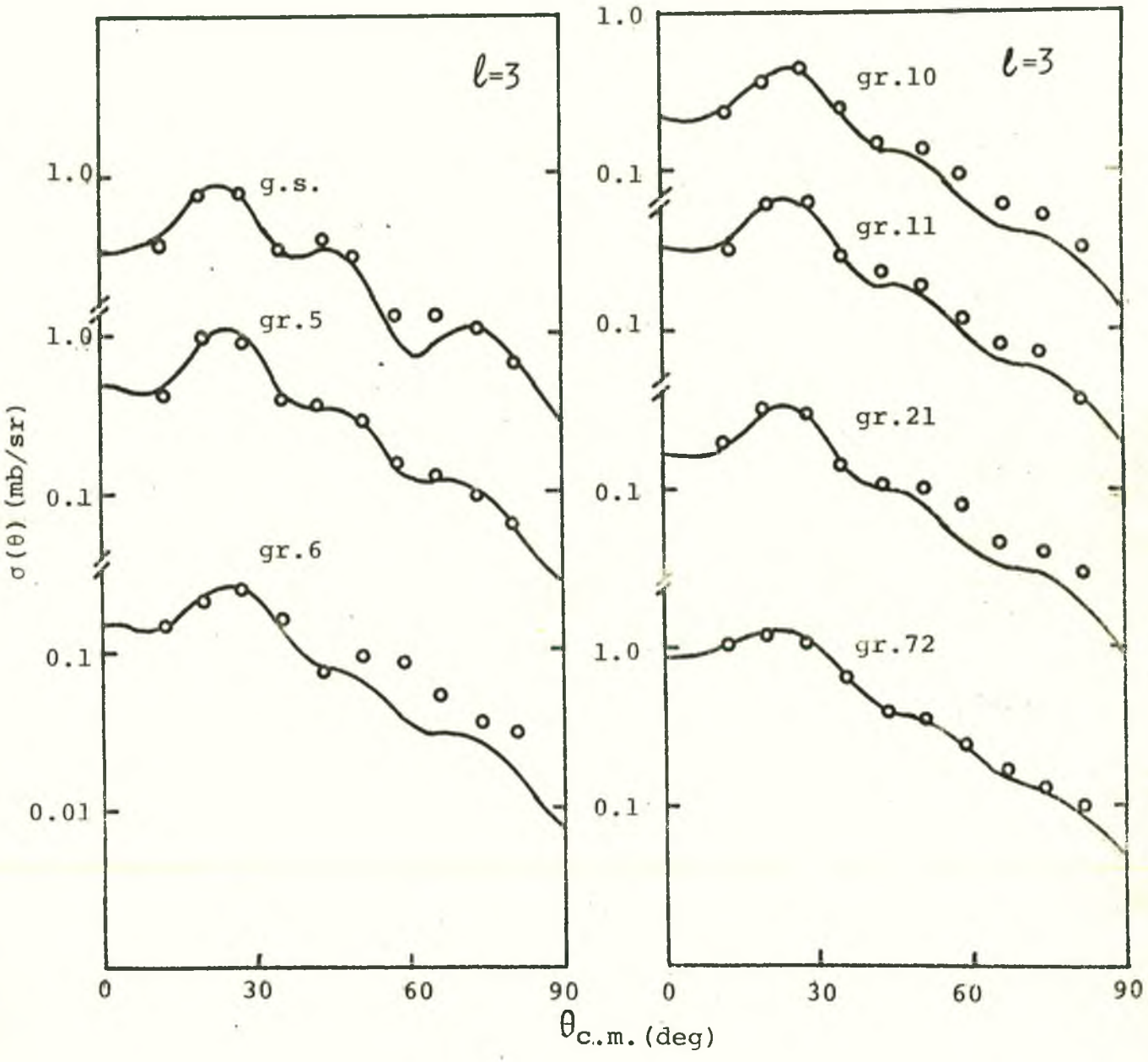

FIG. 4.3. Measured angular distributions fitted with ℓ = 3 DWBA curves.

(section 4.4.2). The remaining transitions together carry about 40% of the $lf_{5/2}$, $T_<$ strength. The selection of parameter sets (table 4.4) increases the $f_{7/2}$ strength by 30-38% and the $f_{5/2}$ strength by 25-30% and thus do not much improve the situation. More $J^{\pi}=5/2^-$ levels thus remain to be identified. Because of the large centrifugal barrier of $\ell=3$ transitions as compared to the $\ell=1$ transitions for example, the spreading will be less for $\ell=3$ than that for $\ell=1$ transitions; such levels are therefore unlikely to lie above $E_x \sim 7.8$ MeV, the excitation energy covered in the present experiment. The lf, $T_<$ transition strength is probably overestimated by Rosner and Holbrow(Ro 67) ; the entire $f_{7/2}$, $T_<$ strength according to them is contained in the g.s.transition. The spectroscopic factor in the present case is smaller than that given by Adam et al. (Ad 76). The present values for the $lf_{7/2}$ levels are twice as strong as those obtained by Hardie et al. (Ha 72) while for the $lf_{5/2}$ levels the present values are somewhat lower than theirs.

4.4.1.3 The $\ell=0, 2$ and 4 transitions

Three $\ell=0$ transitions are observed in the present work (E_x=2.985, 4.938 and 5.228 MeV) and the angular distributions are shown in fig. 4.4. The 2.985 MeV level is strongly excited in the ^{58}Ni(t,α) reaction (Bl 66) and is probably a 2s

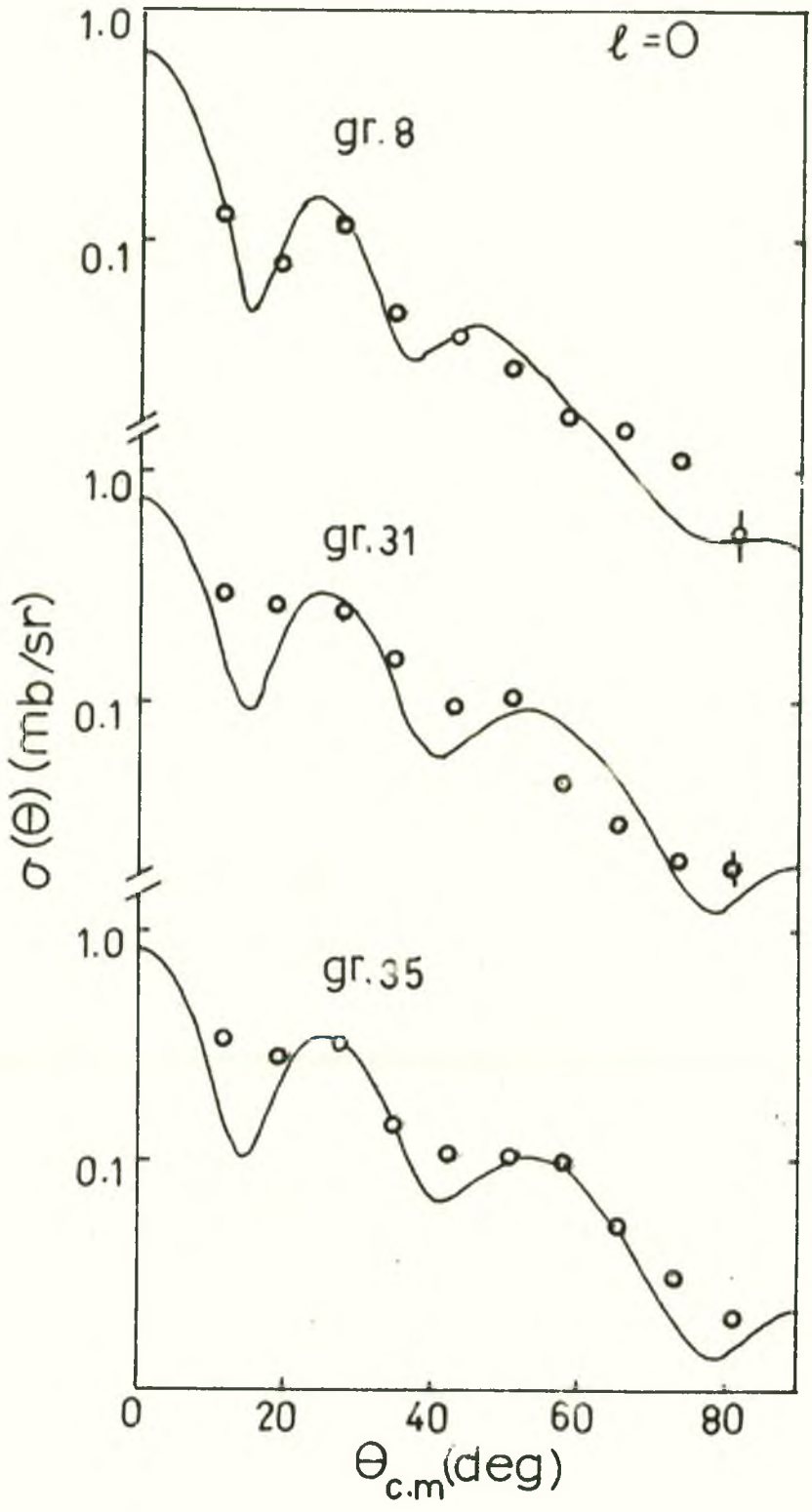

FIG. 4.4. Measured angular distributions fitted with ℓ = 0 DWBA curves.

hole state. The other two transitions are assumed to belong to the 3s state. A discussion on the ℓ=0 transitions is made in section 4.5.

Three ℓ=2 transitions are identified in this experiment two of which lie around E_x=7.8 MeV and are likely to belong to the $2d_{5/2}$ particle state. The other level (E_x=3.862 MeV) is assumed to be a $1d_{3/2}$ hole state and is probably identical with the 3.906 MeV level excited with an ℓ=2 character in the ^{58}Ni(t,α) reaction (Bl 66). No ℓ=2 transition was observed by Hardie et al. (Ha 72) in the ^{56}Fe(τ,d) reaction. The one tentatively assigned in the ^{56}Fe(τ,d) reaction as ℓ=2 by Rosner and Holbrow (Ro 67) at $E_x \sim 4.68$ MeV and later confirmed by Adam et al.(Ad 76) in the ^{56}Fe(d,n) reaction in a tentative ℓ_p=1 according to Hardie et al. (Ha 72) and the present work.

Two ℓ=4 transitions are observed in the present experiment at E_x=3.727 MeV and the doublet at 4.59 MeV. The former is a tentative ℓ=0 transition and the later a mixture of ℓ=2 and 4 in the ^{56}Fe(d,n) reaction (Ok 68). Both the angular distributions are well fitted by the ℓ=4 DWBA curve (fig.4.5).

4.4.1.4 Nonstripping Levels

Several nonstripping levels are observed in the present work (designated n.s. in table 4.4), the angular distributions

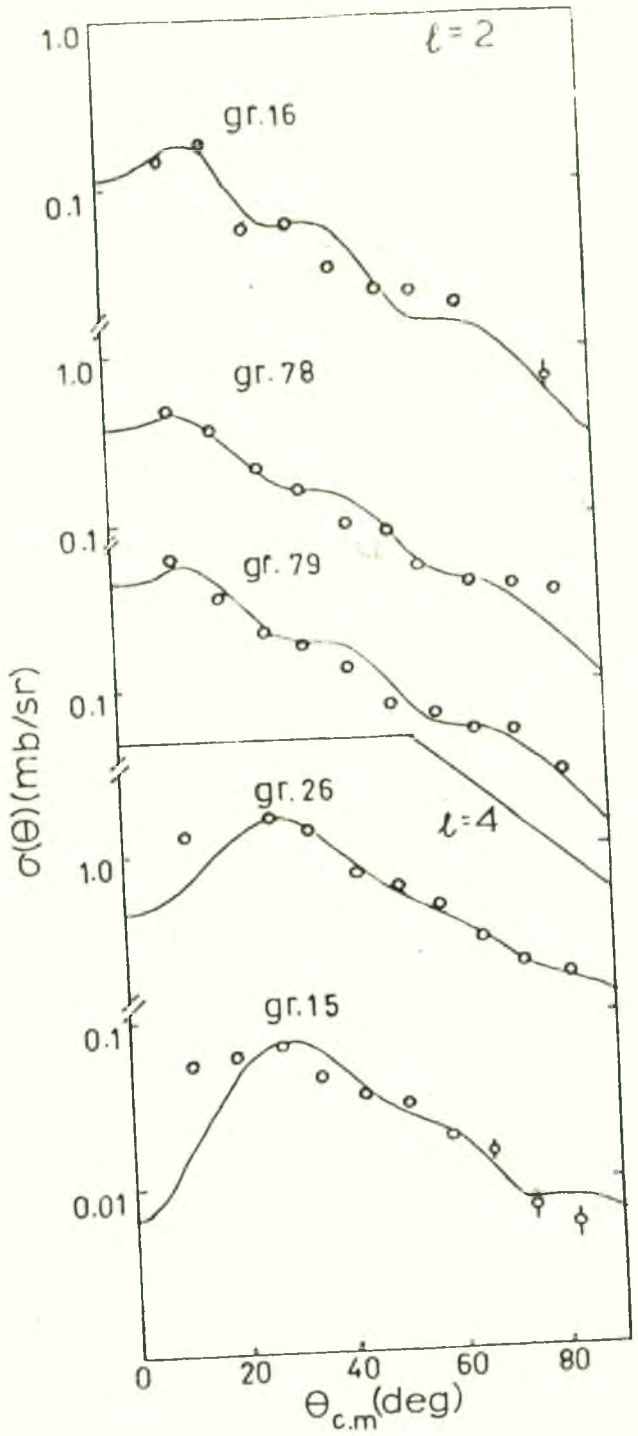

FIG. 4.5. Measured angular distributions fitted with ℓ=2 and 4 DWBA curves.

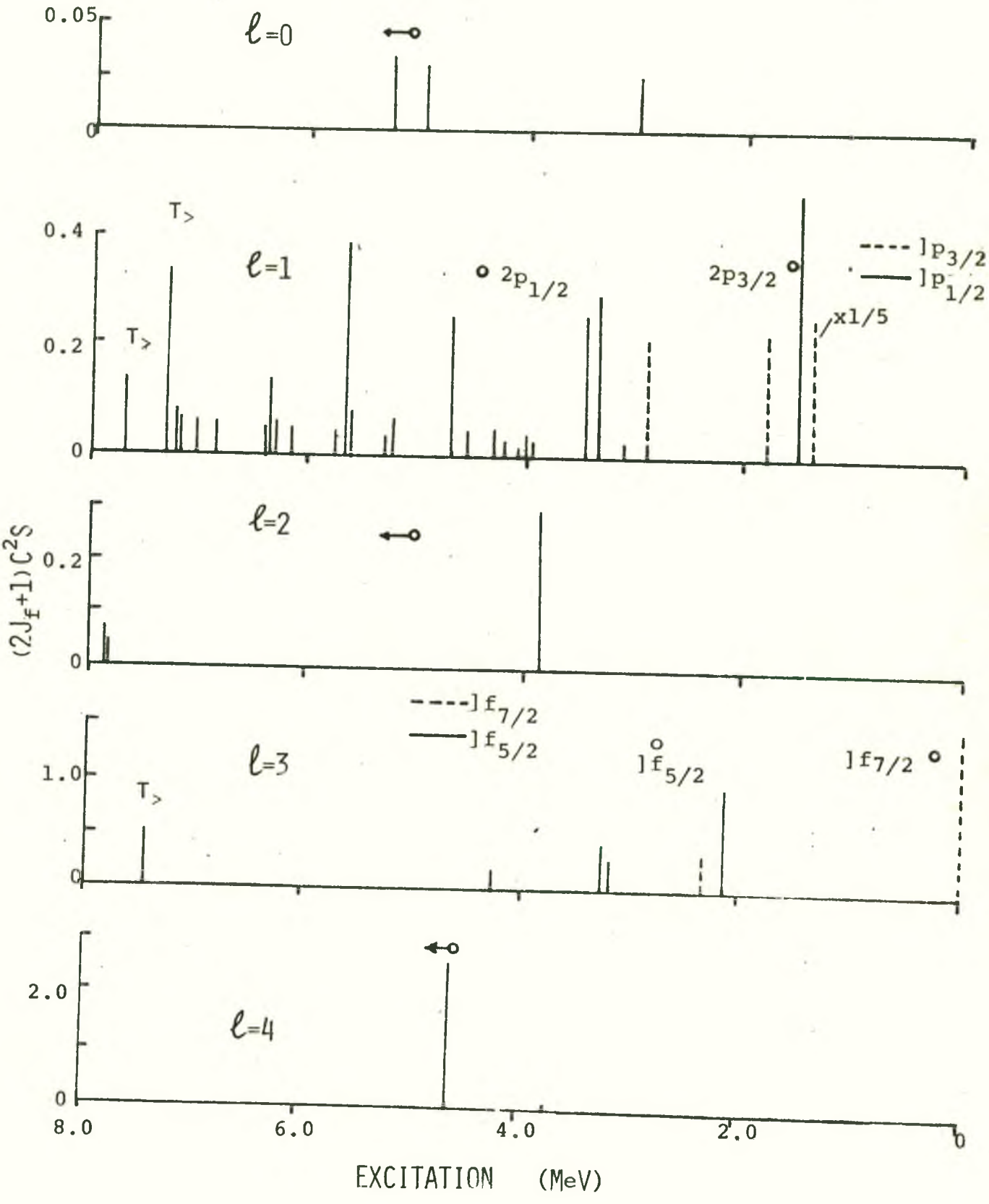

FIG. 4.6. The spectral distributions of single-particle strengths: the centroids of the different $T_<$ states are shown.

to some of which are shown in fig. 4.7. The cross sections rise at forward angles, but the distributions are not given by the direct reaction mechanism. The nonstripping levels are usually weakly excited and the cross sections for many of them are an order of magnitude smaller than the average cross sections for the stripping levels. They cannot be described in terms of a single proton coupled to a ^{56}Fe-core and some of them arise from a collective mode of excitation.

It is interesting to note that the levels with high spin values are either not at all excited in the (τ,d) reaction (levels at 1.224, 1.689 MeV and the multiplets at $\sim$ 2.5 MeV, for example) or have angular distributions not characteristic of a direct process (levels at 1.898, 3.681 MeV for example). Some of the $1d_{3/2}$ hole states (E_x=5.91 MeV) excited in the ^{58}Ni(t,α) reaction have nonstripping angular distributions.

4.4.2 Isobaric analogue states

The ^{56}(τ,d) reaction can excite both the normal ($T_<$) and analogue ($T_>$) states in ^{57}Co. The $T_<$ states were discussed above. Because of the rather large isotopic spin of ^{56}Fe, not enough strengths are available to the analogue states to stand distinctively over the neighbouring $T_<$ states. It has been suggested by Hardie et al. (Ha 72) from a compilation of the

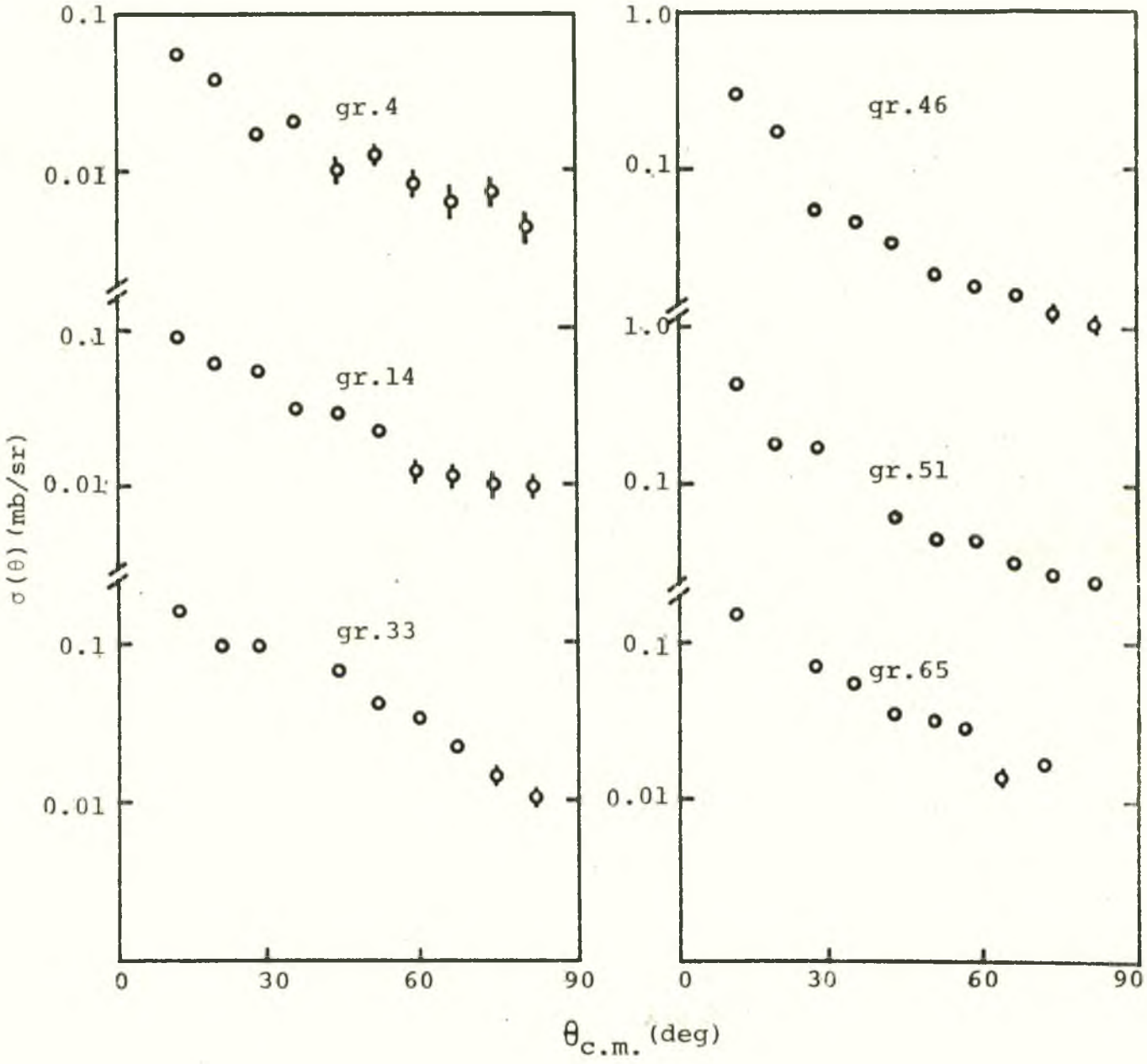

FIG. 4.7. Some of the measured angular distributions displaying a non-stripping character.

available information from the (τ,d) and (p,γ) reactions that there is a confusion over the positive identification of the analogue states. In agreement with Rosner and Holbrow (Ro 67) the levels at 7.271, 7.434 and 7.665 MeV were identified in this work as the analogues of the g.s.+ 14 (unresolved), 136 and 366 keV levels in ^{57}Fe. The relative level spacings and the ℓ_p-values are consistent with the relative level spacings and the J-values of the parent levels. In view of the non-reliability of the DWBA cross sections for (τ,d) reaction at this excitation, as stated earlier, we refrain ourselves from a comparison with the corresponding spectroscopic factors in the ^{56}Fe(d,p) reaction. The Coulomb displacement energy for the isobaric pair of nuclei ^{57}Fe - ^{57}Co comes to be 8.89 MeV for the g.s. analogue.

4.5 The Level Spectrum of ^{57}Co

Several attempts have been made to calculate the level spectrum of ^{57}Co based on the shell model (Ve 66, Mc 67, Ga 69, Ho 73), as well as on the unified model (Sa 68, Co 71, St 71, Go 72). The observed level spectrum is compared with the predictions of the more important theories in fig. 4.8.

The shell model calculation by Vervier (Ve 66) assumes as inert ^{48}Ca core with a proton hole in the $1f_{7/2}$ orbit and the two extra core neutrons only in the $2p_{3/2}$ orbit ; the

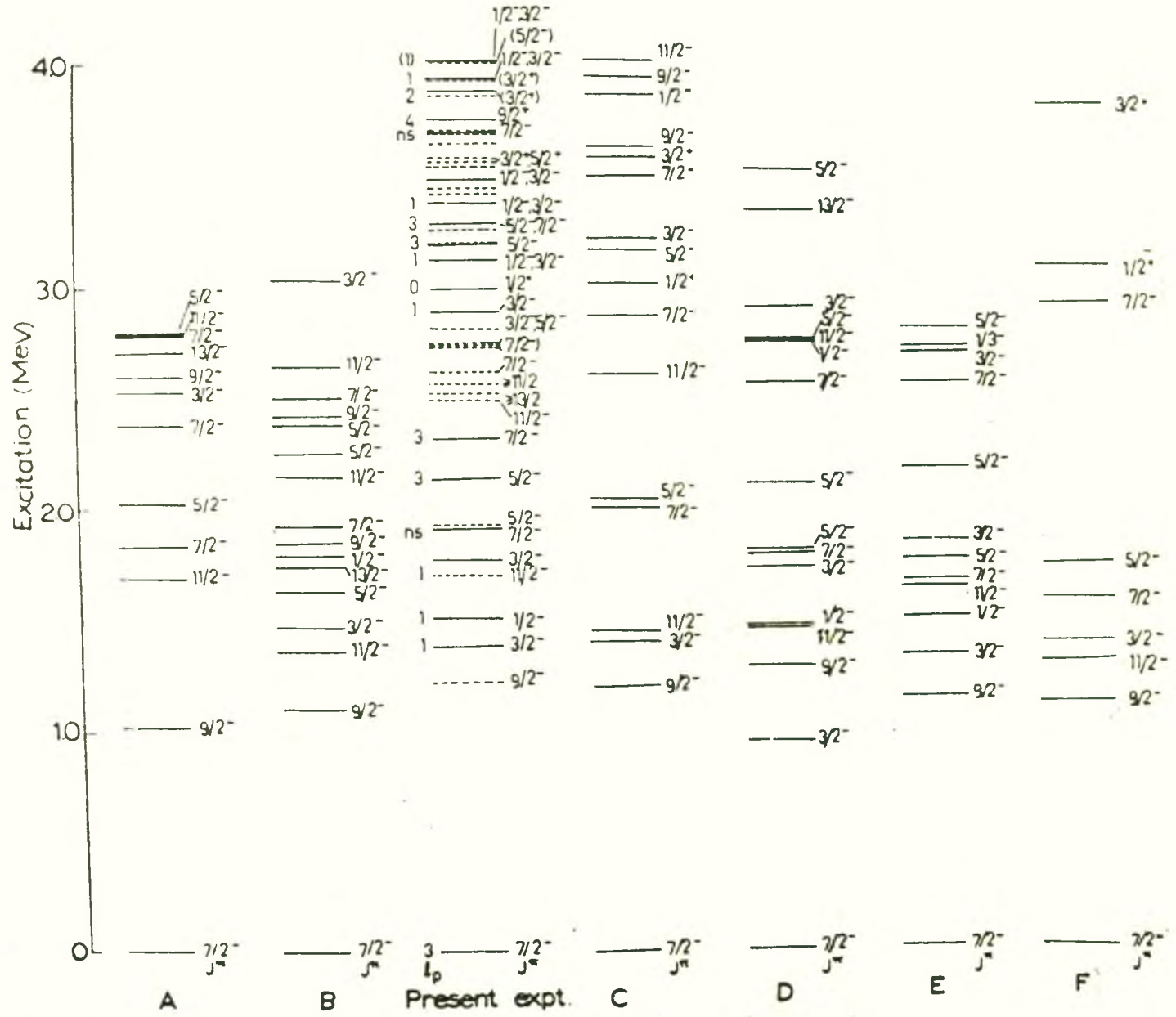

FIG. 4.8. Experimental level spectrum of ^{57}Co compared with theoretical calculations. The levels not observed in the present experiment are shown by broken lines. A: (Ho 73), B: (Ga 73), C: (Sa 68), D: (Go 72), E: (Co 69), F:(Sm 79).

agreement with experiment was poor. The above calculation was then repeated by McGrory (Mc 67) by increasing the model space so as to include also the $2p_{1/2}$ and $1f_{5/2}$ neutron configurations. The residual interaction was taken to give a reasonable agreement with other isotonic nuclei. The agreement with experiment, although somewhat improved, is still unsatisfactory. Several well-known levels are not predicted, in particular there are no calculated $J^{\pi}=1/2^{-}$ and $3/2^{-}$ levels below $E_x \approx 2.5$ MeV, whereas such levels have been observed below $\approx$1.5 MeV.

An extended shell model calculation due to Gatrousis et al.(Ga 69) is based on an inert ^{40}Ca core and includes the neutron configurations $1f_{7/2}$, $1f_{5/2}$, $2p_{3/2}$ and $2p_{1/2}$ and further allows the excitation of protons from the $1f_{7/2}$ shell to the $2p_{3/2}$, $2p_{1/2}$ and $1f_{5/2}$ orbits. The spacings of the single-particle orbits are treated as free parameters and the residual two-body interaction was taken as that given by a free two-nucleon Hamada-Johnston potential. Many more levels are predicted than those by Vervier (Ve 66) and McGrory (Mc 67). A comparision with the experimental level scheme is made in fig. 4.8. Except for the 1.76 MeV level ($J^{\pi}=3/2^{-}$) all the observed levels below $E_x \approx 2$ MeV are reproduced in this calculation, although the sequence and the spacings of the levels

are not exact. Some of the high spin states predicted by Gatrousis (Ga 69), namely the $J^{\pi}=13/2^{-}$ level at ≈1.7 MeV and $J^{\pi}=11/2^{-}$ level at 2.1 and 2.7 MeV, appear to be strong candidates for some of the high spin states (E_x =2.486 MeV, $J^{\pi}=11/2^{-}$; E_x =2.523 MeV, $J \geq 13/2$; E_x =2.555 MeV, $J \geq 11/2$) observed later by Pietzyk et al. (Pi 73) in the ^{57}Fe(p,n) reaction. Two $J^{\pi}=9/2^{-}$ levels predicted by this model at ≈1.8 and ≈2.5 MeV have, however, not been observed in any experiment.

A more recent shell model calculation by Horie and Ogawa (Ho 73) assumes an inert ^{48}Ca core with a proton hole in the $1f_{7/2}$ shell and the extra-core neutron in the 2p and $1f_{5/2}$ orbits. Agreement with the observed level scheme is poor (fig. 4.8). Fewer levels are predicted than observed and the $1/2^{-}$, $3/2^{-}$ levels around E_x =1.5 MeV are not produced. The predicted $3/2^{-}_1$ and $1/2^{-}_1$ levels are respectively 1.1 MeV and 2.1 MeV higher than observed. The spectroscopic factors for the $J^{\pi}=7/2^{-}$, $T_<$ levels populated in single-proton stripping reaction on ^{56}Fe are also calculated by Horie and Ogawa and almost the entire single-particle strength is predicted to be contained in the g.s.transition (table 4.6).

Attempts have also been made to obtain the level of spectrum of ^{57}Co on the weak as well as the intermediate

Table 4.6

Measured transition strengths from (τ,d) and (d,n) reaction compared with theory

E_x (MeV)	J^π	$(2J_f+1)C^2S$									
		a)	b)	c)	d)	e)	f)	g)	I h)	II h)	i)
g.s	$7/2^-$	1.50	0.89	1.80		1.90	1.84	5.20	1.41	1.41	1.98
1.376	$3/2^-$	1.29	0.52	1.80	1.71	1.07	1.11	1.68	1.90	1.60	
1.501	$1/2^-$	0.49	0.35	0.72	0.64	0.45	0.40	0.76	0.75	0.96	
1.758	$3/2^-$	0.23	0.13	0.30	0.35	0.20	0.16		0.86	1.09	
1.898	$7/2^-$								0.44	0.45	0.00
1.920	$5/2^-$								0.04	0.11	
2.134	$5/2^-$	0.98	1.20	2.00		1.18	1.42		3.23	3.58	
2.314	$7/2^-$	0.35	0.20	0.70		0.35			0.95	0.56	0.00
2.611	$7/2^-$								0.04	0.03	
2.731	$5/2^{-j)}$								0.29	0.20	
2.804	$3/2^{-j)}$								0.47	0.43	
2.878	$3/2^-$	0.21	0.11	0.39		0.14	0.17	0.48	0.43	0.32	

a) Present work
b) ^{56}Fe(τ,d) reaction (Ha 72)
c) ^{56}Fe(τ,d) reaction (Ro 67)
d) ^{56}Fe(τ,d) reaction (Ba 75)
e) ^{56}Fe(d,n) reaction (Ad 76)
f) ^{56}Fe(d,n) reaction (Co 69)
g) ^{56}Fe(d,n) reaction (Ok 68)
h) Shell model theory (Go 72); I and II for two different parameters values.
i) Shell model theory (Ho 73)
j) Theoretical values from Gomez (Go 72)

coupling versions of the unified model. The low-lying levels of an odd mass nucleus is given in terms of a single particle (or hole) coupled to an excited even core. The levels of ^{57}Co are thus given by the weak coupling of the $1f_{7/2}$ proton hole to the lowest 2^+ vibrational state of ^{58}Ni and a quintet of negative parity levels with spin 3/2, 5/2, 7/2, 9/2 and 11/2 will be obtained with the centred at $\sim$1.45 MeV (the energy of the lowest 2^+ state in ^{58}Ni). Such levels may be identified with the observed levels at E_x=1.758, 1.919, 1.898, 1.224 and 1.689 MeV respectively by Covello and Manfredi (Co 71). The collective nature of the levels is supported by their much larger B(E2) strengths than the single particle estimates (Co 69, Da 71) and the weak excitation in the (τ,d) and (d,n) reactions. The 1.90 MeV level has a non-stripping angular distribution (fig. 4.8) and the 1.22, 1.69 and 1.92 MeV levels are hardly visible above background. Only the 1.76 MeV level is not weak and the angular distribution leading to this level is of stripping character (fig. 4.2), which probably arises from a mixing with the single particle level of the same J-value. The limitation of the weak coupling model is obvious. The observed splitting ($\approx$0.7 MeV) of the core multiplet is also about 0.2 MeV higher than the energy of the lowest 2^+ state in ^{58}Ni, implying a mixture of states with different numbers of phonons.

The intermediate coupling model as used by Satpathy and Gujrathi (Sa 68) considers upto three phonon states of the core and in addition to the $(1f_{7/2})^{-1}$ proton orbit mentioned above, the $(1d_{3/2})^{-1}$ and $(2s)^{-1}$ proton configurations were also considered. The strength of the coupling was treated as an adjustable parameter. The quintet mentioned above, in particular the doublet nature of the $5/2^-$ and $7/2^-$ levels and of the $11/2^-$ and $3/2^-$ levels, except for a reversal in spin in the later case, is well reproduced (fig.4.8). The $J^\pi=11/2^-$ level at $E_x\approx2.5$ MeV predicted in this model may correspond to one of the high spin levels observed in the $^{57}Fe(p,n)$ reaction (Pi 73) mentioned earlier. This model fails to reproduce the $J^\pi=3/2^-$ and $1/2^-$ levels at $E_x\approx1.5$ MeV and the agreement with experiment is not satisfactory beyond $E_x\approx2.5$ MeV.

It is however, possible that some of the observed levels might be accounted for within the framework of the intermediate coupling model by including additional proton configuration like 2p and $1f_{5/2}$. This is done by Gomez (Go 72) and spacings between the excited proton configurations were taken from experiment and also from the binding energies. The collective parameters were taken from experimental data. Agreement with the experimental level scheme is considerably improved (fig.4.8). The ordering of the low-lying levels is however not correct.

The spectroscopic factors for the single-proton stripping reactions leading to ^{57}Co are calculated by Gomez for some of the strong transitions and the results are summarized in table 4.6. Excepting the g.s. the agreement with the measured values given by (τ,d) and (d,n) reactions is far from satisfactory. The levels at 2.731 and 2.804 MeV predicted to carry reasonable single-particle strengths (table 4.6) are not at all excited in any proton stripping reaction.

In the above weak and intermediate coupling models the core excitation is assumed to follow a pure harmonic vibration. The intermediate coupling model used by Stewart et al.(St 71) considers the phonon states built on an anharmonic vibration. The pairing effects are not ignored and the quasi-particle effects have further been introduced. Quite a significant improvement in the level spectrum is thereby achieved (Fig.4.8); all the level upto E_x~2.3 MeV are reasonably well reproduced.

The above discussions refer to the negative-parity levels. The positive-parity level are calculated only by Satpathy and Gujrathi (Sa 68) and two $1/2^+$ levels (E_x=3.011 and 5.338 MeV) and four $3/2^+$ levels (E_x=3.352, 4.685, 5.448 and 6.416 MeV) are predicted, arising from the 2s and $1d_{3/2}$ proton-hole states, respectively. The observed $J^\pi=1/2^+$ level at E_x=2.99 MeV is clearly the lowest $1/2^+$ level given by

Satpathy and Gujrathi. The difficulty arises with the other $2s_{1/2}$ level. In a previous $^{56}Fe(\tau,d)$ experiment Hardie et al. (Ha 72) observed an $\ell_p=0$ transition to a level close in energy to this predicted level. Two such levels are identified in the present work with an $\ell_p = 0$ stripping angular distribution (fig. 4.4) fairly close to the level under discussion, and the small cross sections are consistent with their identification as 2s hole states. The $1/2^+$ level, however, is not observed in the $^{58}Ni(t,\alpha)$ reaction (Bl 66), although the spectroscopic factor for this level is calculated to be about half that for the $1/2^+_1$ level (Sa 68). This identification of the predicted $1/2^+_2$ level thus remains undecided. Five $\ell_p=2$ transitions (including two doubtful ones) were observed by Blair and Armstrong (Bl 66) in the $^{58}Ni(t,\alpha)$ reaction, some of which may correspond to some of the $3/2^+$ levels given by the calculation of Satpathy and Gujrathi.

In the semimicroscopic model for three nucleon transfer, the transfer of dineutron was taken into account by Smit et al. (Sm 79) by making full use of the collective nature of this transfer and the structure amplitude is factored into two neutron and a proton amplitude. The splitting of multiplets is reproduced by choosing the quadrupole interaction strength. The levels above $\sim$2 MeV is assumed as due to particle-hole

configurations.

The levels at 1.12 MeV ($J^{\pi}=9/2^{-}$), 1.39 MeV ($J^{\pi}=3/2^{-}$), 1.60 MeV ($J^{\pi}=7/2^{-}$), 1.75 MeV ($J^{\pi}=5/2^{-}$), 3.13 MeV ($J^{\pi}=1/2^{+}$), and 3.88 MeV ($J^{\pi}=3/2^{+}$) of the present $^{56}Fe(^{3}He,d)$ reaction are well reproduced by this model. The levels at 1.32 MeV ($J^{\pi}=11/2^{-}$) and 2.98 MeV ($J^{\pi}=7/2^{-}$) of (p,α) reaction by Smit et al. (Sm 79) are well accounted for by this model.

CHAPTER 5

REACTION $^{45}Sc(\tau,d)$

5.1 Introduction

The ^{46}Ti nucleus is assumed as protons and neutrons in excess of 20 belonging to pure $(1f_{7/2})^n$ configurations. The theoretical work is carried out on the assumption that these $1f_{7/2}$ nucleons outside the core are in interaction and the nuclear spectra are due entirely of states of pure configuration by this residual nucleon-nucleon interaction.

The energy levels in ^{46}Ti have been measured from a variety of nuclear reactions and compiled by Lederer and Shirley (Le 78) and Auble (Au 78). The excitation energies determined from a previous $^{45}Sc(\tau,d)$ reaction (Br 68) are systematically larger than those of the complications and also those given by a recent high resolution gamma ray study (Dr 78) following the (α,n) reaction on ^{43}Ca. It was therefore thought worthwhile to redetermine the energy levels in ^{46}Ti so as to make a meaningful comparison with the adopted levels (Le 78,Au 78) as well as with those levels observed in gamma ray studies (Dr 78,De 73,Fo 76).

Yntema (Yn 62) studied (d,t) reaction on ^{47}Ti at 21.4 MeV and identified a few levels up to E_x= 5.84 MeV.

Kashy et al. (Ka 64) studied the $^{47}Ti(p,d)$ reaction at 17 MeV. They measured ℓ_p transfer and transition strengths from DWBA calculation.

In the study of the $^{46}Ti(p,p')$ reaction (Mo 66, Pe 68, Le 68, Ga 71) the level structure of ^{46}Ti have been investigated upto $E_x \sim 4.316$ MeV and J^π assignments of the low-lying levels have been made.

Maher et al. (Ma 67) studied the (O^{16}, N^{15}) reaction on several nuclei including ^{45}Sc and observed a few levels upto $E_x = 5.187$ MeV.

The $^{47}Ti(^3He,\alpha)$ reaction was studied by Broman and Pullen (Br 68) at 15 MeV covering an excitation of 10.943 MeV.

Properties of the levels of ^{46}Ti have been investigated by Priest et al. (Pr 69) through the $^{45}Sc(\alpha,t)$ reaction covering an excitation energy upto $E_x \sim 5.967$ MeV and the spectroscopic factors were extracted.

Faraggi et al. (Fa 71) investigated the $^{42}Ca(O^{16},C^{12})$ reaction and identified a few levels upto $E_x = 7.26$ MeV.

Rapaport et al. (Ra 73) and Kong et al. (Ko 72) studied

the properties of ^{46}Ti through (p,t) reaction. Rapaport et al. measured transition strengths and J^{π}-assignments were obtained from both the studies.

The present work is concerned with the (τ,d) reaction on ^{45}Sc at E_{τ}=16 MeV. This reaction was previously studied by Broman and Pullen (Br 68) at E_{τ}=15 MeV, Barnard and Jones (Ba 68) at E_{τ}=38 MeV and Ohmura et al. (Oh 68) at E_{τ}=24 MeV covering angular distribution measurements respectively upto $E_x \sim 7.6$, 3.9 and 5.6 MeV. The experiment of Broman and Pullen was later extended by Broman and Larsson (Br 71) to include excitation beyond 7.6 MeV using the same set of nuclear plates. There are several discrepancies in the assignment of orbital angular momentum transfer in the different measurements (see table 5.3); more serious is the systematically large difference in the spectroscopic factors, varying by a factor of 2 even for strong transitions, given by Broman and Pullen on the one hand and Barnard and Jones, and Ohmura et al.on the other, eventhough the error in the absolute cross sections is quoted as less than 40% in the different measurements. In the $^{45}Sc(\alpha,t)$ reaction studied by Priest and Vincent, the relative spectroscopic strengths were extracted, while another proton stripping reaction (^{16}O, ^{15}N) by Maher et al. was naturally concerned more with reaction mechanism itself than with the spectroscopic

factors, eventhough absolute cross section was measured. The present work was therefore undertaken with an energy resolution better than in previous experiments and special care was taken in measuring the absolute cross section values. Properties of most of the levels upto $E_x \sim 9.9$ MeV are given.

5.2 Experimental Procedure

The plates exposed with products of $^{45}Sc(\tau,d)$ reaction were scanned at the Nuclear Physics Laboratory, University of Dacca, Dacca. A typical spectrum at 26.25^{o} is shown in fig. 5.1. Each peak is labeled with a number which corresponds to the level numbering of table 5.3. Contaminant groups are labeled using the corresponding level energy in the residual nuclei. Because of the uncertainty in the spectrograph calibration at the high magnetic field used in the present experiment ($B \sim 13.57$ K-gauss), an internal calibration was made using least squares parabolic fits to several well known levels in ^{46}Ti namely (2.011, 3.298, 3.936, 4.526 and 5.554), and ground state of the $^{12}C(\tau,d)^{13}$ reaction. The later provided a useful calibration point in a region of the plates where density of the levels is high.

Above levels are shown underlined in table 5.3. The

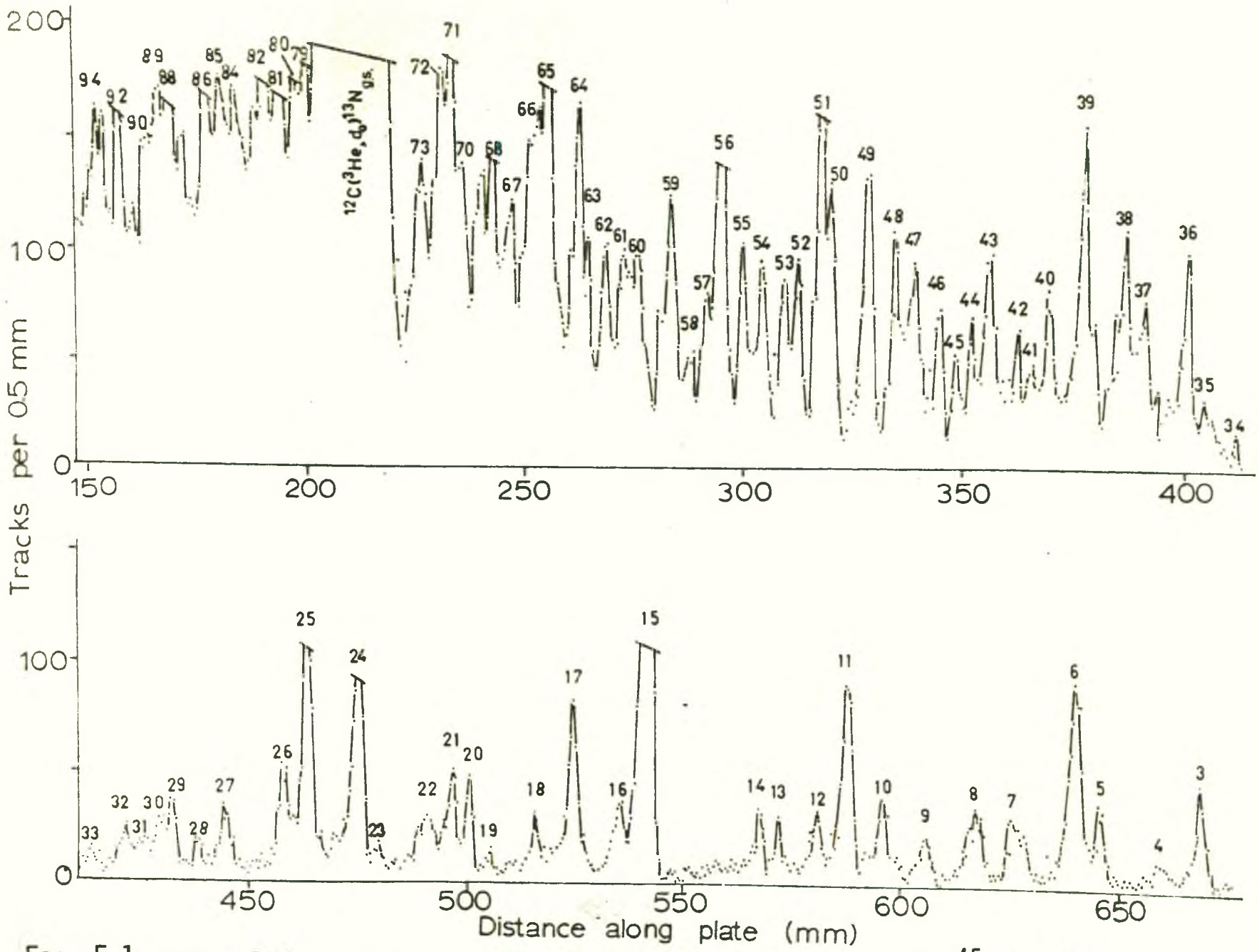

FIG. 5.1. Part of the energy spectrum of deuterons arising from the $^{45}Sc(\tau,d)$ reaction at 26.25^{o} showing the region of high density.

values of a_o, a_1, a_2 for each channel in two regions are given in table 5.1. The overall energy resolution (FWHM) was found to be ~22 keV. Levels upto E_x ~ 9.9 MeV have been identified and angular distributions have been measured for most of the levels. The effective target thickness was found to be 53 $\mu gm.cm^{-2}$. The total uncertainty in the absolute value of the (τ,d) cross section, resulting mainly from the target thickness, scanning and background subtraction, is less than 15%.

5.3 DWBA Analysis

The angular distribution data were analyzed in terms of the DWBA theory of direct stripping reaction in the local zero range approximation. The calculations were carried out by Professor H.M.Sen Gupta at Oxford using the code DWUCK due to Kunz with the IBM 360/195 Computer of Rutherford High Energy Laboratory.

The optical model potential used was of the same form as that in chapter 4.(Equ 4.3.1). The optical model potential was of the standard Woods-Saxon form for the ^{3}He-potential and real part of the deuteron potential. The bound state wave function was generated by using the real potential of the form

$$V\, f(r,r_o,a) + \frac{V\lambda}{45.2}\,\frac{1}{r}\,\frac{d}{dr}\, f\,(r,\, r_o,\, a)\; \underline{\ell}.\underline{s}$$

where $f(r,r_o,a) = \left(1+\exp \frac{r-r_o A^{1/3}}{a}\right)^{-1}$ is the form factor and $\lambda = 25$.

Table 5.1

Constants of least squares fit for $^{45}Sc(\tau,d)$ reaction

Region	Channel	a_o	a_1	a_2
1	2	12.777	-42.179	23.409
	3	12.851	-43.859	27.250
	4	12.649	-42.837	24.515
	5	12.638	-43.690	26.186
2	2	11.146	-17.348	-71.548
	3	11.321	-21.286	-56.930
	4	11.051	-17.579	-76.860
	5	11.082	-19.156	-70.900

The strength of the potential was adjusted, with r_o=1.25 fm, a=0.65 and Coulomb radius parameter r_o=1.3 fm, so as to give the correct binding energy of the transferred proton.

The potential parameters used in the DWBA calculations are shown in table 5.2. ref.(Oh 68, Ba 66, Ch 74). This combination approximately satisfies the condition 4.3.1 as given in chapter 4 (sect.4.3). The spectroscopic transition strengths $(2J_f+1)C^2S/2J_i+1)$ were obtained by normalising the computed cross section $\sigma_{DW}(\theta)$ to the measured value $\sigma_{Exp}(\theta)$ through the relation 4.3.2. in chapter 4 (sect.4.3). The normalization constant N=4.42 was obtained from the ref.(Ba 66).

5.4 Results and Discussions

A large numbers of levels, including a few analogues, have been observed up to $E_x \sim$ 9.9 MeV. The angular distributions have been measured for all the groups and transition strengths extracted for many of them. The results are summarised in table 5.3.

Typical examples of the DWBA fits to the measured angular distributions are shown in figs. 5.2-5.7. The levels for which the cross sections at the first two forward angles are missing, either due to the presence of a contaminant or

Table 5.2

Optical Model Parameters

Particle	V_o (MeV)	r_o (fm)	a (fm)	W_o (MeV)	$4W_D$ (MeV)	r_I (fm)	a_I (fm)	$V_{s.o.}$ (MeV)	$r_{s.o.}$ (fm)	$a_{s.o.}$ (fm)	r_C (fm)	Ref.
^{3}He	139.0	1.08	0.80	12.3		1.743	0.721				1.4	(Oh 68), (Ba 66)
d	94.8	1.12	0.79		61.2	1.32	0.74	6.6	0.90	1.16	1.3	(Ch 74)
p	a)	1.25	0.65					λ=25			1.3	

a) adjusted to reproduce the binding energy

to an emulsion disturbance, are excluded from the DWBA analysis ; these are marked n.a. in table 5.3. A few levels do not have angular distributions characteristics of a direct stripping process. Such levels are denoted by n.s. in table. Also included in the table for a comparison are the results from previous (τ,d) reactions on ^{45}Sc(Br 68, Ba 68, Oh 68). The transition strengths in all these studies as well as in the present work are extracted using the same normalization constant (N=4.42) and should therefore be directly comparable (Columns 9-12).

5.4.1 The angular distribution and transition strengths

5.4.1.1 The ℓ=1 and 3 transitions

The 1f and 2p single particle strength are heavily fragmented and the 2p strength is more or less evenly distributed over the entire range of excitation energy studied, while a good amount of the 1f shell model strength is carried by a few low lying levels (table 5.3, fig.5.8). A number of angular distributions required a mixture of ℓ=1 and 3 transfers signifying a high degree of mixing of the 1f and 2p shell model configurations. Such a mixture was considered during the DWBA analysis, only when the quality of a fit was thereby improved significantly and the ℓ=3 components had an appreciable

Table 5.3

Summary of the level properties ^{46}Ti

Level	E_x(MeV)		$\sigma_{max}(\theta)$ (mb/sr)	ℓ_p transfer				$(2J_f+1)C^2S/(2J_i+1)$			
	a)	b)		a)	c)	d)	e)	a)	c)	d)	e)
0	0	0	0.11	3	3	3	3	0.26	0.53	0.27	0.17
1	0.890	0.891	0.76	1+3	1+3	1+3	1+3	0.082+0.29	0.25+0.96	0.06+0.28	0.10+0.34
2	2.011	2.010	0.68	1+3	1+3	1+3	1+3	0.078+0.28	0.20±0.72	0.04+0.22	0.09+0.25
3	2.960	2.962	0.14	3	3	3	1+3	0.29	0.50	0.22	0.04+0.06
4	3.060	3.059	0.50	2	2		(1+3)	0.054	0.09		(0.12+0.09)
5	3.234	3.263	0.081	1+3	1+3	3	(1)	0.012+0.15	0.01+0.24	0.58	(0.07)
6	3.298	3.299	0.29	3	3		3	0.54	0.90		0.64
7	3.441	3.438	0.12	2	2	3	(1+2)	0.11	0.27	0.16	(0.006+0.01)
8	3.573	3.572	0.12	3	1+3		1+3	0.22	0.02+0.36		0.008+0.24
9	3.726	3.724	0.26	1	1		1+(2)	0.024	0.06		0.02+(0.07)
10	3.842	3.842	0.26	1+3	1+3	1+3	1+2	0.021+0.12	0.06+0.31	0.09+0.36	0.02+0.22
11	3.930	3.930	0.49	1+3	1+3		(1+3)	0.037+0.28	0.09+0.57		(0.05+0.36)
12	4.031	4.021	0.38	1	1		1	0.034	0.08		0.04

Table 5.3 (continued)

Level	E_x(MeV)		$\sigma_{max}(\theta)$ (mb/sr)	ℓ_p transfer				$(2J_f+1)C^2S/(2J_i+1)$			
	a)	b)		a)	c)	d)	e)	a)	c)	d)	e)
13	4.136	4.130	0.12	1+3	1+3			0.009+0.037	0.02+0.14		
14	4.199	4.206	0.065	3	3		(0)+3	0.12	0.23		(0.02)+0.20
		4.394			1				0.004		
15	4.526	4.524	0.655	3	3		(0)+3	1.04	2.11		(0.04)+0.84
16	4.617	4.620	0.25	1+3	1			0.022+0.067	0.06		
17	4.719	4.723	0.29	1+3	1+3		(0)+3	0.025+0.28	0.03+0.59		(0.01)+0.39
18	4.845	4.846	0.11	1+3	1+3		1+3	0.008+0.062	0.03+0.08		0.03 +0.05
19	4.966	4.950	0.10	n.s	1+3				0.01+0.05		
20	5.036	5.045	0.12	0	0			0.028	0.06		
21	5.094	5.098	0.39	1	1		1+3	0.033	0.13		0.08 +0.19
22	5.167	5.187	0.16	1+3	1+3			0.012+0.075	0.02+0.17		
23	5.317	5.326	0.29	1	1			0.25	0.02		
24	5.379	5.383	0.39	1+3	1+3		1+3	0.019+0.31	0.07+0.40		0.09 +0.22
25	5.554	5.557	0.60	1+3	1+3		1+3	0.045+0.21	0.14+0.41		0.08 +0.38

Table 5.3 (continued)

Level	E_x(MeV)		$\sigma_{max}(\theta)$ (mb/sr)	ℓ_p transfer				$(2J_f+1)C^2S/(2J_i+1)$			
	a)	b)		a)	c)	d)	e)	a)	c)	d)	e)
26	5.618	5.610	0.13	1+3	1			0.005+0.12	0.06		
27	5.811	5.816	0.14	0	0			0.030	0.06		
28	5.897	5.899	0.11	1+3	1+3			0.006+0.031	0.02+0.04		
29	5.980	5.982	0.19	1+3	1+3			0.012+0.65	0.02+0.31		
30	6.021	6.029	0.19	1	1			0.015	0.05		
31	6.094	6.088	0.20	n.a.	0				0.03		
32	6.140	6.141	0.35	n.a.	1+3				0.01+0.08		
33	6.217	6.214	0.20	n.a.	0				0.01		
34	6.251	6.246	0.23	n a.							
35	6.337	6.335	0.19	2	1			0.10	0.06		
36	6.424	6.427	1.01	1	1			0.070	0.16		
37	6.550	6.556	0.76	1	1+3			0.059	0.09+0.22		
38	6.616	6.623	0.60	1	1			0.046	0.03		
39	6.742	6.744	0.85	1+3	1+3			0.052+0.25	0.13+0.51		
40	6.851	6.856	0.14	1+3	1+3			0.012+0.041	0.02+0.33		

Table 5.3 (continued)

Level	E_x(MeV)		$\sigma_{max}(\theta)$	ℓ_p transfer				$(2J_f+1)C^2S/(2J_i+1)$			
	a)	b)	(mb/sr)	a)	c)	d)	e)	a)	c)	d)	e)
41	6.899	6.897	0.44	1	1			0.030	0.04		
42	6.974	6.979	0.16	n.a.	1+3				0.02+0.14		
43	7.041	7.049	0.36	1+3	1+3			0.031+0.18	0.09+0.18		
44	7.101	7.101	0.36	1	1			0.032	0.08		
45	7.147	7.147	0.33	1	1			0.032	0.06		
46	7.201	7.204	0.75	1	1+3			0.044	0.09+0.20		
47	7.288	7.294	0.22	1+3	1			0.007+0.12	0.06		
48	7.347	7.349	0.89	1	1			0.066	0.16		
49	7.429	7.433	0.92	1	1			0.063	0.25		
50	7.558	7.565	0.76	1	1			0.052	0.42		
51	7.584		1.38	1				0.096			
52	7.611	7.665	0.57	1	1			0.040	0.15		
53	7.712	7.707	0.56	1				0.38			
54	7.780	7.764	1.02	1	1			0.066	0.16		
55	7.849	7.849	0.72	1	1			0.045	0.10		

Table 5.3 (continued)

Level	E_x(MeV)		$\sigma_{max}(\theta)$ (mb/sr)	ℓ_p transfer				$(2J_f+1)C^2S/(2J_i+1)$			
	a)	b)		a)	c)	d)	e)	a)	c)	d)	e)
56	7.917	7.920	1.30	1	1			0.094	0.30		
57	7.979	7.971	0.41	1				0.029			
58	8.038	8.026	0.16	n.s.							
59	8.088	8.090	0.70	1	1			0.052	0.14		
60	8.182	8.115	0.92	1	1			0.063	0.15		
61	8.228	8.230	0.78	1				0.054			
62	8.293	8.303	0.53	1	1			0.042	0.05		
63	8.346		0.64	1				0.044			
64	8.384	8.402	0.51	1+3	1			0.024+0.18	0.13		
65	8.467	8.466	0.76	1+3	1			0.044+0.17	0.03		
66	8.530	8.513	1.77	1				0.12			
67	8.574	8.552	0.54	1+3	1			0.033+0.062	0.09		
68	8.621	8.625	1.14	1	1			0.083	0.06		
69	8.662	8.673	0.24	1	1			0.028	0.11		
70	8.709		0.19	1				0.026			

Table 5.3 (continued)

Level	E_x(MeV)		$\sigma_{max}(\theta)$ (mb/sr)	ℓ_p transfer				$(2J_f+1)C^2S/(2J_i+1)$			
	a)	b)		a)	c)	d)	e)	a)	c)	d)	e)
71	8.761		1.32	1				0.16			
72	8.808	8.797	1.18	1	1			0.10	0.029		
73	8.860	8.884	2.76	1	1			0.21	0.10		
74	8.940	8.945	1.29	1	1			0.10	0.09		
75	9.984	9.019	1.52	1	1			0.13	0.12		
76	9.070	9.053	0.68	1				0.055			
77	9.111	9.124	1.34	1+3	1			0.10+0.18	0.06		
78	9.141		0.31	n.s.							
79	9.176	9.197	0.35	3	3			0.28	1.07		
80	9.205	9.242	0.94	1				0.064			
81	9.253		1.00	1				0.082			
82	9.304		0.82	1				0.066			
83	9.345		0.40	1				0.030			
84	9.385	9.418	0.50	1	1			0.041	0.11		
85	9.426		0.34	3				0.29			

Table 5.3 (continued)

Level	E_x(MeV)		$\sigma_{max}(\theta)$ (mb/sr)	ℓ_p transfer				$(2J_f+1)C^2S/(2J_i+1)$			
	a)	b)		a)	c)	d)	e)	a)	c)	d)	e)
86	9.474	9.472	1.23	1	1			0.085	0.11		
87	9.519		0.30	2				0.20			
88	9.572	9.608	0.41	3				0.28			
89	9.618		0.43	1				0.040			
90	9.649	9.670	0.52	1				0.049			
91	9.682		0.21	n.s.							
92	9.718	9.741	0.58	2				0.058			
93	9.761		0.41	n.a.							
94	9.790	9.816	0.38	n.a.							
		9.847									
95	9.864	9.887	0.42	n.a.							

The estimated errors in energies in present work are ± keV. n.s. Non stripping angular distribution. n.a. Data not analysed.

a) Present work.

b) Refs.(Le 78, Au 78, Dr 78)

c) The (τ,d) reaction at E_τ=15 MeV (Br 68); ℓ-values and transition strengths above E_x=7.6 MeV are from ref.(Br 71)

d) The (τ,d) reaction E_τ=37.7 MeV (Ba 68)

e) The (τ,d) reaction at E_τ=24.3 MeV (Oh 68)

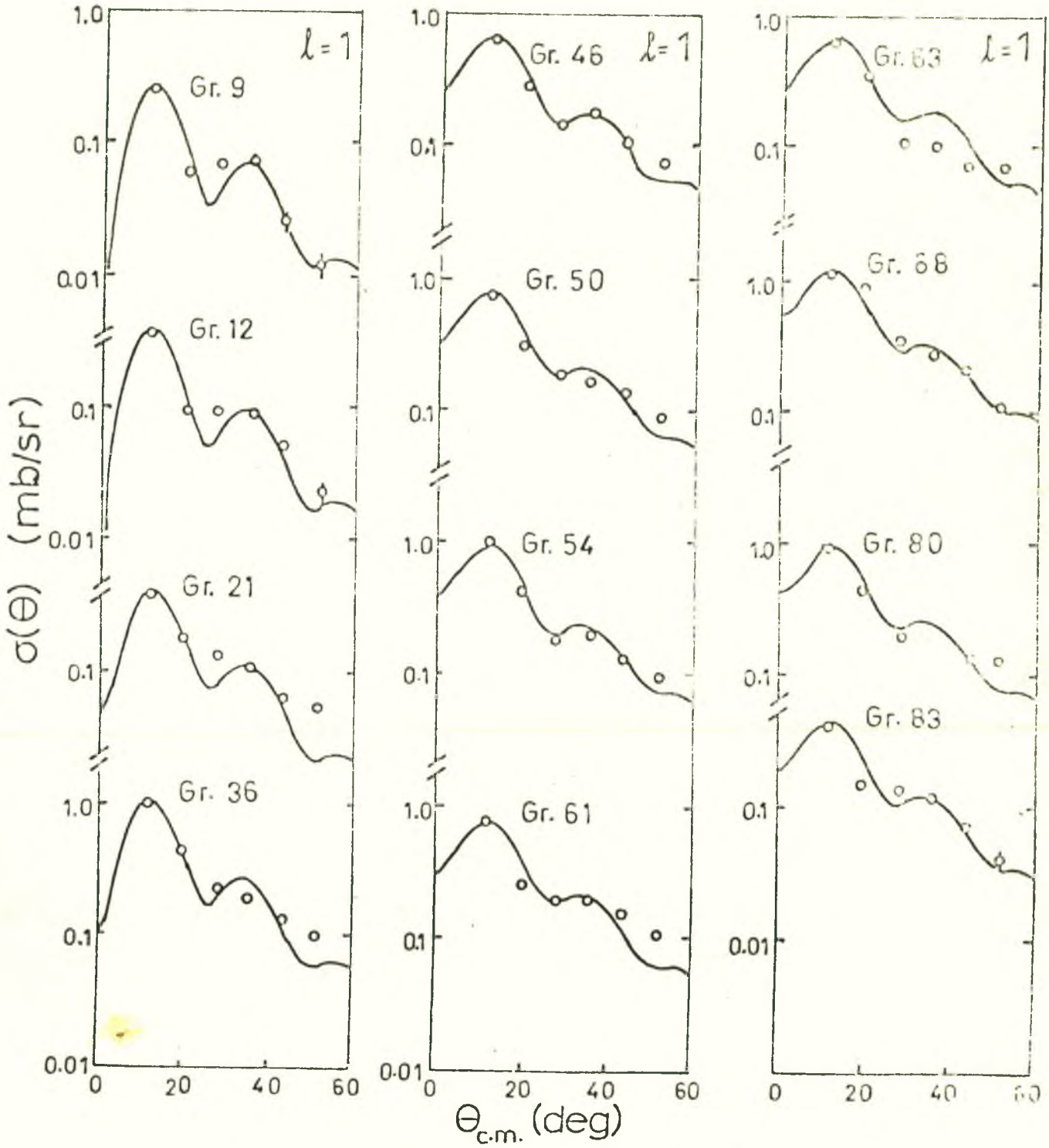

FIG. 5.2. Measured angular distributions fitted with ℓ = 1 DWBA curves.

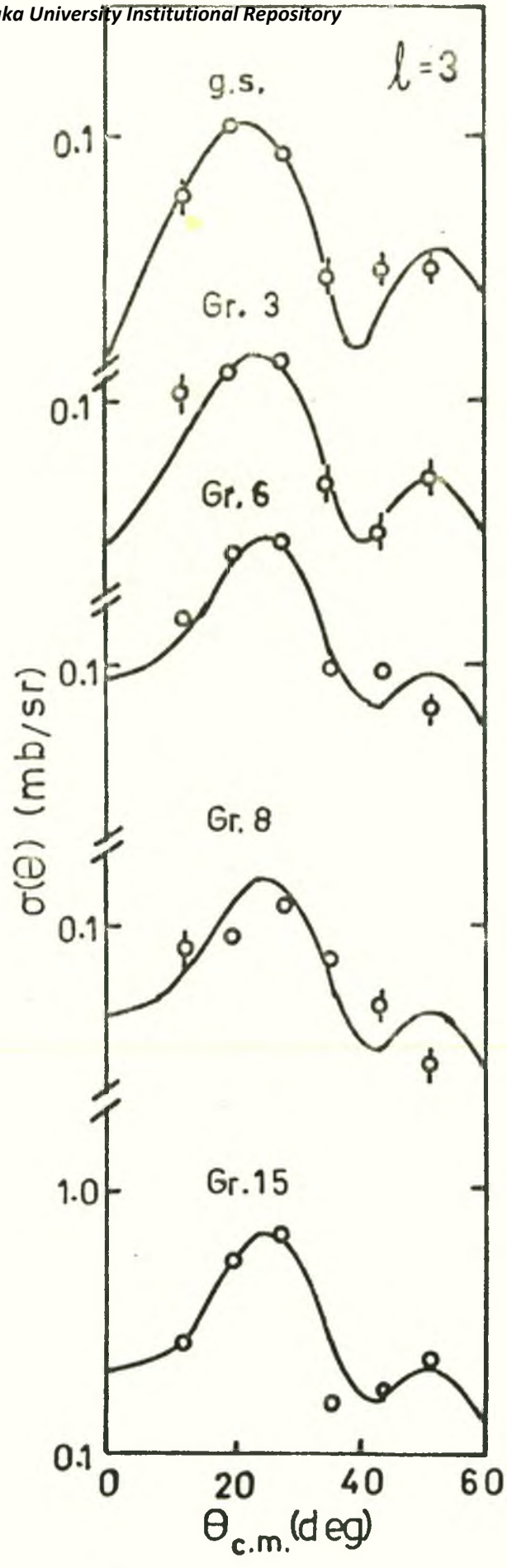

FIG. 5.3. Measured angular distributions fitted with $\ell = 3$ DWBA curves.

contribution. A few examples are given in fig. 5.4, where fits from individual ℓ-value are also shown in some cases.

The transition strengths in table 5.3 were deduced by assuming that all ℓ=1 and 3 transitions populate respectively the $2p_{3/2}$ and $1f_{7/2}$ shell model states. The summed transition strengths so obtained are shown in table 5.4 for comparison with the shell model values. The $T_<$ component of the total 1f strength thus becomes 6.3, as against the single-particle limit 10.5 for $1f_{7/2}$+ $1f_{5/2}$ shells. It is possible that some of the ℓ=3 transitions actually correspond to the $1f_{5/2}$ shell rather than the assumed $1f_{7/2}$ shell, for which the spectroscopic strength increases by 60% as found by the DWBA calculations and the summed strength comes closer to the shell model value. For 2p transitions the observed strength is 3.7, being fairly close to the expected $T_<$ component of the total $2p_{3/2}$ + $2p_{1/2}$ strength of 4.5. The possibility of excitation of $2p_{1/2}$ orbital cannot be totally ruled out, in which case the strength increases by about 20% and the summed 2p strength becomes further close to the expected limit. It could then be assumed that most of the $T_<$ component of the 1f and 2p shell model strengths have been reached within the excitation ($E_x \sim 10$ MeV) covered in the present work.

Broman and Pullen (Br 68) calculated the 1f and 2p

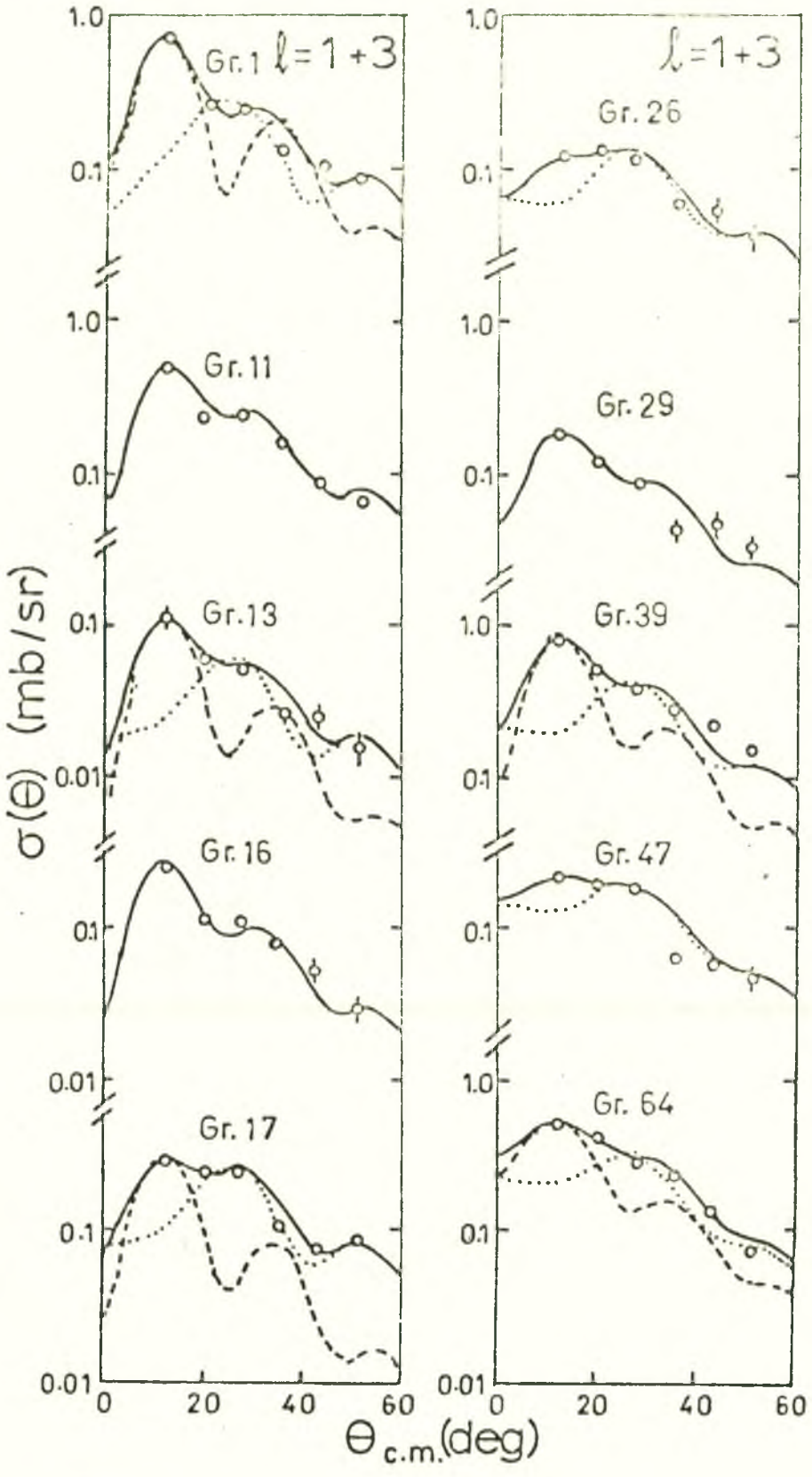

FIG. 5.4. Measured angular distributions fitted with ℓ=1+3 DWBA curves: solid line, ℓ=1+3; broken line, ℓ=1; dotted line, ℓ=3.

Table 5.4

Results of the sum rule analysis for the proton $T_<$ states in ^{46}Ti

Single particle state	$\Sigma(2J_f+1)C^2S/(2J_i+1)$			
	Shell model limit		a)	b)
$1f_{7/2}$	6	10.5	6.3	11.3
$1f_{5/2}$	4.5			
$2p_{3/2}$	3	4.5	3.7	4.9
$2p_{1/2}$	1.5			

The strengths are deduced by assuming that all ℓ_p = 1 and 3 transitions belong to the $2p_{3/2}$ and $1f_{7/2}$ shell respectively; the possibility of excitation of $1f_{5/2}$ and $2p_{1/2}$ shells increases the strengths.

a) Present work

b) Ref.(Br 68)

strength assuming $1f_{7/2}$ and $2p_{3/2}$ states and obtained 11.3 and 4.9 closer to the single-particle limits. A similar increase in their results of spectroscopic strength would also be expected if $2p_{1/2}$ and $1f_{5/2}$ configurations are considered in the ℓ=1 and 3 transitions and in that case the agreement of the observed values with single-particle limit may not be that good.

5.4.1.2 The ℓ=0 and 2 transitions

A few angular distributions were fitted with ℓ=0 and 2 transfers (figs.5.5,5.6). The transitions to the negative parity states are a result of the $(2s_{1/2})^{-2}$ $(1f_{7/2})$ and $(1d_{3/2})^{-2}$ $(1f_{7/2})$ configurations in ^{45}Sc, i.e. the negative parity states arise from the $(2s_{1/2})^{-1}$ $(1f_{7/2})$ two-proton configurations in ^{46}Ti. The negative parity states thus have the characteristics of a deformed rotational band and based on the energy spacings, the characteristic cascade and crossover transitions and an enhanced E2 transition, the levels at E_x= 3.059, 3.442, 3.853, 4.663, 5.198 and 6.150 MeV with respective J^{π}= 3^-, 4^-, (5^-), (6^-), (7^-) and (8^-) have been identified in the ^{43}Ca$(\alpha,n\gamma)$ reaction (Dr 78) as the members of a rotational band. It is therefore possible that the negative parity levels populated in the (τ,d) reaction have a contribution from a non-single

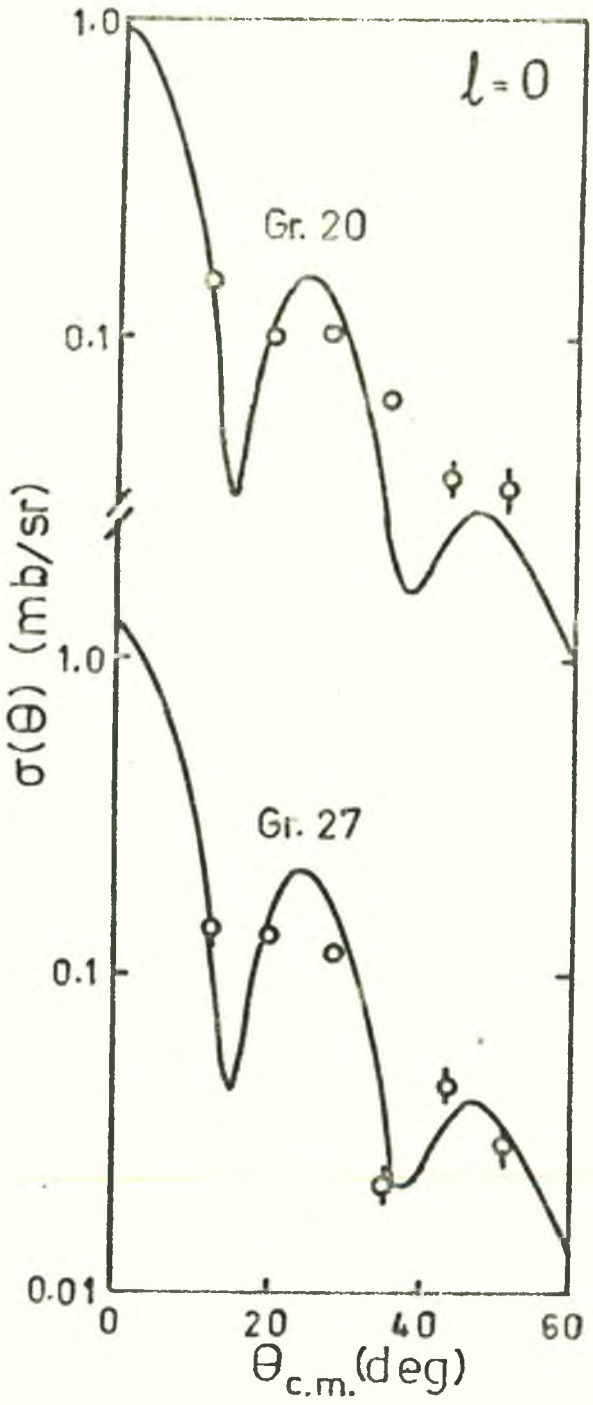

FIG. 5.5. Measured angular distributions fitted with $\ell = 0$ DWBA curves.

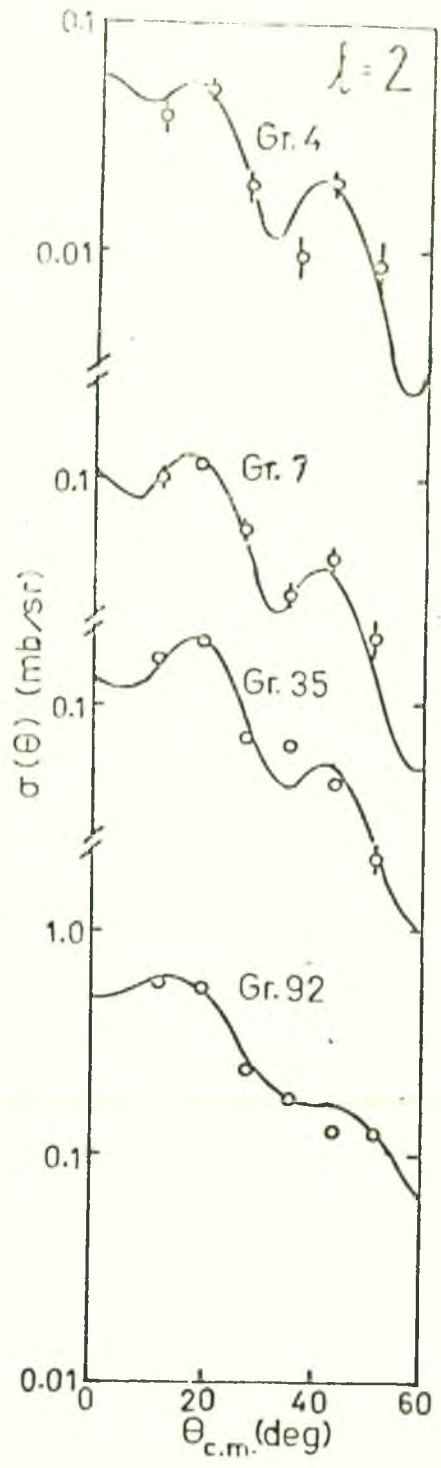

FIG. 5.6. Measured angular distribution fitted with ℓ=2 DWBA curves.

step process. In fact the measured angular distributions for ℓ=0 transitions (fig. 5.5) do not follow the detailed shape of the single-step DWBA curve and thus in view of the limited data in the present experiment the contribution from a multi-step process cannot be ruled out. The ℓ=0 transfers may be considered in view of the negative parity of the two levels.

The levels at 3.059 and 3.44 MeV have contradictory ℓ_p-assignment in previous $^{45}Sc(\tau,d)$ experiments (table 5.3). The present experiment in agreement with Broman and Pullen (Br 68) assigns ℓ_p=2 to both these levels. This ℓ_p-value is consistent with the negative parity of these levels clearly given by the life-time measurements in the $^{43}Ca(\alpha,n\gamma)$ and $^{32}S(^{16}O,2p\gamma)$ reactions (Dr 78,De 73). These levels as mentioned above are the lowest two members of the negative parity hand in ^{46}Ti. No other member of the band is populated in the (τ,d) reaction.

5.4.2 Isobaric Analogue States

A few low-lying levels is ^{46}Sc are fairly strongly excited in (d,p) reaction on ^{45}Sc and it would be expected that the corresponding analogues in ^{46}Ti lie above E_x~9 MeV. On the basis of relative level spacings and the consistency between the ℓ_p-transfer in (τ,d) reaction and ℓ_n-transfer

in (d,p) reaction, four levels, namely 9.176, 9.426, 9.474 and 9.572 MeV, have been identified as analogues. The results are summarized in table 5.5 for a comparison with the levels in the ^{45}Sc(d,p) reaction (Ra 66, Ro 81). There is a reasonable resemblance between the transition strength given by the present (τ,d) work and the (d,p) work of ref. (Ro 81). It may be mentioned that level at 9.250 MeV was previously identified as the analogue of the first excited level of ^{46}Sc (Ra 66, Ro 81). The level in the present experiment is populated with angular distribution typical of ℓ_p=1 transfer (fig. 5.2) rather than ℓ_p=3 expected from the corresponding (d,p) reaction. Eventhough the background in the region of the plate where the group lies is relatively high, repeated scans yielded a consistent set of cross section data, never differing by more than 10% among different scannings. It is surprising then that the analogue of a very strong group, found in a previous (τ,d) work (Br 71), is missing in the present experiment. There is no evidence of an ℓ_p=1+3 mixture in this angular distributions as found in many other distributions (fig. 5.7 and table 5.3).

5.5 Level Spectrum of ^{46}Ti

The level spectrum of ^{46}Ti has been calculated by several authors (Oh 68, Pr 69, Ku 78) on the basis of the McCullen-

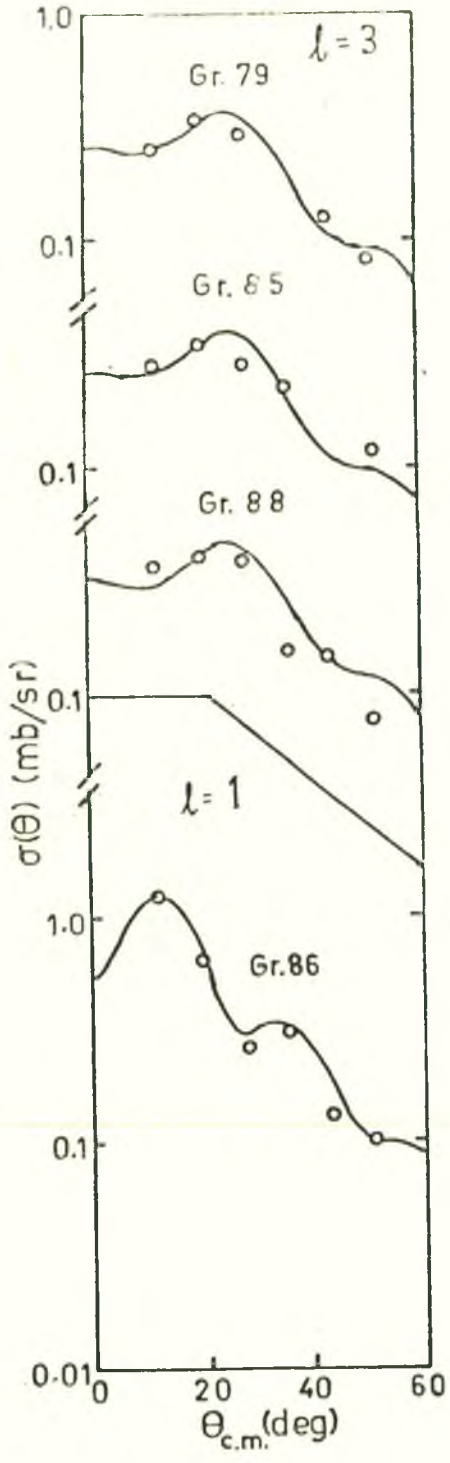

FIG. 5.7. Measured angular distribution for analogue states.

Table 5.5

Summary of the results on the isobaric analogue states in ^{46}Ti

$^{45}Sc(\tau,d)\ ^{46}Ti$ a)				$^{45}Sc(d,p)\ ^{46}Sc$						ΔE_c (MeV)
E_x^A (Mev)	$E_x^{b)}$ (MeV)	ℓ_p	$(2J_f+1)C^2S$	E_x^P (MeV)	ℓ_n		$(2J_f+1)C^2S$		J^π	
					c)	d)	c)	d)		
9.176	0	3	2.24	0	3	3	4.64	2.88	4^+	7.591
9.426	0.250	3	2.32	0.228	3	3	4.96	2.86	3^+	7.613
9.474	0.298	1	0.68	0.279	(1)	1+3	(0.80)	0.44 e)	5^+	7.610
9.572	0.396	3	2.24	0.444	3	3	2.48	1.60	2^+	7.643

a) Present work.

b) Excitation in '^{46}Sc' obtained with the 9.176 MeV level as the ground state analogue.

c) Ref. (Ra 66)

d) Ref. (Ro 81)

e) The strengths of the $\ell_n = 1$ component.

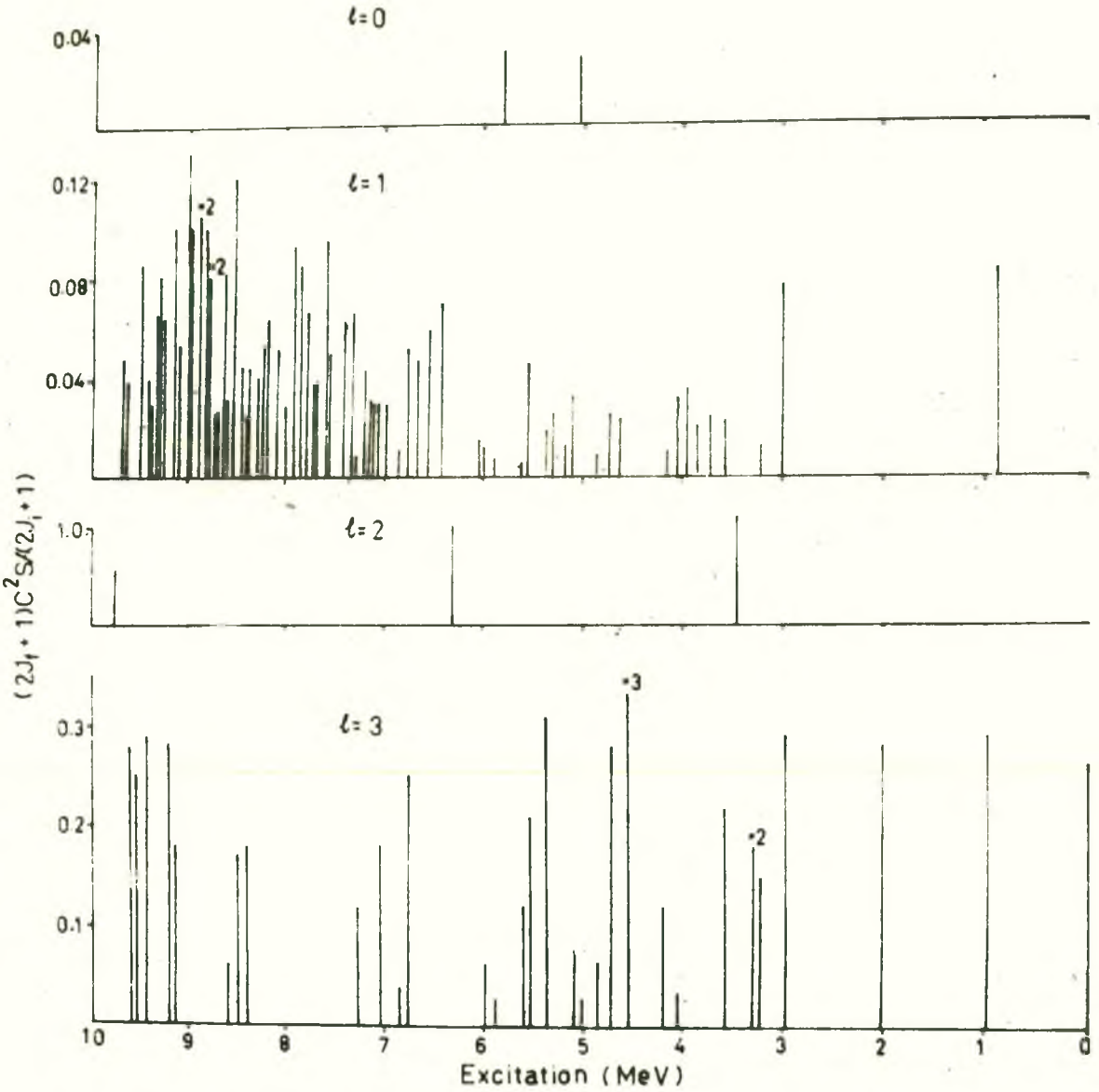

FIG. 5.8. The spectral distributions of single-particle strengths.

Bayman-Zamick (MBZ) model (Mc 64). The spectroscopic strengths relevant to the ℓ_p=3 transitions in the ^{45}Sc(τ,d) ^{46}Ti reactions have also been calculated (Oh 68, Pr 69) within the framework of the model.

The MBZ model starts with a closed ^{40}Ca-core and the states are built on the pure $(1f_{7/2})^n$ configurations. Furthermore the two-body residual interaction is assumed to be independent of the number of particles in the $f_{7/2}$ orbit. The different calculations differ from one another only in the details of the interaction.

The levels in ^{46}Ti up to E_x=5 MeV which are excited in the present investigation with ℓ_p=3 character (table 5.3) are shown in solid lines in fig. 5.9 for a comparison with the predictions of the MBZ model (Pr 69, Ku 78); also included by dotted lines are the other positive parity levels that are known to exist in this excitation region. The J^π-values of the most of the low-lying levels in ^{46}Ti are established on a firm basis (see a discussion by Dracoulis et al. Dr 78), but a definite correspondence between theory and experiment can be made to only a few of them. A comparison of the transition strengths for such levels given by theory (Pr 69) and all (τ,d) experiments (present work and refs. Br 68, Ba 68, Oh 68) is made in fig. 5.10. It is observed that the strengths given by

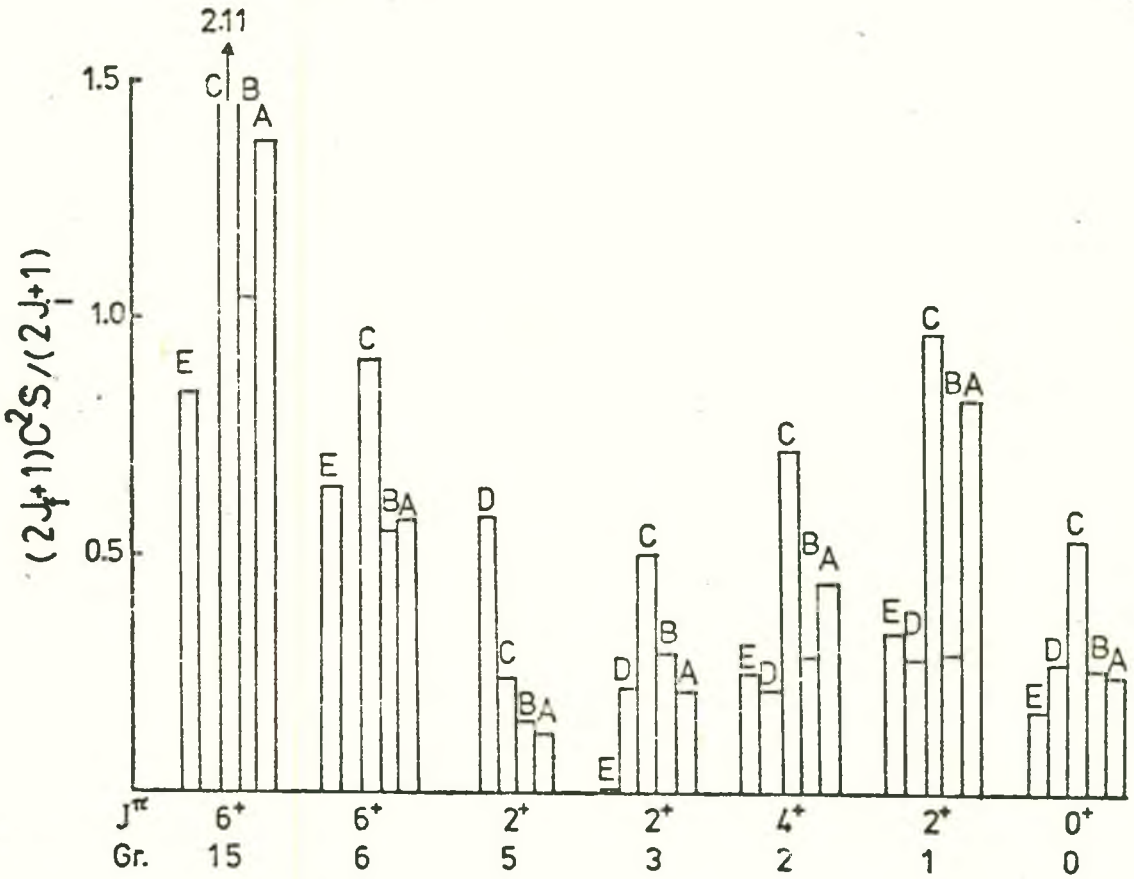

FIG. 5.10. Measured spectroscopic strengths compared with theory.

A : MBZ theory (Pr 69), B : Present work, C : (Br 68), D : (Ba 68),

E : (Oh 68).

the present experiment are in excellent agreement with the MBZ theory (fig. 5.10) for all but the first excited level (2^+_1); the strength for the latter group given by the present work is much smaller than that predicted. The strength given by Broman and Pullen (Br 68) on the other hand agrees with theory only for this 2^+_1 level. Several low-lying 2^+ states are observed in the (τ,d) experiments, only three of which are given by the MBZ model (figs. 5.9 and 5.10). It is, however, interesting to note that the summed strength 1.13 measured in the present experiment for all the 2^+ states up to $E_x \sim 4$ MeV, namely groups 1, 3, 5, 10 and 11, (group 9 is excluded for not having an ℓ=3 component) is indeed in excellent agreement with the summed strength 1.16 given by the theory (Pr 69) for the 2^+_1, 2^+_2 and 2^+_3 states and one may be tempted to account for the difference in strenght between theory and experiment for the 2^+_1 state in terms of this fragmentation.

A 4^+ level at E_x= 3.90 MeV is predicted (Pr 69) to be strongly populated in the (τ,d) reaction (predicted strength = 1.01), but no single level is found in the experiment that may be a possible candidate for this. Whether or not the predicted strength is distributed over several of the levels with undetermined J^π-values excited with ℓ_p=1+3 character (table 5.3) is difficult to say. Another 4^+ state at 3.22 MeV

is predicted to have a small strength.

A detailed comparison with the (τ,d) experiment thus shows the inadequacy of the MBZ model; a satisfactory description of only a few low-lying levels in ^{46}Ti is given by the simple $(1f_{7/2})^n$ configuration. Further indications of the existence of more complicated configuration come from the excitation of low-lying negative parity states and several states excited with ℓ=1 character in the (τ,d) reaction and also from the existence of two low-lying 0^+ states (Le 78,Au 78) other than the ground state. An augmented basis of 6 particles and 8p-2h configurations employed later by Skouras (So 75) is a step in that direction. Since it is extremely difficult to perform such a shell model calculation on the full $(fp)^6$ basis, a deformed scheme was adopted. Other than reproducing the 0^+_2 state the improvement is however not significant.

A passing mention may be made here on the band structure of ^{46}Ti. From gamma ray studies following (τ,n) reaction on ^{43}Ca, a ground state band has been proposed (Dr 78) comprising of the levels at E_x= 0, 0.889, 2.010, 3.299, 4.897 and 6.244 MeV with respective $J^\pi=0^+$, 2^+, 4^+, 6^+, (8^+), and (10^+) values. This is slightly different from the band suggested by Fortuna et al. (Fo 76) from the ^{40}Ca(^{12}C,α2pγ) reaction, namely

levels at E_x= 0, 0.889, 2.010, 3.299, 4.643, 6.244 and 6.519 MeV with respective J = 0^+, 2^+, 4^+, 6^+, (8^+), (10^+) and $(11^+, 12^+)$ values. The difference is probably due to the uncertainty in the spin assignments to higher members of the proposed band. Only the lowest four members of the band (and not the high spin levels) are populated in the (τ,d) reaction. The E2 transition strengths were derived by Dracoulis et al.(Dr 78) from the lifetime measurements and it is interesting to note that the enhancements of these transitions are approximately given by the MBZ model (Ku 78), as well by the more detailed calculations by Skouras (So 75).

A second positive parity band with the 2.613 keV level ($J^\pi=0^+$) has also been tentatively proposed by Dracoulis et al. (Dr 78). The excitation energies of the levels at E_x= 2.613, 2.962, 3.827, 4.416, 5.280 and 6.027 MeV, with $J^\pi=0^+$, 2^+, (4), (5^-), (6) and (7) respectively, are remarkably linear against J(J+1) and it is thus possible that some of the levels (obviously all these cannot be members of the even-J band) really belong to the same band. Only one member, namely the one at E_x=2.962 MeV is populated in the (τ,d) reaction and only weakly so.

CHAPTER 6

REACTION ^{59}Co(t,p)

6.1 Introduction

The ^{61}Co nucleus may be described by an $f_{7/2}$ proton hole and 6 neutrons distributed in the $2p\text{-}1f_{5/2}$ orbitals beyond Z=N=28 closed shell. Theoretical studies have been attempted to describe the ^{61}Co states with models based on excited core concept in which an $f_{7/2}$ proton hole is coupled to the ground state or to the excited states of the ^{62}Ni core.

Experimental information on the level structure of ^{61}Co has been derived using a variety of reactions. The β-decay studies (St 66, Gu 67, Gr 67) show very few levels and their energy levels are all consistent, from their studies the spin-parity assignments upto E_x= 1.995 MeV were made.

Spectrometer studies of levels of ^{61}Co on the decay of ^{61}Fe were performed by Bron et al.(Br 75). Spin-parity assignments upto E_x= 3.365 MeV were made by assuming the ground state spin as $3/2^-$.

The properties of low-lying levels of ^{61}Co were studied by Coop et al.(Co 69,70) through (p,α) and (p,αγ) reactions.

Mateja et al.(Ma 76) later studied the $^{64}Ni(p,\alpha)$ reaction at E_p= 13-16 MeV using magnetic spectrograph covering levels upto E_x= 3.937 MeV.

The $^{62}Ni(t,\alpha)$ reactions were studied by Blair et al. (Bl 66) and Hudson et al. (Hu 71) and properties of several levels are given.

The level properties of ^{61}Co were studied by Hudson et al.(Hu 71) through the $^{59}Co(t,p)$ reaction at E_t= 12 MeV covering levels upto 3.965 MeV with an energy resultion of ~20 keV. Discrepencies are observed in parity assignment of some levels studied by Hudson et al. in (t,p) reaction and by Blair et al. (Bl 66) in (t,α) reaction. Mateja et al.(Ma 76) observed all the levels excited by different reactions including (t,p) upto E_x= 3.965 MeV in addition to several new levels. The present (t,p) reaction on ^{59}Co at 15 MeV was studied with a slightly better resolution to re-examine the level properties of the ^{61}Co and also to extend to as high an excitation energy as possible.

6.2 Experimental Procedure

The plates exposed with the $^{59}Co(t,p)$ reaction were scanned at the Nuclear Physics Laboratory, University of Dacca,

Dacca. Scannings have been done for all the plates. But the spectra were lousy at high excitation, so that no significant results were obtained above 5.23 MeV. A typical spectrum at 11.25^{o} is shown in the fig. 6.1. The numbers adjacent to the peaks refer to the level numbering of the table 6.3. Contaminant groups resulting from (t,p) reactions from different impurities like ^{12}C, ^{14}N, ^{16}O and ^{56}Fe in the target are labeled using the corresponding level energy in the residual nuclei. Energy calibrations were performed at four angles using least squares fit with known energy levels namely 1.027, 1.619, 2.231, 2.343, 2.639, 2.864 and 3.104 MeV taken from Nuclear Data sheet (Au 75). The procedure has been mentioned in Chapter 2 (Section 2.6), these levels are shown underlined in the table 6.3. The values of a_o, a_1 and a_2 for each channel are shown in table 6.1. The overall energy resolution (FWHM) was found to be 18 keV. Levels upto E_x~5.23 MeV have been identified and angular distributions have been measured for most of the transitions.

The relative cross sections were measured for each level with method as described in Chapter 2 (Section 2.8).

6.3 DWBA Analysis

The Distorted Wave Born approximation (DWBA) calculations

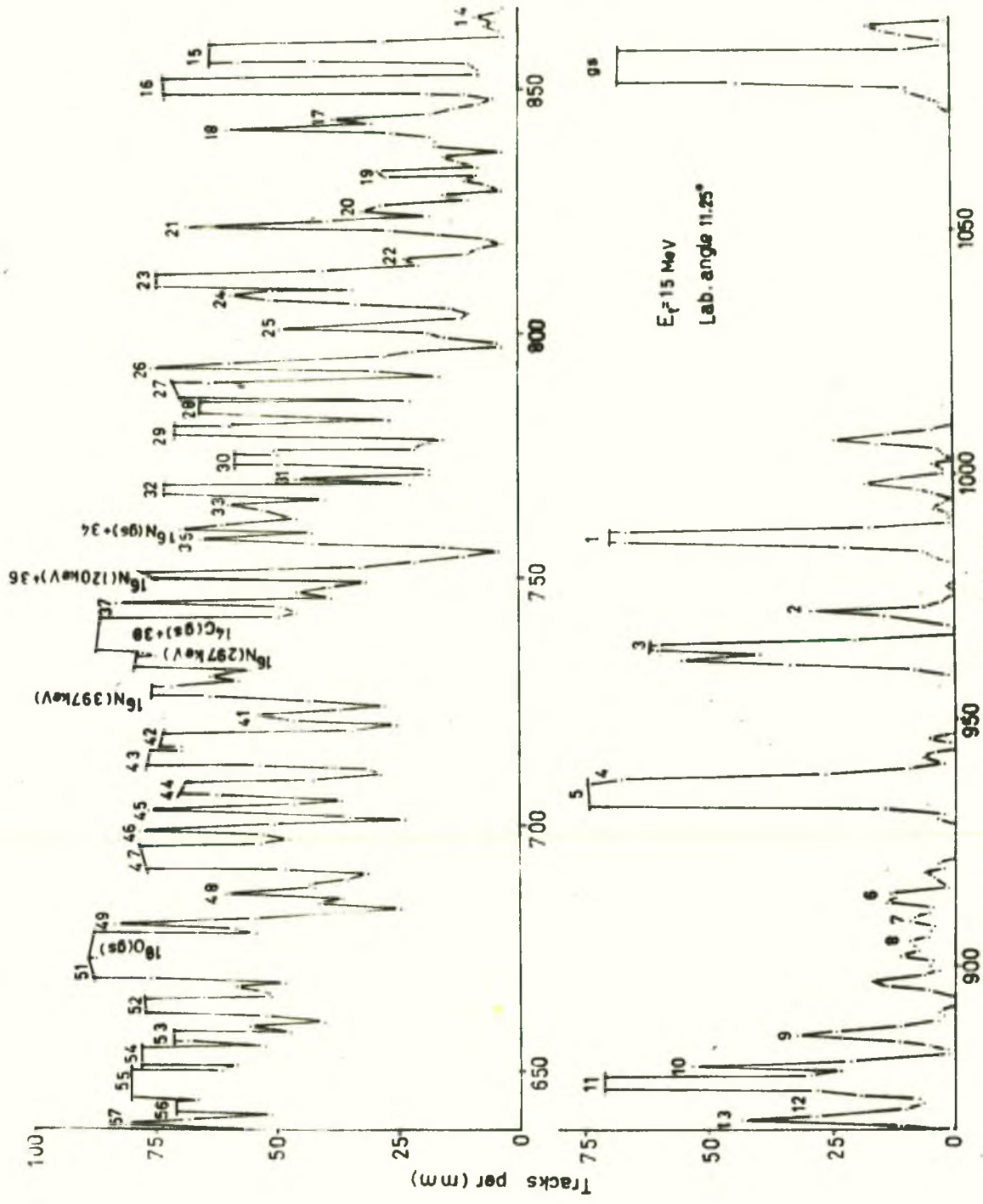

FIG. 6.1, Proton spectrum from ^{59}Co(t,p) reaction at 11.75°.

Table 6.1

Constants of least squares fit for ^{59}Co (t,p) reaction

Channel	a_o	a_1	a_2
2	13.516	-33.953	5.976
3	14.120	-37.565	10.858
4	14.107	-38.111	12.191
5	14.089	-38.559	11.816

were made for the ^{59}Co(t,p) reaction with the code DWUCK of Kunz by the present author with the help of Professor H.M.Sen Gupta using the IBM 370/115 Computer of Bangladesh University of Engineering and Technology, Dacca.

The optical model potential used was of the same form as that in Chapter 4, but without the spin-orbit term. Triton potential and the real part of the proton potential were of the standard Woods-Saxon form, while the imaginary part of the proton potential was the Woods-Saxon derivative. All calculations were performed with local potential using a zero range approximation without any lower cut off. The real depth of the bound state was adjusted to give the correct binding energy. Because of non availability of triton elastic scattering data around E_t= 15 MeV for the mass of Co nuclei, parameters determined from ^{62}Ni (Ha 67) for set A and ^{59}Ni (Fl 69) for set B, were used for the entrance channel. Triton potential parameters of set A were chosen from the survey of Hafele et al. (Ha 67) and for set B (r_o= 1.16 fm family) from the survey of Flynn et al.(Fl 69) ; this was also used by Nann et al. (Na 78) in ^{59}Ni(t,p) reaction. Proton potential parameters, set A, are taken from individual data sets of Makofske et al. (Ma 72) and for set B the global potential of Perey (Pe 65) ; this was also used in the ^{59}Ni(t,p)

reaction by Nann et al.(Na 78) with slightly increasing the real well depth. The optical model parameters are listed in table 6.2.

For the DWBA analysis the configurations used were of different L-transfers as follows :

L=0 : $(1f_{5/2} \quad 1f_{5/2})$

L=2 : $(2p_{1/2} \quad 1f_{5/2})$ and $(2p_{3/2} \quad 1f_{5/2})$

L=3 : $(3s_{1/2} \quad 1f_{5/2})$

L=4 : $(3s_{1/2} \quad 1g_{9/2})$

For each L-transfer the DWBA calculations were made with different J-values 7/2, 5/2 and 3/2. For each L-transfer calculations were carried out for excitation energies E_x= 0, 1.5, 3.0 and 4.5 MeV. DW calculation for ground state was also done by reducing the strength of the optical model parameters for set A A to 10% to see the effect of the parameter variation (fig.6.2).

Angular momentum transfers were measured with DWBA calculation of set A A for all states. But set B B was attempted for those states which were not fitted with set A A and/or had disagreement with the assignments of previous (t,p) reaction of Hudson et al. (Hu 71).

Table 6.2

Optical model parameters used for the ^{59}Co(t,p) reaction

Particle	Symbol	V (MeV)	r_o (fm)	a (fm)	W (MeV)	$4W_D$ (MeV)	r_1 (fm)	a_1 (fm)	r_e (fm)	Ref.
t	A	151.0	1.24	0.692	29.0		1.36	0.890	1.25	(Ha 67)
t	B	169.7	1.16	0.732			1.51	0.796	1.25	(Fl 69)
p	A	50.92	1.214	0.751		52.32	1.323	0.457	1.25	(Ma 72)
p	B	47.5	1.25	0.65		54.0	1.25	0.47	1.25	(Pe 65)
n		a)	1.25	0.65	λ=25		1.25			

a) adjusted to reproduce the binding energy.

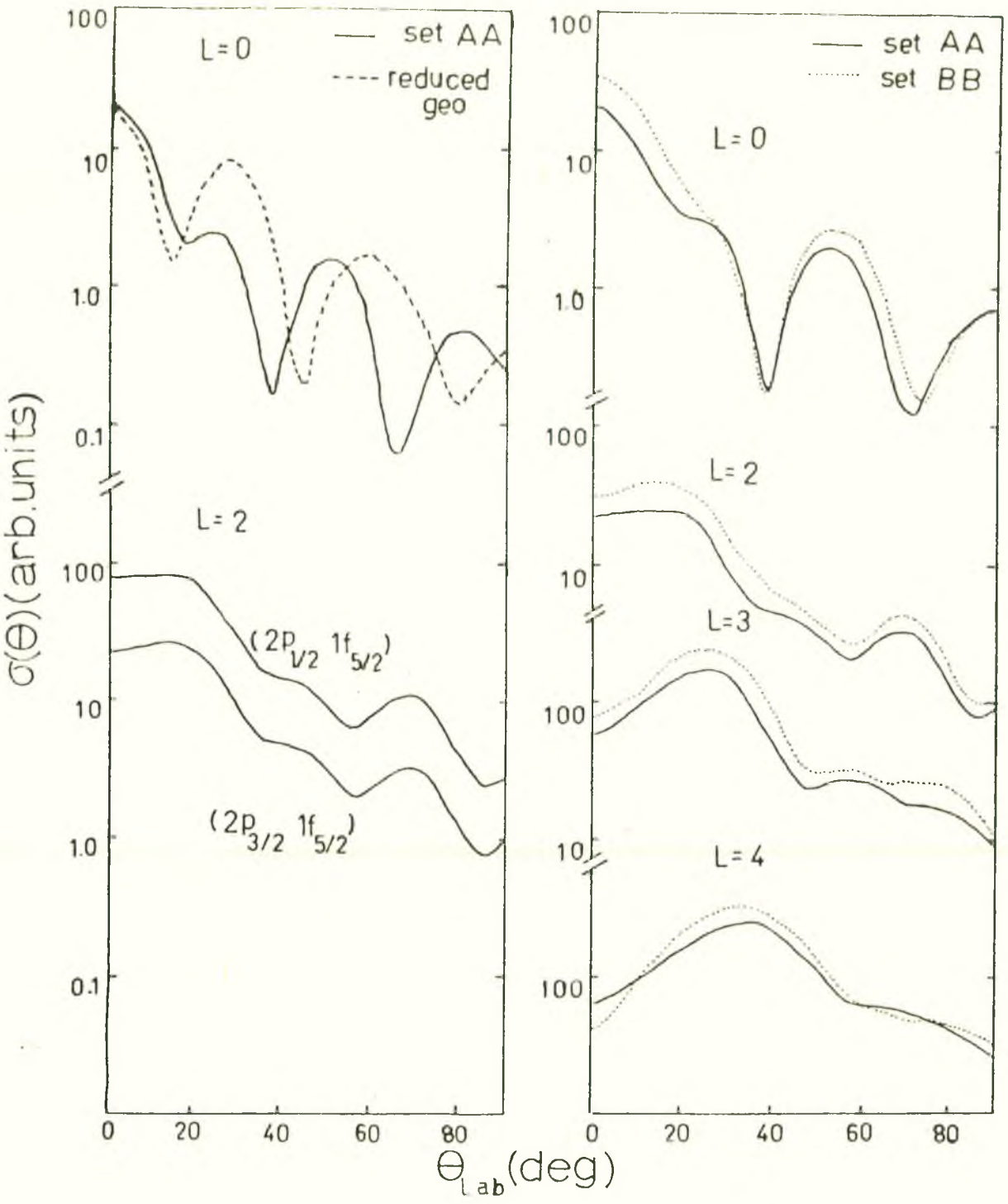

FIG. 6.2. Effects of potential parameters and configuration on DWBA calculations.

6.4 Energy Levels of ^{61}Co

A summary of the levels observed in ^{61}Co with the (t,p) reaction is given in table 6.3. The second and third columns of this table identify the excitation of the levels by means of present and previous (t,p) experiments (Hu 71). For convenience in comparison of individual states the excitation energies from both (t,p) and (p,α) data (Ma 76) and those from recent compilation are presented in a separate table 6.4. The energy values are correct upto three decimal places except where shown otherwise.

The levels populated in previous ^{59}Co(t,p) reaction (Hu 71) upto E_x= 2.765 MeV are all observed in the present study and the energy values are also consistent with theirs. Within this excitation energy there are four states at 1.89, 1.96, 2.01 and 2.48 MeV excited in present work, but not found in the previous (t,p) reaction by Hudson et al. These levels were identified in the ^{64}Ni(p,α) reaction (Co 69,70 , Ma 76). Hudson et al.(Hu 71) observed two levels at 1.903 and 1.971 MeV in the (t,α) studies. The levels at 2.012 and 2.484 MeV are excited in the β - decay (Br 75). The level at 2.94 MeV observed in present (t,p) work is excited in (p,α) reaction (Co 69, Ma 75). This is also observed in the β - decay(Br 75), but was not found in the previous (t,p)

Table 6.3

Summary of the results of ^{61}Co

Level	E_x(MeV)		L - transfer		Cross Section (arb.units)	J^π
	a)	b)	a)	b)	a)†	c)
gs	0	0	0	0	5293	$7/2^-$
1	1.026	1.026	2	2	269	$3/2^-$
2	1.20	1.213	2	2	65	$3/2^-,5/2^-$
3	1.286	1.286	2	2	224	$\geq 7/2^-$
4	1.622	1.620	0 or 2	0	150	$7/2^-$
5	1.666	1.66	2	2	847	$\geq 7/2^-$
6	1.89		n.a		52	
7	1.96		n.a		26.71	$3/2^-$
8	2.01		2+4		24.9	$3/2^-,5/2^-$
9	2.231	2.239	2	2	148.3	$1/2^{+d)},3/2^--11/2^{-e)}$
10	2.303	2.313	2+4	2+4	89	$3/2^-,5/2^-$
11	2.343	2.348	0+2	0+2	315	$7/2^-$
12	2.37	2.386	4	4	83	$(1/2^-)$
13	2.429	2.436	2+4	2+4	84	
14	2.48		n.s		75	3/2,5/2
15	2.564	2.568	2	2	431	$3/2^{+d)},3/2^--11/2^{-e)}$
16	2.639	2.639	2	2	604	
17	2.71	2.728	2	2	100	
18	2.74	2.765	2	2	95	$3/6^-,5/6^-$

Table 6.3 (Continued)

Level	E_x(MeV)		L - transfer		Cross Section (arb.units)	J^π
	a)	b)	a)	b)	a)†	c)
19	2.857	2.882	2+4	2	52	$5/2^{-g)}, 2/2^{-d)}$
20	2.94		2		58	$3/2^-, 5/2^-$
21	2.984	2.975	2+4	2	150	
		3.017		2		
22	0.064		2+4		44	
23	3.109		2+4		230	
24	3.16	3.151	4	(2+4)	147	$(1/2^-)$
25	3.22	3.220	0+2	(0+2)	103	$7/2^{-e)}, (3/2^+)^{d)}$
26	3.331		2+4		194	
27	3.388	3.394	2+4	(2+4,3)	381	
28	3.446	3.450	2+4	0+2	356	$(7/2^-)$
29	3.501	3.515	2+4	0+2	239	
30	3.570	3.578	2+4	2+4	212	$(3/2^+)^{d)}, 3/2^- - 11/2^{-e)}, (3/2^+, 5/2^+)^{f)}$
31	3.618		n.s		58	
32	3.651	3.653	2+4	2+4	321	
33	3.68		(2+4)		103	
34	3.72	3.713	0	4	123	$7/2^-$
35	3.766	3.746	2+4	2+4	152	$(7/2^-)$
36	3.857	3.870	3	(2+4)	230	$(3/2, 5/2)^+$

Table 6.3 (Continued)

Level	E_x (MeV)		L - transfer		Cross Section (arb.units)	J^π
	a)	b)	a)	b)	a)†	c)
37	3.93		n.s		113	
		3.965		2+4		
38	4.010		2+4		318	
39	4.09		0		141	$7/2^-$
40	4.13		n.s		115	
41	4.21		2+4		111	
42	4.26		0		205	$7/2^-$
43	4.31		(0+4)		262	$(7/2^-)$
44	4.40		n.s		247	
45	4.44		n.s		142	
46	4.53		2+4		143	
47	4.57		(2)		300	
48	4.67		n.s		110	
49	4.73		2+4		119	
50	4.80		n.s		181	
51	4.84		0		452	$7/2^-$
52	4.92		2+4		147	
53	5.04		0+4		192	$7/2^-$
54	5.08		2+4		304	
55	5.13		2+4		400	

Table 6.3 (Continued)

Level	E_x (MeV)		L - transfer		Cross Section (arb.units)	J^π
	a)	b)	a)	b)	a)†	c)
56	5.18		n.s		214	
57	5.23		n.s		191	

n.s - non stripping angular distribution.

n.a - data not analyzed.

a) Present work

b) The ^{59}Co(t,p) reaction at E_t= 12 MeV, Hudson et al.(Hu 71)

c) Previous experiments, summarized by the present author, consistent with present L-assignment (Br 75, Co 70, Bl 66, Ma 76).

d) The (t,α) reaction of Blair et al.(Bl 66).

e) Present work

a)† Peak cross section

f) The (p,α) reaction of Mateja et al.(Ma 76)

g) β-decay by Bron et al.(Br 75)

The estimated errors in energies in present work are ± 15 keV.

reaction by Hudson et al. (Hu 71).

The levels at 3.109, 3.618 and 3.68 MeV found in the present work were not observed in the previous (t,p) study, but were identified in (p,α) reaction by Mateja et al.(Ma 76). The present (t,p) experiment populates the states at 3.064 and 3.331 MeV which are not observed in any previous work.

The level at 3.93 MeV (the present study) is possibly an unresolved doublet of 3.924 and 3.937 in (p,α) of Mateja et al.(Ma 76). In the present (t,p) reaction some unresolved levels are observed such as 2.564, 2.71, 3.22, 3.388, 3.570 and 3.766 MeV resolved into 2.559 and 2.572, 2.707 and 2.727, 3.204 and 3.240, 3.384 and 3.397, 3.565 and 3.575, 3.758 and 3.775 MeV in the (p,α) reaction of Mateja et al. (Table 6.4)

6.5 Angular momentum transfer and spin-parity assignment

Angular momentum transfers of states were determined from a comparison of the measured angular distribution with that given by the DWBA calculations (listed in the fifth column of table 6.3). The solid lines in fig. 6.2 represent the theoretical cross sections normalized to the experimental angular distributions. The L-transfer of states due to different mixtures is obtained by taking a sum of theoretical

Table 6.4

Energy levels of ^{61}Co

Level	E_x (MeV) a)	b)	c)	d)
gs				
1	1.026	1.027	1.026	1.028
2	1.20	1.205	1.213	1.206
		1.272		
3	1.286	1.286	1.286	1.286
		1.325		1.323
4	1.622	1.619	1.620	1.619
		1.646		1.646
5	1.666	1.664	1.66	1.665
6	1.89	1.889		1.889
7	1.96	1.953		1.953
8	2.01	2.012		2.014
9	2.231	2.231	2.239	2.232
		2.258		
10	2.303	2.303	2.313	2.304
11	2.343	2.343	2.348	2.346
12	2.37	2.386	2.386	2.374
13	2.429	2.432	2.436	2.432
14	2.48	2.484		2.484
		2.558		

Table 6.4 (continued)

	E_x (MeV)			
Level	a)	b)	c)	d)
15	2.564	2.568	2.568	2.559 2.572
16	2.639	2.639	2.639	2.642
17	2.71		2.728	2.707 2.727
18	2.74	2.754	2.765	2.757
				2.780
19	2.857	2.864	2.882	2.867
20	2.94	2.920		2.922
21	2.984	2.875	2.975	2.980
			3.017	2.998
22	3.064			
23	3.109	3.104		3.102
				3.126
24	3.16		3.151	3.152
				3.176
				3.190
				3.204
25	3.22		3.220	
		3.239		3.240

Table 6.4 (continued)

	E_x (MeV)			
Level	a)	b)	c)	d)
26	3.331			
				3.349
				3.357
		3.365		3.364
27	3.388		3.394	3.384 3.397
				3.410
				3.428
28	3.446		3.450	3.445
				3.471
				3.485
29	3.501		3.515	3.493
				3.514
				3.536
30	3.570		3.578	3.565 3.575
				3.600
31	3.618			3.609
32	3.651		3.653	3.654
33	3.68			3.692
34	3.72		3.713	3.700 3.728
				3.753

Table 6.4 (continued)

	E_x (MeV)			
Level	a)	b)	c)	d)
35	3.766		3.746	3.758 3.775
				3.806
				3.815
				3.827
36	3.857		3.870	3.871
				3.890
				3.906
				3.916
				3.924
37	3.93			
				3.937
			3.965	
38	4.010			
39	4.09			
40	4.13			
41	4.21			
42	4.26			
43	4.31			
44	4.40			

Table 6.4 (continued)

Level	E_x (MeV) a)	b)	c)	d)
45	4.44			
46	4.53			
47	4.57			
48	4.67			
49	4.73			
50	4.80			
51	4.84			
52	4.92			
53	5.04			
54	5.08			
55	5.13			
56	5.18			
57	5.23			

a) Present work

b) Summarised by Auble (Au 75)

c) The ^{59}Co(t,p) reaction by Hudson *et al.* (Hu 71)

d) The ^{64}Ni(p,α) reaction by Mateja *et al.* (Ma 76)

angular distributions of two L-transfers in a proportion that gives the best fit to the measured values. The experimental angular distribution is then fitted by this sum which is represented by the solid lines and the components are represented by the broken lines.

The results of the calculations show that shapes of the angular distributions are essentially independent of the configurations assumed and of different J-values for an L-transfer.

The distorted wave calculation also does not show any significant dependence on the variation of optical model parameter. For the odd A nuclei the selection rules governing the (t,p) reaction (S=0) are

$$\underline{J_f} = \underline{L} + \underline{J_i} \ , \quad \pi_i \, \pi_f = (-1)^L .$$

These selection rules allow more than one L-value for a given transition. A definite spin assignments is not usually possible from the above selection rules. Only parity and limits on the possible spin of a state are given. Spin and parity assignments of the levels have been made for those cases where angular momentum for same levels have been measured in (t,p) reactions and (t,α) or β-decay, since in

(t,α) or β-decay only one J^{π} value is allowed in the transition. The ground state spin of ^{59}Co is $7/2^-$, so a state excited by L = 0 transfer in ^{61}Co has $J^{\pi} = 7/2^-$. The states with mixed L-transfers are produced when the two neutrons coupled to the $f_{7/2}$ proton hole will mix with proton states of the same spin. Therefore the expected J^{π}- value would be in the limit $3/2^-$- $11/2^-$ for L = 2 + 4 and $7/2^-$ for L = 0 + 2 transitions.

6.5.1 L = 0 transfer

The angular distributions for six states including ground state are fitted with L = 0 transfer (fig. 6.3). The spin of these states is therefore $7/2^-$. Two sets of potential parameters were used to fit the ground state angular distribution. A better fit is suggested by the set BB specially for the forward angles. The level at 1.622 MeV is characterized by both L = 0 and 2 transfers (fig. 6.3) as against only L = 0 found by Hudson et al.(Hu 71). An attempt was also made to fit the angular distribution of this level with potential parameter of set BB for L = 0 and 2. No improvement is observed. Blair et al.(Bl 66) from (t,α) reaction and Bron et al.(Br 75) in the β-decay assign $J^{\pi} = 7/2^-$ for this state ; either of L = 0 and L = 2 transition is consistent with this J^{π}- value.

The present study shows an L = 0 transfer for the state at 3.72 MeV as against an L = 4 transition given by previous (t,p) reaction (Hu 71). Both L = 0 and L = 4 transfers are shown in the fig. 6.3. The parameter set BB also gives an L = 0 transfer. Unfortunately the data point at the forward-most angle is missing. This could perhaps help distinguishing between L = 0 and L = 2 assignments.

The angular distribution for the remaining three levels (E_x = 4.09, 4.26 and 4.84 MeV) are all fitted quite well with an L=0 transfer. Though the data at the first forward angles are missing, the 4.09 MeV level shows the characteristics of an L = 0 transfer.

6.5.2 L = 2 transfer

The angular distributions for eleven states are observed to have characteristic of an L = 2 transfer shown in fig. 6.4, the J^{π}-limits for an L = 2 transfer are $3/2^{-}$ - $11/2^{-}$.

Of these states the ones at 1.026, 1.20, 1.286, 1.666, 2.231, 2.564, 2.639, 2.71 and 2.74 MeV are well fitted by L = 2 DWBA curves. Hudson et al.(Hu 71) also identified these levels as L = 2 transfer in (t,p) reaction. Blair et al.(Bl 66) in (t,α) reaction assigned $J^{\pi} = 3/2^{-}$ for the level at 1.027 MeV.

Bron et al.(Br 75) assigned $J^{\pi}= 3/2^{-}$ for 1.027, $3/2^{-}$, $5/2^{-}$ for 1.205 and $3/2^{-}$, $5/2^{-}$ for 2.754 MeV levels. The absence of β-feeding to the level at 1.286 MeV gives the probable $J^{\pi} \geq 7/2^{-}$. Smit et al.(Sm 79) and Mateja et al.(Ma 76) assigned high spin value to this level. Coop et al.(Co 69,70) identified the J^{π}-values of the 1.027 and 1.206 MeV levels as $3/2^{-}$ and $3/2^{-}$, $5/2^{-}$ in (p,α) reaction. The present L-assignments are consistent with these J^{π}-values. Blair et al.(Bl 66) predicted $J^{\pi}= 1/2^{+}$ and $3/2^{+}$ for the 2.247 and 2.575 MeV levels and Coop et al.(Co 69) in (p,α) reaction assigned $J^{\pi}= 1/2^{+}$ for the 2.230 and $3/2^{+}$ for 2.563 MeV level. If 2.231 and 2.564 MeV level in the present (t,p) reaction may correspond to the 2.247 and 2.575 MeV of Blair et al. The present L-transfers of these two levels disagree with theirs (Co 69, Bl 66). The (t,p) angular distribution leading to the level at 2.71 MeV is characterized by an L = 2 transfer (present work and Hu 71). Mateja et al. (Ma 76) observed two levels at 2.707 and 2.727 MeV in place of 2.71 MeV. The spin of the level at 2.727 MeV is believed to be 1/2 - 5/2 (Ma 76).

Hudson et al. observed the level at 1.66 MeV through an L = 2 transfer and made the tentative assignments as $(5/2^{-})$. Bron et al.(Br 75) observed the level at 1.645 MeV with $J^{\pi}= (3/2^{-})$, $5/2^{-}$. But Mateja et al.(Ma 76) identified three levels at 1.619, 1.646 and 1.665 MeV. They also predicted

that the last one might be a high spin state $J^{\pi} \geq 7/2^{-}$. Among these levels, the first two were observed by Bron et al. (Br 75) in β-decay. Smit et al. (Sm 78) predicted the level at 1.656 with J^{π} as high as $11/2^{-}$. The level at 1.666 MeV in the present study is very strongly populated and the L-assignment is consistent with the predicted J^{π}-value.

The angular distribution of the level at 2.94 MeV has been satisfactorily reproduced through an L = 2 transfer. Bron et al. (Br 75) predicted J = 3/2, 5/2 of the level at 2.94 MeV from β-decay. The J^{π} of the level would thus be $3/2^{-}$, $5/2^{-}$. The 4.57 MeV level is populated by an L = 2 transition and is poorly fitted by DWBA calculation. The 2.94 and 4.57 MeV levels have not been observed by Hudson et al. in the (t,p) reaction.

6.5.3 L = 3 transfer

Only one level at 3.857 MeV is excited with angular distribution characterized by an L = 3 transfer (fig. 6.5) ; Hudson et al. (Hu 71) however made a tentative L = 2+4 transfer in (t,p) reaction. Mateja et al. (Ma 76) tentatively assigned $J^{\pi} = 3/2^{+}$, $5/2^{+}$ and Blair et al. (Bl 66) through $^{62}Ni(t,\alpha)$ reaction assigned $J^{\pi} = 3/2^{+}$ to this level. The J^{π}-limits from the present work are $1/2^{+}$ - $13/2^{+}$, being consistent

with their assignments.

6.5.4 L = 4 transfer

Two states at 2.37 and 3.16 MeV exhibit the characteristics of an L = 4 transfer (fig. 6.5). In the previous (t,p) reaction studied by Hudson et al.(Hu 71) the state 2.37 MeV state was excited by L = 4 transition, while the other state is observed with tentative L = 2 + 4 character. The DWBA analysis is tried with the set BB which again requires an L = 4 transition.

6.5.5 L = 0 + 2 transfer

Levels at 3.043 and 3.22 MeV are found to be populated by L = 0 + 2 transitions and the angular distributions are well fitted by the DWBA calculation (fig. 6.6). This L = 0+2 assignment is consisten with the (t,p) work of Hudson et al. (Hu 71). The J^{π}-value of these states is $7/2^{-}$. The level at 3.22 MeV with L = 0 + 2 may correspond to the state at 3.215 MeV with $J^{\pi} = (3/2)^{+}$ observed by Blair et al.(Bl 66) in (t,α) reaction. Bron et al.(Br 76) observed two levels at 3.204 and 3.239 MeV assignd $J^{\pi}= 3/2^{-}$, $5/2^{-}$ and J = 3/2, 5/2 to both the levels. The present L-assignment then contradicts the parity assignment made by Blair et al.

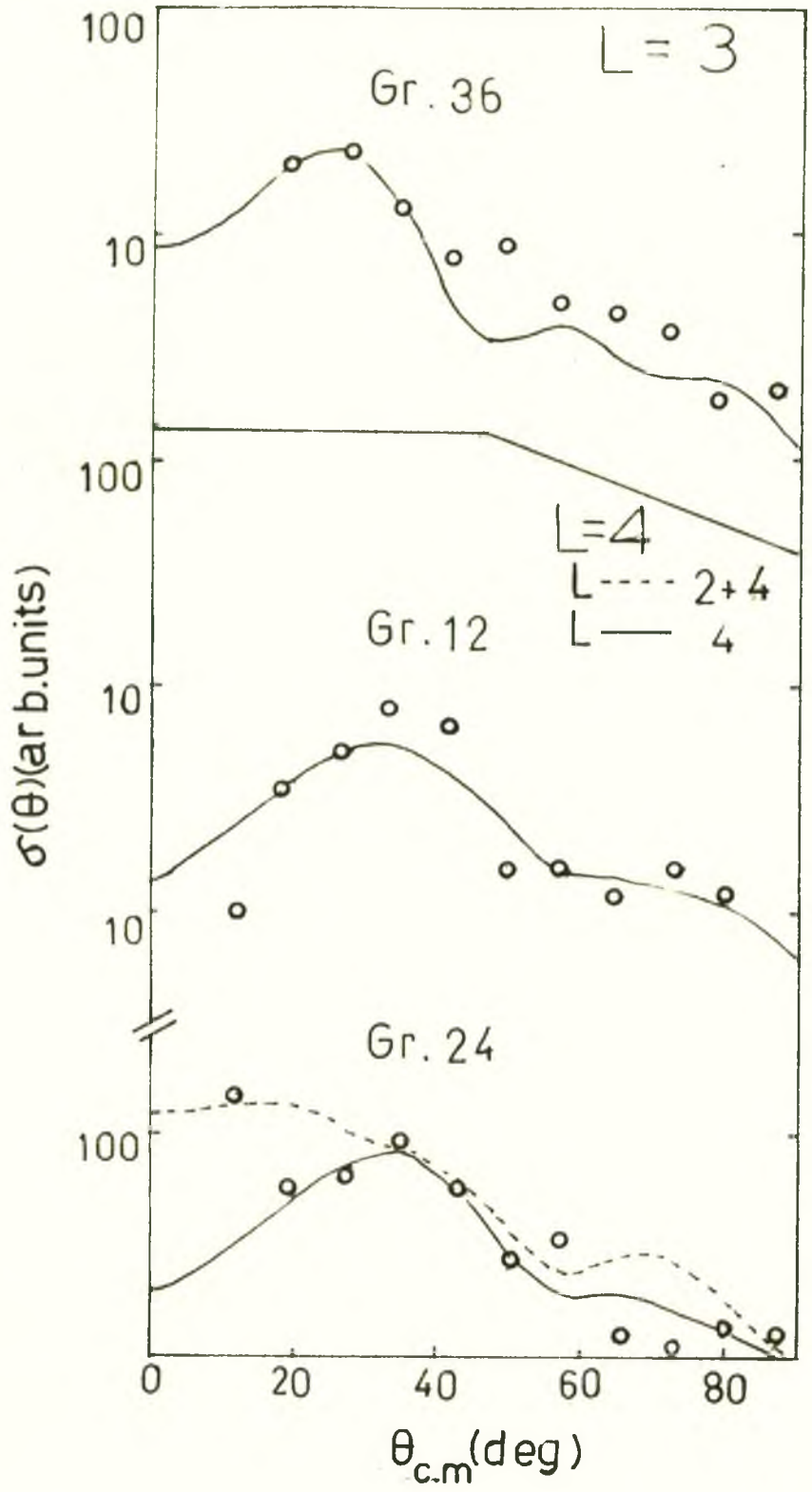

FIG. 6.5. Experimental angular distributions fitted to L = 3 and 4 DWBA curves.

6.5.6 L = 0 + 4 transfer

Two states at 4.31 and 5.04 MeV populated in the present (t,p) reaction through L = 0 + 4 transitions, have not been found in any previous works (fig. 6.6). The angular distribution of the level 4.31 MeV is well fitted, while the fit to the 5.04 MeV level is poor. These states are assigned to have $J^{\pi} = 7/2^{-}$.

6.5.7 L = 2 + 4 transfer

The angular distributions of a large number of levels are fitted by mixed L = 2 + 4 transfers (figs. 6.7, 6.8). Six of these levels, namely at 2.303, 2.429, 3.388, 3.570, 3.651 and 3.766 MeV, are in agreement with previous (t,p) results (Hu 71, fig. 6.7). Because of the consistency in L-transfer the 3.766 MeV level in the present study may be compared with the level 3.746 MeV of Hudson et al. For the level at 3.388 MeV Hudson et al. assigned an ambiguous L = 2 + 4 or 3 transfer whereas in the present work an L = 2 + 4 gives a good fit to the measured angular distribution (fig. 6.7). An L = 3 distribution with both the parameter sets AA and BB gives a poor fit to the data. The L-transfer values for the levels at 2.857, 2.984, 3.446 and 3.501 MeV made in the two (t,p) works (present work and Hudson et al.) are not in agreement with each other.

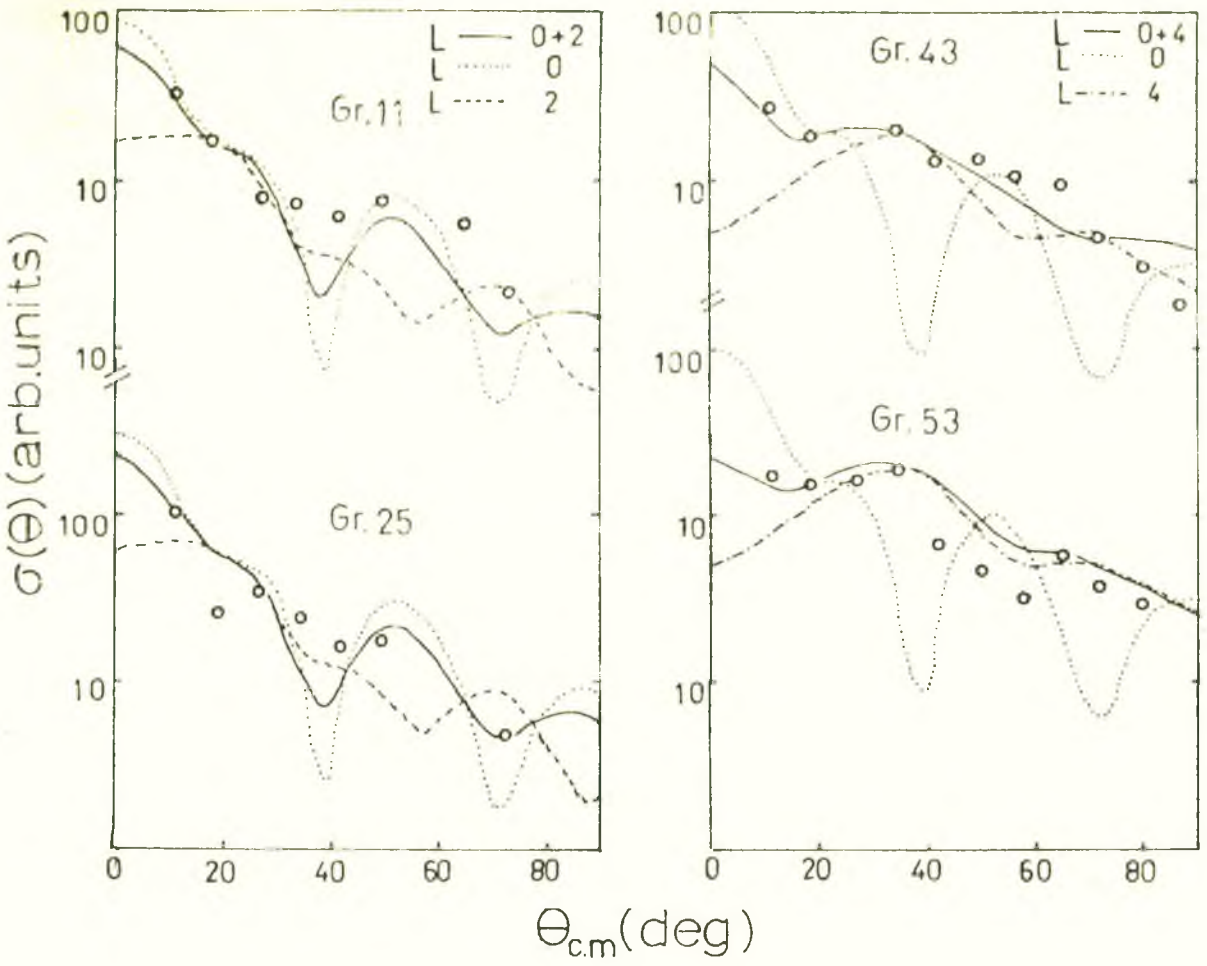

FIG.6.6. Experinental angular distribution fitted with L=0+2 L=0+4 DWBA curves.

Bron et al.(Br 75) assigned J = 3/2, 5/2 to the level at 2.01 MeV from β-decay. Coop et al. (Co 70) also suggest the same J-value. The present L-assignment for the level gives $J^{\pi} = 3/2^{-}, 5/2^{-}$. Bron et al.(Br 75) observed the levels at 2.303 and 2.857 MeV with $J^{\pi} = 3/2^{-}$, $5/2^{-}$ and $5/2^{-}$ respectively. The state at 2.857 and 3.466 MeV excited through L = 2 + 4 characteristics in the present study may be considered the same level as the 2.893 and 3.470 MeV found in (t,α) reaction (Bl 66) with $J^{\pi} = 7/2^{-}$ and $(7/2^{-})$. Blair et al.(Bl 66) also observed the level at 3.776 MeV with $J^{\pi} = (7/2^{-})$. Mateja et al.(Ma 76) observed two levels at 3.758 and 3.775 MeV and tentatively assigned the J^{π}-value of $(3/2^{-}, 3/2^{-})$ to the 3.758 MeV. The L = 2 + 4 transfer to the levels at 2.303, 2.857, 3.466 and 3.776 MeV are consistent with J-assignments made earlier (Bl 66, Br 75, Ma 76).

In the study of the ^{62}Ni(t,α) reaction (Bl 66), the state at 3.578 MeV was observed with $J^{\pi} = 3/2^{+}$; corresponding to this the observed level at 3.570 MeV in the present (t,p) reaction is excited through an L = 2 + 4 transition with J^{π}-limits $3/2^{-}$ - $11/2^{-}$. The present work is then in disagreement with their work.

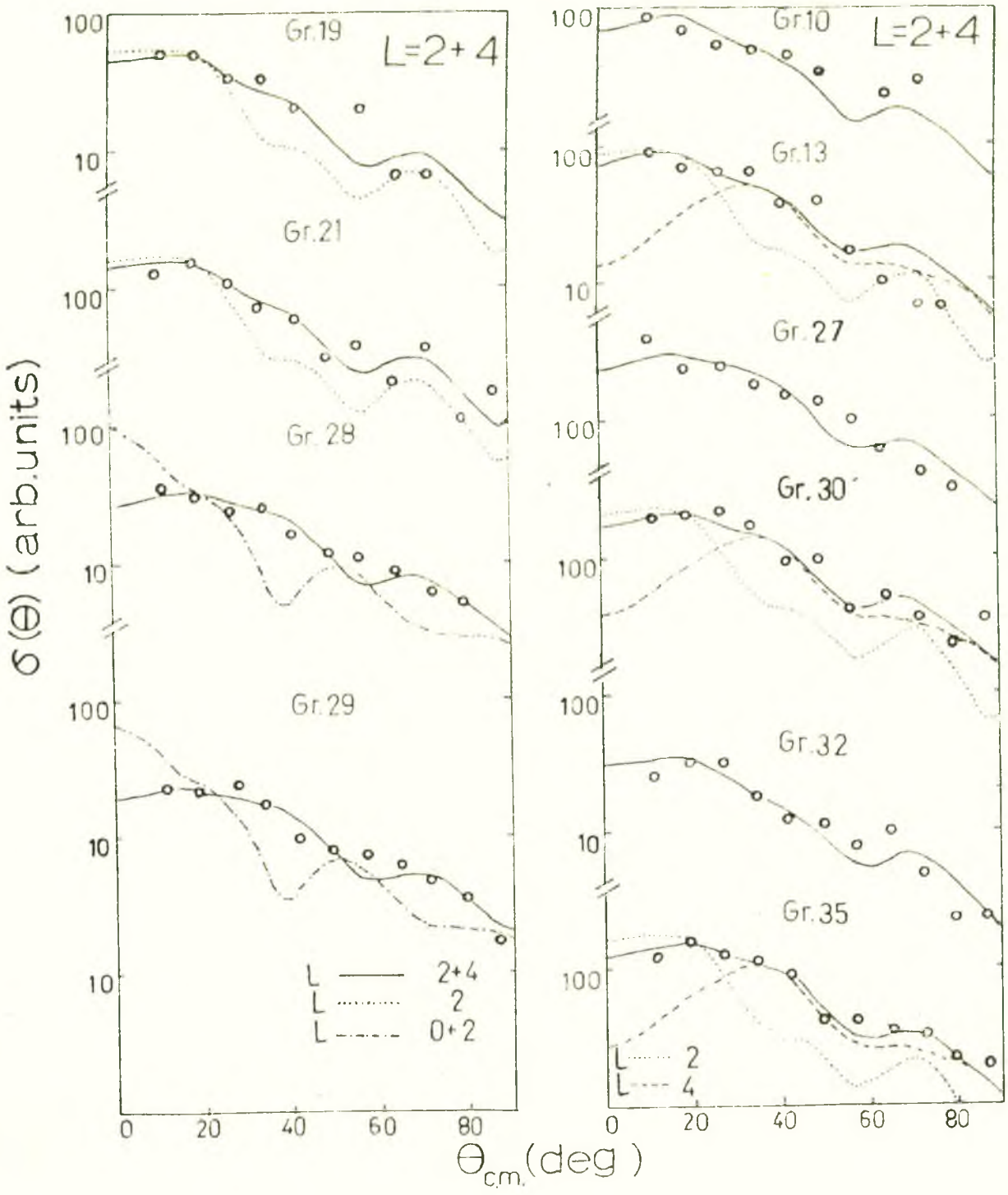

FIG. 6.7. Experimental angular distributions fitted with L=2+4 transfer. Left: disagreement and right: agreement with previous study (Hu 71).

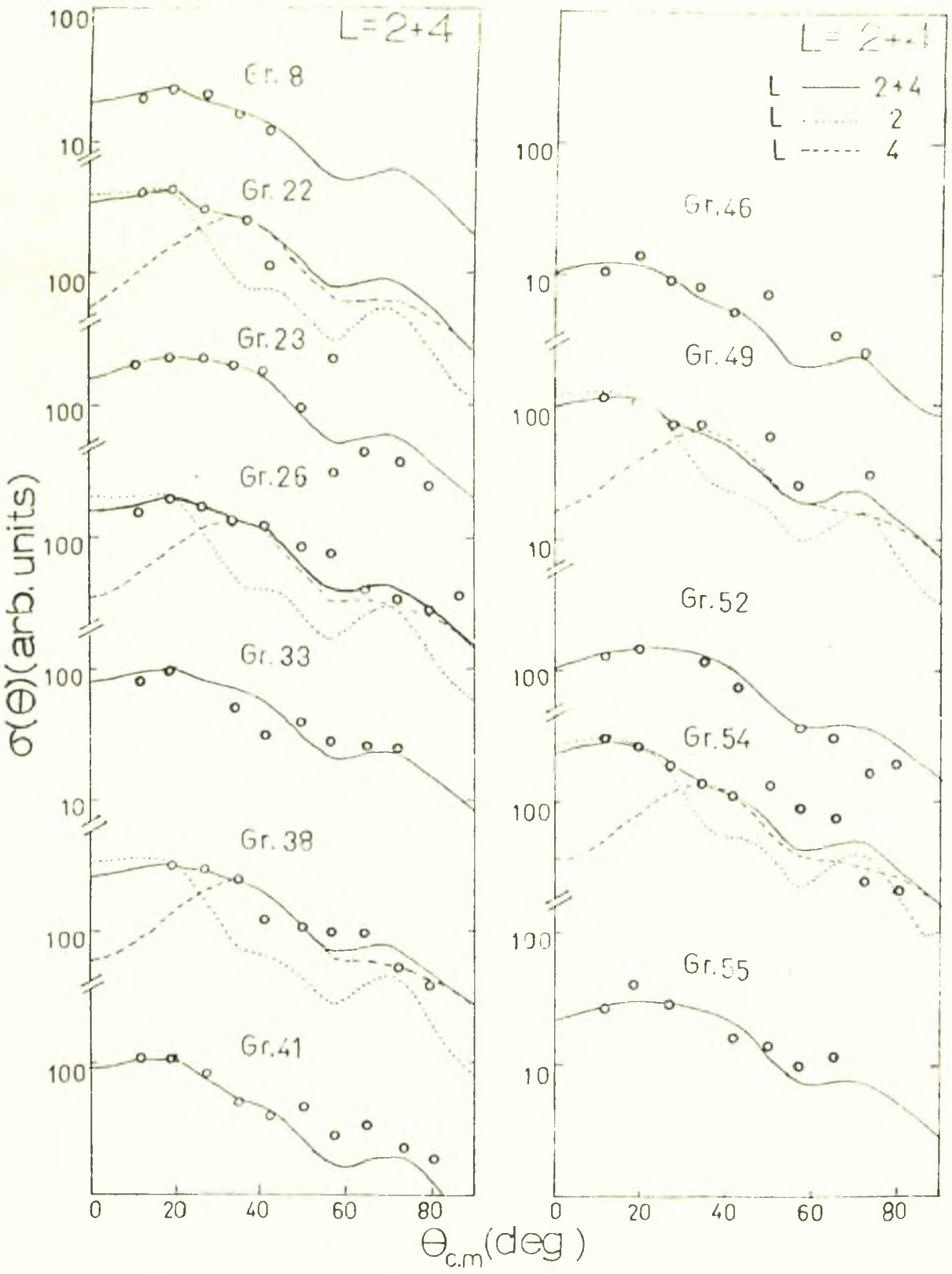

FIG.6.8. Experimental angular distributions fitted with L=2+4 transfer new in the present study.

6.5.8 Non-stripping level

There are eleven states (fig. 6.9) that show feature-less angular distribution and are not given by a single-step process. Spin-parity assignments of the level 2.48 MeV made in different studies are given in table 6.3.

6.6 Structure of ^{61}Co

Several theoretical works have been done to study the level properties of the odd - mass Co-isotopes and these have been found to be successful in explaining the low-lying levels. Earlier studies were limited only to ^{57}Co and ^{59}Co isotopes because of lack of availability of properties of excited states of ^{61}Co.

The level properties of ^{61}Co are tried to explain on the basis of theoretical work of Satpathy and Gujrati (Sa 68), Stewart et al.(St 71), Gomez (Go 72) and Smit et al.(Sm 79) as described in Chapter 4 (Section 4.5) (fig.6.10).

The theoretical levels calculated by Stewart et al.(St 71) and Gomez (Go 72) are similar in structure upto 2.3 MeV but the predicted level spacings are different. The first excited state

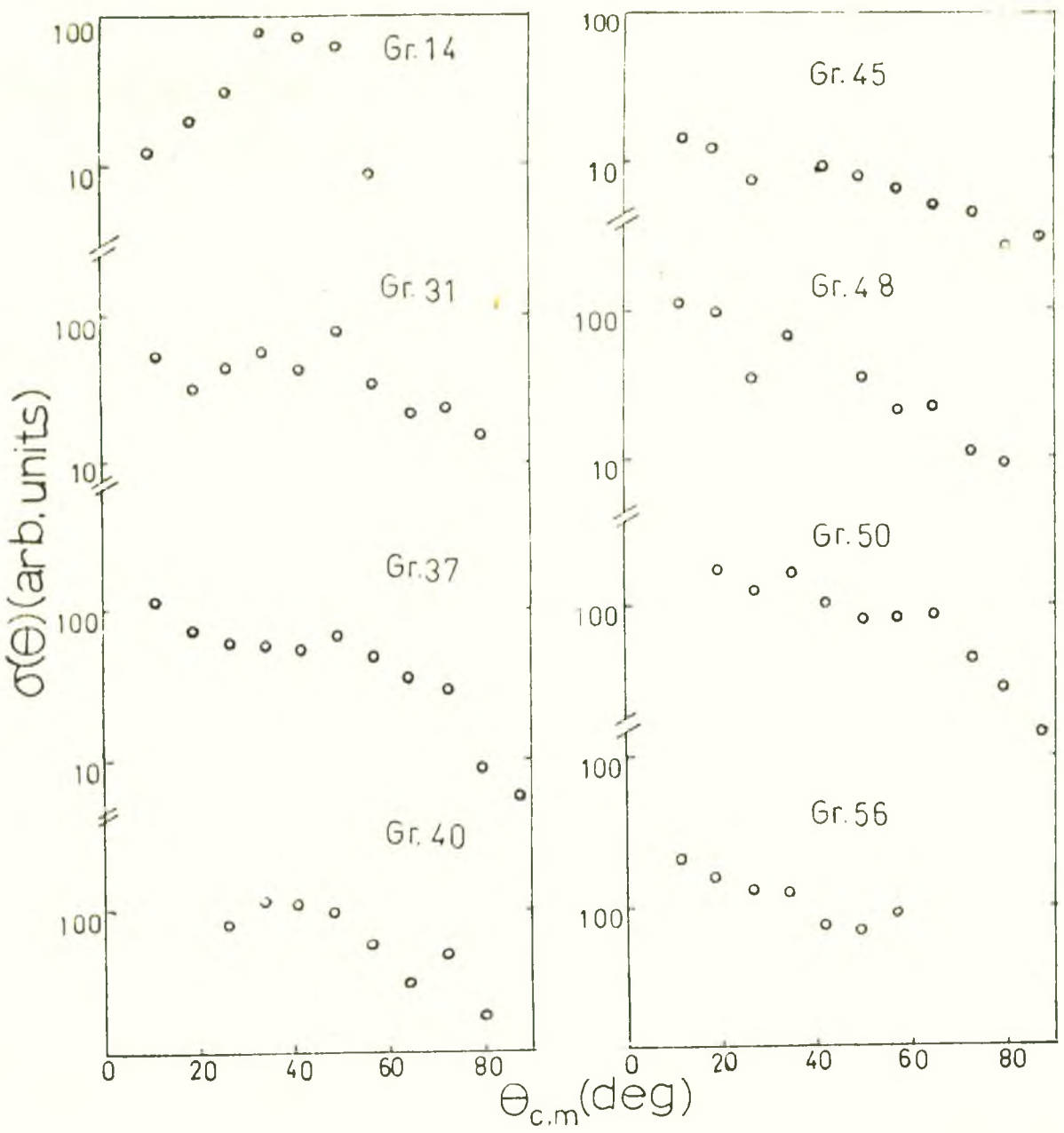

FIG. 6.9. Some of the measured angular distributions displaying a non-stripping character.

$J^{\pi} = 9/2^{-}$ predicted by Satpathy et al. is raised in these two models and becomes approximately degenerate with the $11/2^{-}$ level as a lower member. The sequance of the levels is much better given in the calculations by Stewart et al.(St 71) than those found in the work of Satpathy. Theoretical levels calculated by the three models (Sa 68, St 71, Go 72) are found to be in agreement with few experimental levels upto 2.5 MeV.

The level at 1.272 and 1.287 MeV were observed by Hudson et al.(Hu 71) in (t,α) reaction as a doublet. These two are expected to have high spin values. Bron et al.(Br 75) observed the 1.287 MeV level without direct β-feeding. So expected spin would be $\geq 7/2$. Mateja et al.(Ma 76) observed a triplet at 1.619, 1.646 and 1.665 in place of a doublet. The 1.665 MeV level is populated very strongly which is consistent with the high spin assignment. Mateja et al. did not observe the 1.272 MeV state in their study of the ^{64}Ni(p,α) reaction. Smit et al.(Sm 78) predicted that 1.28 and 1.65 MeV levels were of high spin state. The level at 1.666 MeV is also observed as one of the strongly excited states in the present study with L = 2 transfer.

The 1.287 and 1.665 MeV may therefore be compared with the theoretically predicted spin state $9/2^{-}$, $11/2^{-}$ the position

of the 1.665 MeV state is higher than the predicted one.

The level at 1.027 MeV with $J^{\pi} = 3/2^{-}$ is explained well by Satpathy et al.(Sa 68) and Stewart et al. (St 71). The levels at 2.247 MeV ($J^{\pi}= 1/2^{+}$), 3.573 MeV ($J^{\pi}= 3/2^{+}$) and 2.575 MeV ($J^{\pi}= 3/2^{+}$) observed by Blair et al.(Bl 66) in (t,α) reaction are well accounted for by Satpathy et al.(Sa 68). The levels at 1.623 MeV $J^{\pi}= 7/2^{-}$ and 1.65 MeV $J^{\pi}= 3/2^{-}$, $5/2^{-}$ identified by Coop et al.(Co 69,70) in (p,α) and in β-decay study by Bron et al.(Br 75) may be compared with the doublet of spin states $7/2^{-}$, $5/2^{-}$ predicted by Satpathy et al.(Sa 68). The observed levels at 1.325 MeV ($J^{\pi}=1/2^{-}$), 2.015 MeV ($J^{\pi}=3/2^{-}$, $5/2^{-}$), 2.37 MeV ($J^{\pi}=(1/2)^{-}$), 2.343 MeV ($J^{\pi}=7/2^{-}$) and 2.484 MeV (J =3/2, 5/2) are well accounted for by the calculations of Stewart et al.(St 71). The level at 3.343 MeV is excited in both (t,p) reactions (the present work and Hudson et al.(Hu 71)) through L = 0 + 2 and may be compared with the calculated level at 3.368 MeV ($J^{\pi}=7/2^{-}$) by Satpathy et al.(Sa 68). The observed levels at 1.20 MeV ($J^{\pi}=3/2^{-}$, $5/2^{-}$), 1.65 MeV ($J^{\pi}=3/2^{-}$, $5/2^{-}$), 1.623 MeV ($J^{\pi}=7/2^{-}$) are also well reproduced in the model of Stewart et al.(St 71).

Smit et al.(Sm 79) successfully calculated the level structure of ^{57}Co using semimicroscopic model. They have

predicted that satisfactory description of three transfer reaction can be obtained by extending the work of this model in this mass region. The hole states at 2.22 MeV ($J^{\pi}=1/2^{+}$) and 3.56 MeV ($J^{\pi}=3/2^{+}$) may be compared to the 2.247 MeV ($J^{\pi}=1/2^{+}$) and 3.573 MeV ($J^{\pi}=3/2^{+}$) levels observed by Blair et al.(Bl 66) in (t,α) reaction.

Hudson et al.(Hu 71) tried to explain the general features of the levels of ^{61}Co produced via (t,p) reaction by assuming a simple model. They described the ^{59}Co nucleus by an $f_{7/2}$ proton hole and four neutrons outside Z = N = 28 shell closure. When two neutrons transfer to ^{59}Co nuclei through (t,p) reaction, the ^{61}Co states can be reached by coupling the $f_{7/2}$ proton hole to two transferred neutrons generating states with $J^{\pi} = 0^{+}$, 2^{+} and 4^{+}.

Hudson et al. observed transitions below 2.24 MeV as pure L = 2 transitions followed by two L = 2 + 4 transfers ; several L = 2 transitions were afterwards observed upto 3.02 MeV. Thereafter only L = 2 + 4 transfers are found. They interpreted the result as follows : There are several neutron configurations that can be coupled to spin 2^{+}. But $(p_{3/2}, p_{1/2})$ and $(p_{1/2}, f_{5/2})$ would exhibit pure L = 2 character, when coupled to the $f_{7/2}$ proton hole. The

$(p_{3/2}, f_{5/2})$ and $(f_{5/2}, f_{5/2})$ configurations can be coupled to both 2^+ and 4^+ spin. Thus mixed transitions are possible. Among these L = 2 + 4 and L = 4 transitions occur.

The same sequence is also observed in the present (t,p) study.

CHAPTER 7

REACTION ^{102}Ru(t,p)

7.1 Introduction

The ^{104}Ru is an even-even nucleus and exhibits vibrational levels in low excitation energy. The information on the levels of ^{104}Ru is rather meagre. This nucleus has been studied only through the Coulomb excitation and β^-- decay.

The Coulomb excitation studies have identified the 362 keV level (Te 56, St 58) and 893 keV level (St 61). Later McGowan et al.(Mc 68) reported another level at 983 keV.

The level scheme of ^{104}Ru was studied by Zander et al. (Za 66), Pinston et al.(Pi 70), Tivin et al.(Ti 75 and Summerer et al. (Su 78a) through decay of Tc. The middle two measurements report levels upto 3.77 MeV and later upto 4.268 MeV. Pinston et al.(Pi 70) made J^π- assignments to several levels, some tentatively on basis of ground state ^{104}Tc as 2^-. Summerer et al.(Su 78b) deduced J^π- values of some low-lying levels upto 2.481 MeV by γ-γ correlation measurements.

The (t,p) reaction was therefore undertaken in an attempt

to provide spectroscopic information on ^{104}Ru, to examine whether the levels excited in β- decay may be populated in (t,p) reaction and also to extend the excitation above 4.268 MeV.

The theoretical calculation of the level structure of this nucleus is also rather inadequate and is calculated upto 1.8 MeV. The present experimental information may then guide to a future theoretical study.

7.2 Experimental Procedure

The emulsion plates exposed to the ^{104}Ru (t,p) reaction were scanned at the Nuclear Physics Laboratory, University of Dacca, Dacca. Although the entire length of the plates were scanned, the excitation energy could not be measured above E_x~5.08 MeV due to lousy spectra at high excitation energy. The proton groups corresponding to the ground state of ^{104}Ru could not be scanned at the first four angles because of emulsion disturbance. A typical spectrum at 11.25° is shown in fig. 7.1. The numbers adjacent to the peaks refer to the level numbering of table 7.3. Different contaminant groups are labeled with corresponding level energy in the residual nuclei. Energy calibrations were done using the least squares method

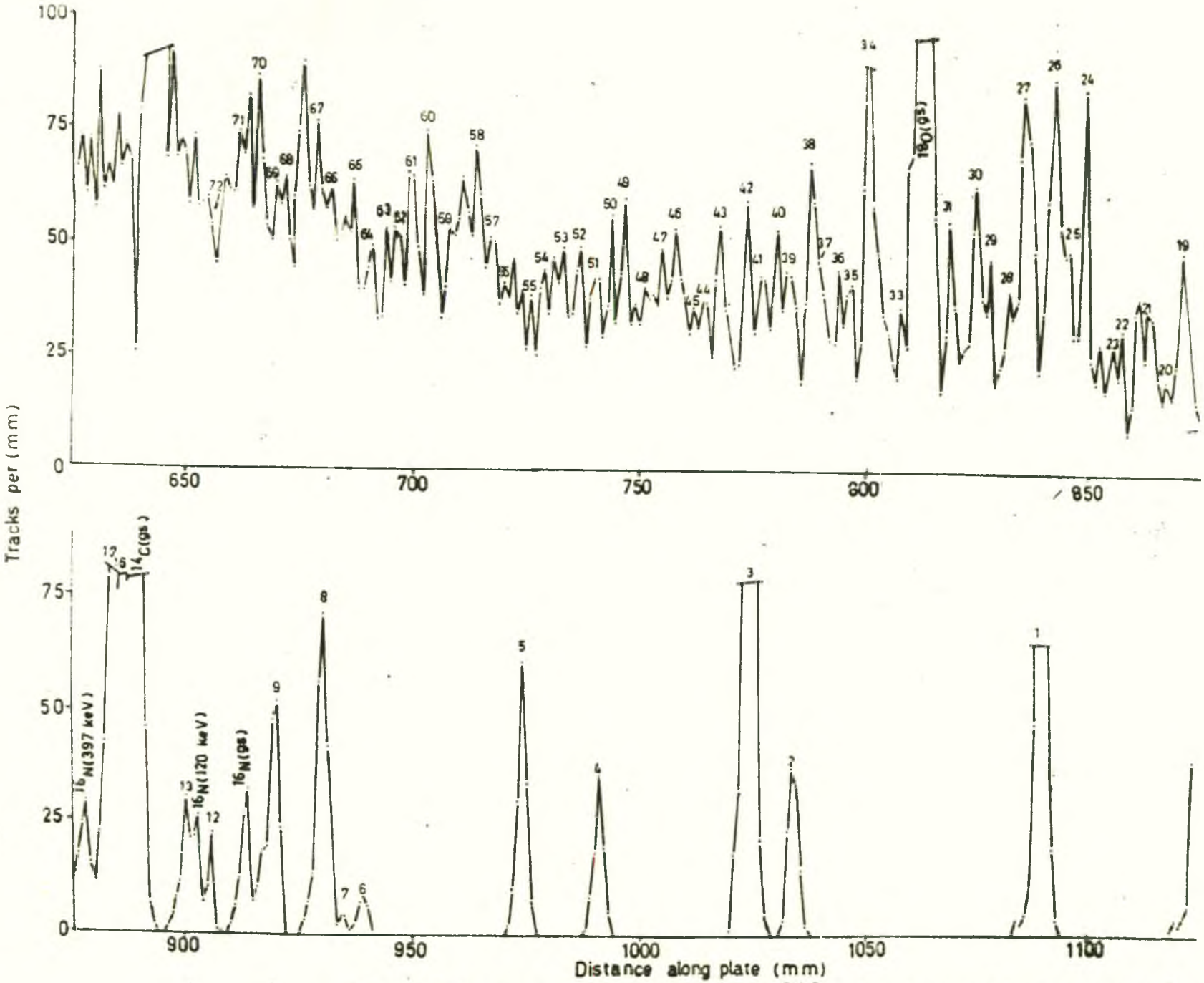

FIG. 7.1. Proton spectrum from ^{102}Ru(t,p) reaction at 11.75°.

at four angles using several known levels namely the levels at 0.352, 0.994, 1.981, 2.487 and 2.866 Mev (Sa 76) as discussed in Chapter 2, Section 2.6. These levels are shown underlined in table 7.3. The constants of the least squares fit are given in table 7.1. The overall resolution (FWHM) is ~20 keV. A total of 72 levels are identified upto E_x~5.08 MeV and angular distributions were measured for these levels. The relative cross sections were measured for each level as described in Chapter 2, Section 2.8.

7.3 DWBA Analysis

The DWBA analysis were performed for the ^{102}Ru(t,p) reaction with the code DWUCK of Kunz using the IBM 370/115 Computer at the Bangladesh University of Engineering and Technology, Dacca. The present author was helped by Professor H.M. Sen Gupta in these calculations.

The optical model potential was of the same form as in ^{59}Co(t,p) reaction (Chapter 6). Triton elastic scattering data are not available around E_t=15 MeV for Ru nuclei. Triton potential for set A was from elastic triton scattering from ^{116}Sn at 20 MeV (Ha 67) and set B from interpolation of neighbouring nuclei (Fl 69). The set C was actually refitted (De 75) with the requirement that the real radius and diffussivity parameters

Table 7.1

Constants of least squares fit for $^{102}Ru(t,p)$ reaction

Channel	a_o	a_1	a_2
2	14.006	-37.938	15.171
3	14.212	-39.082	16.377
4	13.915	-37.877	15.264
5	12.990	-33.557	9.055

r_o and a_o remain close to the corresponding values for the proton parameters. The real well depth for tritons is approximately three times the proton real well depth so that the well matching condition be satisfied.

Proton potential for set A was taken from elastic scattering of proton on ^{106}Pd at 13 MeV (Ro 66) and set B was from the global potential given by Becchetti and Greenlees (Be 69).

The potential parameters for set AA were earlier used in (d,t) reaction on ^{105}Pd at E_t= 17 MeV (Di 69) and sets BB and CB were used in the analysis of the ^{101}Rh(p,t) reaction by Del Vecchio (De 75). Real depth of bound state is adjusted to reproduce the binding energy. The potential parameters are given in table 7.2.

The bound state configurations were constructed on the basis of the simple shell model. The transferred neutrons are expected to be captured into $2d_{5/2}$, $2d_{3/2}$, $3s_{1/2}$, $1g_{7/2}$ and $1h_{11/2}$ levels. The configurations used for set AA in the DWBA calculations for different L-transfers are as follows :

Table 7.2

Optical model parameters used for the ^{102}Ru(t,p) reaction

Particle	Symbol	V (MeV)	r_o (fm)	a (fm)	W (MeV)	$4W_D$ (MeV)	r_1 (fm)	a_1 (fm)	r_e (fm)	Ref.
t	A	153.0	1.24	.70	20.8		1.42	.890	1.24	(Ha 67)
t	B	171.0	1.16	.752	16.5		1.498	.817	1.24	(Fl 69)
t	C	134.0	1.166	.784	14.0		1.55	.795	1.24	(De 75)
p	A	56.0	1.156	.804		40.2	1.355	.584	1.25	(Ro 66)
p	B	55.4	1.17	.75		36.02				(Be 69)
n		a)	1.25	.65	λ=25					

a) adjusted to reproduce the binding energy.

L = 0 : $\underline{(2d_{5/2}\ \ 2d_{5/2})}$

L = 1 : $\underline{(2d_{5/2}\ \ 2f_{7/2})}$, $(2g_{7/2}\ \ 2f_{7/2})$

L = 2 : $\underline{(1g_{7/2}\ \ 2d_{3/2})}$, $(1g_{7/2}\ \ 2d_{5/2})$, $(3s_{1/2}\ \ 2d_{3/2})$, $(1g_{7/2}\ \ 1g_{7/2})$

L = 3 : $\underline{(2d_{5/2}\ \ 1h_{11/2})}$, $(3s_{1/2}\ \ 2f_{7/2})$

L = 4 : $\underline{(1g_{7/2}\ \ 2s_{1/2})}$, $(1g_{7/2}\ \ 1g_{7/2})$

For each L-transfer the DWBA calculations were made with excitation energy E_x = 0, 2 and 4 MeV.

For sets BB and CB only the configurations (fig. 7.2) that are underlined above were used. DWBA calculations with the set AA were found to fit most of angular distribution, while some of the distributions not fitted by the set AA are well accounted for by sets BB and CB. The calculated angular distributions using the three sets are represented by solid line for set AA, dots for set BB and, dot and dash for set CB in the fig. 7.3.

7.4 Energy Levels of ^{104}Ru

The results of the reaction ^{102}Ru(t,p) are summarized in

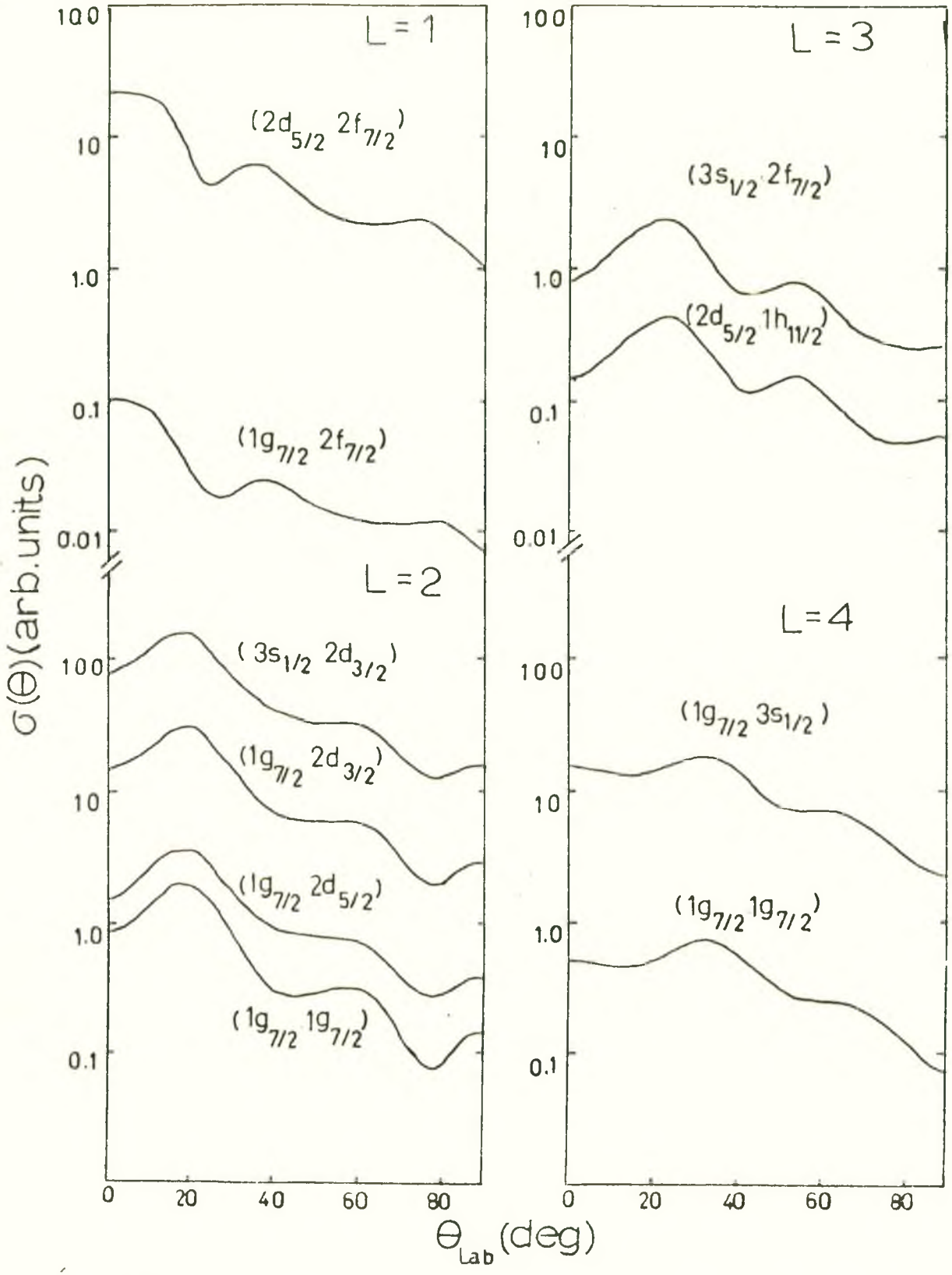

FIG. 7.2. DWBA curves with different configurations using parameter set AA.

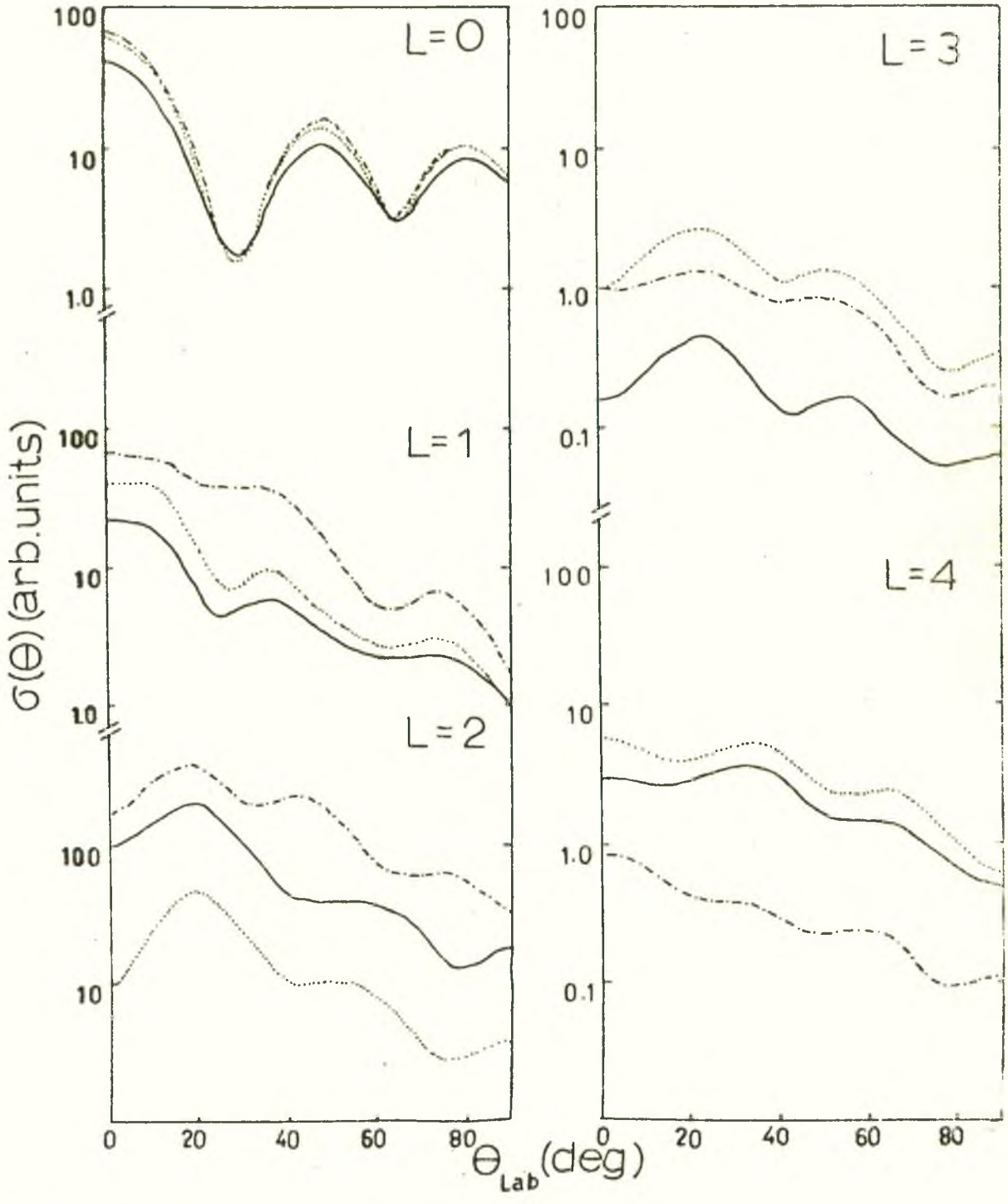

FIG. 7.3. DWBA curves with different potential parameters.

table 7.3. This table also includes for a comparison the excitation energy of the ^{104}Ru compiled by Samuelson et.al. (Sa 76). The energy values in the present work are significant to three decimal places except where shown otherwise.

Most of the adopted levels upto E_x~3.776 MeV (Sa 76) are identified in the present experiment. The levels at 1.504, 1.88, 1.979, 2.295, 2.487, 3.495 MeV found in the present study are in excellent agreement with previous β-decay studies (Pi 70, Ti 75, Su 78a). The first two β-decay experiments excite the levels at 2.55, 3.716 and 3.780 MeV of present study. The present (t,p) reaction populates states at 2.088, 2.17, 2.610, 3.016, 3.522 and 3.557 MeV which are identified in the β-decay study by Tivin et al.(Ti 75), whereas Summerer et al. (Su 78a) observed 2.088 and 2.610 MeV levels. The level at 3.463 MeV was found by Tivin et al.(Ti 75) and Zander et al. (Za 66) in the β-decay studies. The levels at 1.34, 2.387, 2.425, 3.36, 3.410, 3.61, 3.645, 3.68, 3.86 and 4.278 MeV excited in the present study, are not listed in the Nuclear Data Sheet (Sa 76). Among these, the 1.34, 3.36 and 3.645 MeV levels are observed by Pinston et al.(Pi 70) and rest are identified by Summerer et al.(Su 78a) in β-decay experiments.

In the present study fifteen new levels within E_x~3.778 MeV and twenty-seven levels above this are identified.

Table 7.3

Summary of the results of ^{104}Ru

Level	E_x (MeV) a)	E_x (MeV) b)	Cross Section arb.units a)	L-trans. a)	J^π a)	J^π c)
gs						0^+
1	0.353	0.358	450	2	2^+	2^+
		0.889				4^+
2	0.896	0.893	144	2	2^+	2^+
3	0.991	0.988	1881	(3)	(3^-)	0^+
		1.242				$3(2)^+$; 3^{+d}
4	1.34	1.355[e]	85	(1)	(1^-)	
5	1.504	1.502	134	1	1^-	$(3,4)^+, 3^d$
		1.515				2^d
		1.685				
6	1.81		89	(3)	(3^-)	
7	1.88	1.874	22	4	4^+	
		1.899[e]				
		1.933				
8	1.979	1.971	220	3	3^-	$(1,2)^+, 3^{-d}$
		1.933[e]				
		2.035				$(2,3)^\pm, 3^{-d}$
9	2.088	2.087	161	2	2^+	
		2.094[e]				$(1,2)^+$
10	2.17	2.175		n.a		

Table 7.3 (continued)

Level	E_x (MeV) a)	E_x (MeV) b)	Cross Section arb.units a)	L-trans. a)	J^π a)	J^π c)
11	2.20			n.a		
12	2.24		53	(4)	(4^+)	
		2.269				$(2,3)^+,3(4)^d$
13	2.295	2.289	99	3	3^-	$(2,3)^+,2^{+d}$
		2.329[f]				$(1,2,3)^d$
14	2.387	2.394[f]	56	n.s		3(1)
15	2.425	2.430[f]		n.s		
16	2.454		251	1	1^-	
		2.482[e,f]				$(2,3)^\pm$ 3^-
17	2.487	2.490	308	4,3	4,3	$(2,3)^\pm$
		2.524				
18	2.55	2.547	60	n.a		$(1,2)^\pm$
19	2.610	2.616	150	2	2^+	
20	2.66		69			
21	2.704		88	3	3^-	
		2.759[f]				
22	2.775		102	(4)	(4^+)	
23	2.801		133			
		2.823[e,f]				$(2,3)^\pm$
24	2.866		204	3	3^-	
		2.886				

Table 7.3 (continued)

Level	E_x (MeV)		Cross Section arb.units	L-trans.	J^π	
	a)	b)	a)	a)	a)	c)
25	2.904		100	n.s		
26	2.945		342	1	1^-	
27	3.016	3.016	265	2	2^+	
28	3.054		75	3	3^-	
		3.075[f]				
29	3.107		88	(2)	(2^+)	
30	3.144		155	3	3^-	
31	3.208	3.221	133	2	2^+	
32	3.293		161	(4)	(4^+)	
		3.334[f]				
		3.355				
33	3.36	3.369[e,f]	51	4	4^+	
34	3.410	3.414[f]	176	2	2^+	
		3.443				
35	3.463	3.462	108	1	1^-	
36	3.495	3.501	69	n.s		
		3.508				
37	3.522	3.513	37	n.a		
38	3.557	3.559	153	2	2^+	
		3.583				
		3.584[f]				

Table 7.3 (continued)

Level	E_x (MeV) a)	E_x (MeV) b)	Cross Section arb.units a)	L-trans. a)	J^π a)	J^π c)
39	3.61	3.618	135	2	2^+	
40	3.645	3.635[e]	87	3	3^-	$(1,2)^\pm$
41	3.68	3.677[f]	90	n.a		
42	3.716	3.712	114	(3)	(3^-)	$(1,2)^\pm$
43	3.780	3.776	109	(3)	(3^-)	$(1,2,3)^-$
44	3.822		83	3	3^-	
45	3.86	3.875[f]	79	n.s		
46	3.899		122	(3)	(3^-)	
47	3.941		78	2,4	2,4	
48	3.98		70	4	4^+	
49	4.037		70	n.s		
50	4.063			4	4^+	
51	4.111		108	2	2^+	
52	4.148		73	n.s		
53	4.193		91	2	2^+	
54	4.230		81	n.s		
55	4.278		109	n.s		
56	4.35		81	n.s		
57	4.38		75	n.s		
58	4.404		187	1	1^-	

Table 7.3 (continued)

Level	E_x (MeV)		Cross Section arb.units	L-trans.	J^π	
	a)	b)	a)	a)	a)	c)
59	4.478		107	2	2^+	
60	4.533		108	2	2^+	
61	4.584		117	n.s		
62	4.62		82	n.s		
63	4.65		99	4	4^+	
64	4.69		107	3	3^-	
65	4.73		86	4	4^+	
66	4.79		116	3	3^-	
67	4.83		201	2	2^+	
68	4.88		84	(3)	(3^-)	
69	4.93		108	3	3^-	
70	4.99		132	3	3^-	
71	5.02		207	1	1^-	
72	5.08		70	n.s		

a) Present work
b) Nuclear Data Sheet (Sa 76)
c) β-decay study by Pinston et al.(Pi 70)
d) β-decay study by Summerer et al.(Su 78b)
e) β-decay study (Pi 70) not included in the N.D.S.(Sa 76)
f) β-decay study (Su 78a)

The estimated errors in energies in present work are ± 15 keV.

7.5 Angular momentum transfer and spin parity assignment

The angular momentum transfers of the levels of ^{104}Ru are obtained by comparing the DWBA calculations with the measured distributions as listed in table 7.3. The best fits are shown in the figs. 7.4-7.7. For even-even target nuclei the spin parity of the ground state is $J_i^\pi = 0^+$, the residual states in (t,p) reactions thus have angular momentum.

$$J_f = L \text{ and parity } \Pi_f = (-1)^L$$

The J^π assignment is made for the levels whose angular distributions are well fitted by the DWBA calculations.

7.5.1 L = 1 transfer

Seven levels at 1.34, 1.504, 2.454, 2.945, 3.463, 4.404 and 5.02 MeV are obtained with L = 1 transfer (fig. 7.4) i.e. with $J^\pi = 1^-$. The angular distribution of the level at 1.34 MeV is poorly fitted by the DWBA calculations for all the three sets of optical model parameters. The level at 1.504 MeV observed with $J^\pi = 1^-$ in the present study (fig. 7.4) is in disagreement with the previous assignment of $J^\pi = (3,4)^+$ made by Pinston et al.(Pi 70) in the β - decay study.

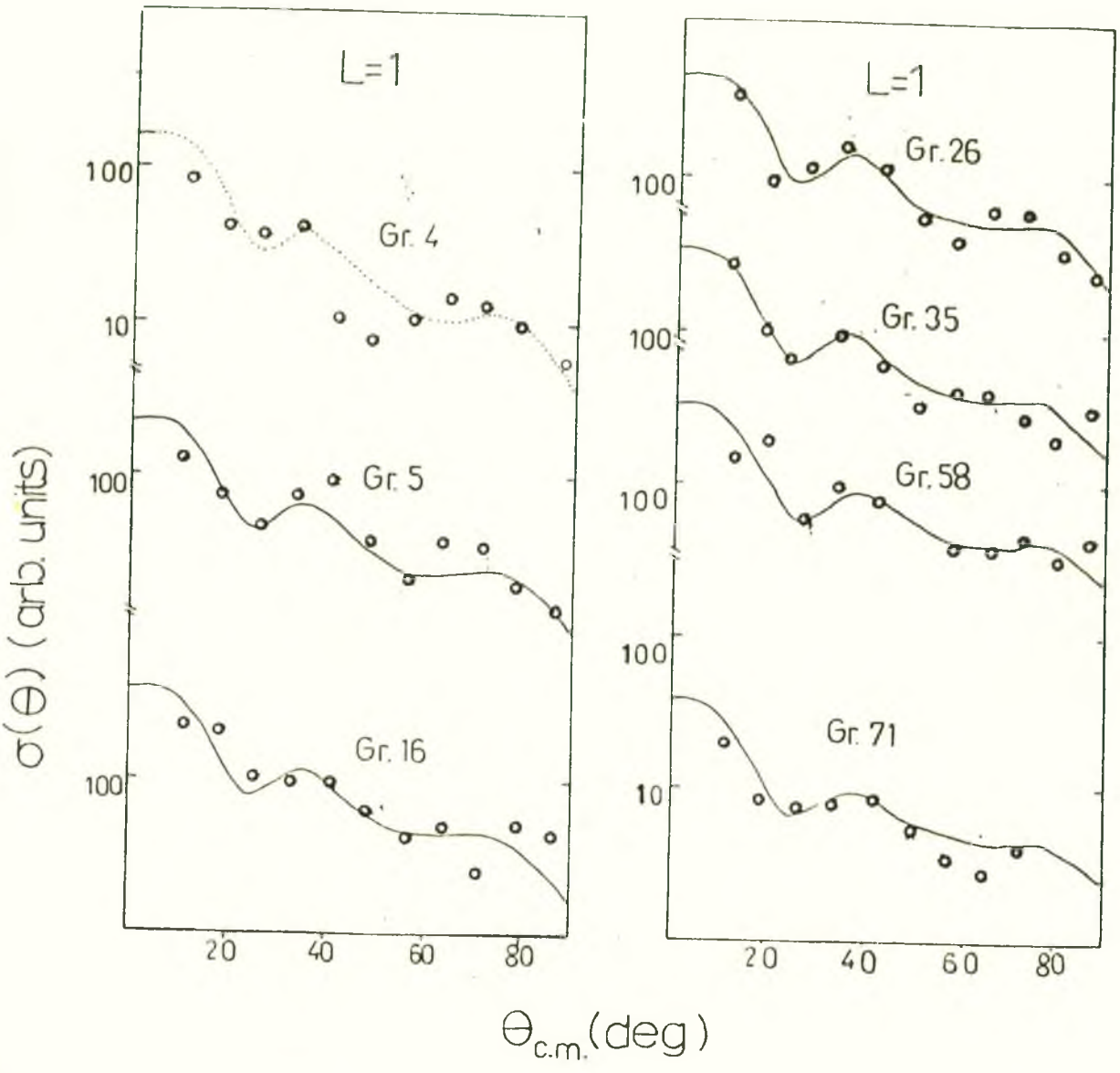

FIG. 7.4. Experimental angular distributions fitted with L=1 DWBA curves.

7.5.2 L = 2 transfer

Several levels are observed with L = 2 transition (fig. 7.5) as shown in table 7.3. The J^{π} assignment for these level is 2^{+}. The levels at 0.353 and 0.896 MeV show the characteristic feature of L = 2 transfer and the J^{π} assignment of the level 0.353 MeV is in agreement with previous β-decay study (Pi 70) and Coulomb excitation (Mc 68). The level at 0.896 MeV with $J^{\pi} = 2^{+}$ is an unresolved doublet of 0.882, $J^{\pi} = 2^{+}$ MeV observed in β-decay (Pi 70). The angular distribution of the level at 3.016 MeV is fitted partially by potential parameters of sets AA and CB. The angular distributions of the levels at 3.107, 4.111, 4.193, 4.78 and 4.533 MeV are reproduced through L = 2 transfer with set CB, with a poor fit to the level at 3.107 MeV.

7.5.3 L = 3 transfer

L = 3 transitions (fig. 7.6) are observed for several levels which give $J^{\pi} = 3^{-}$ as shown in table 7.3. The angular distributions of the levels at 0.991, 1.81 and 2.801 Mev are poorly fitted by L = 3 DWBA curves ; only general trends are observed. The tentative J^{π} assignment of 3^{-} for 0.991 MeV in the present experiment is not in agreement with the $J^{\pi} = 0^{+}$ assignment made in the β - decay (Pi 70) and Coulomb excitation

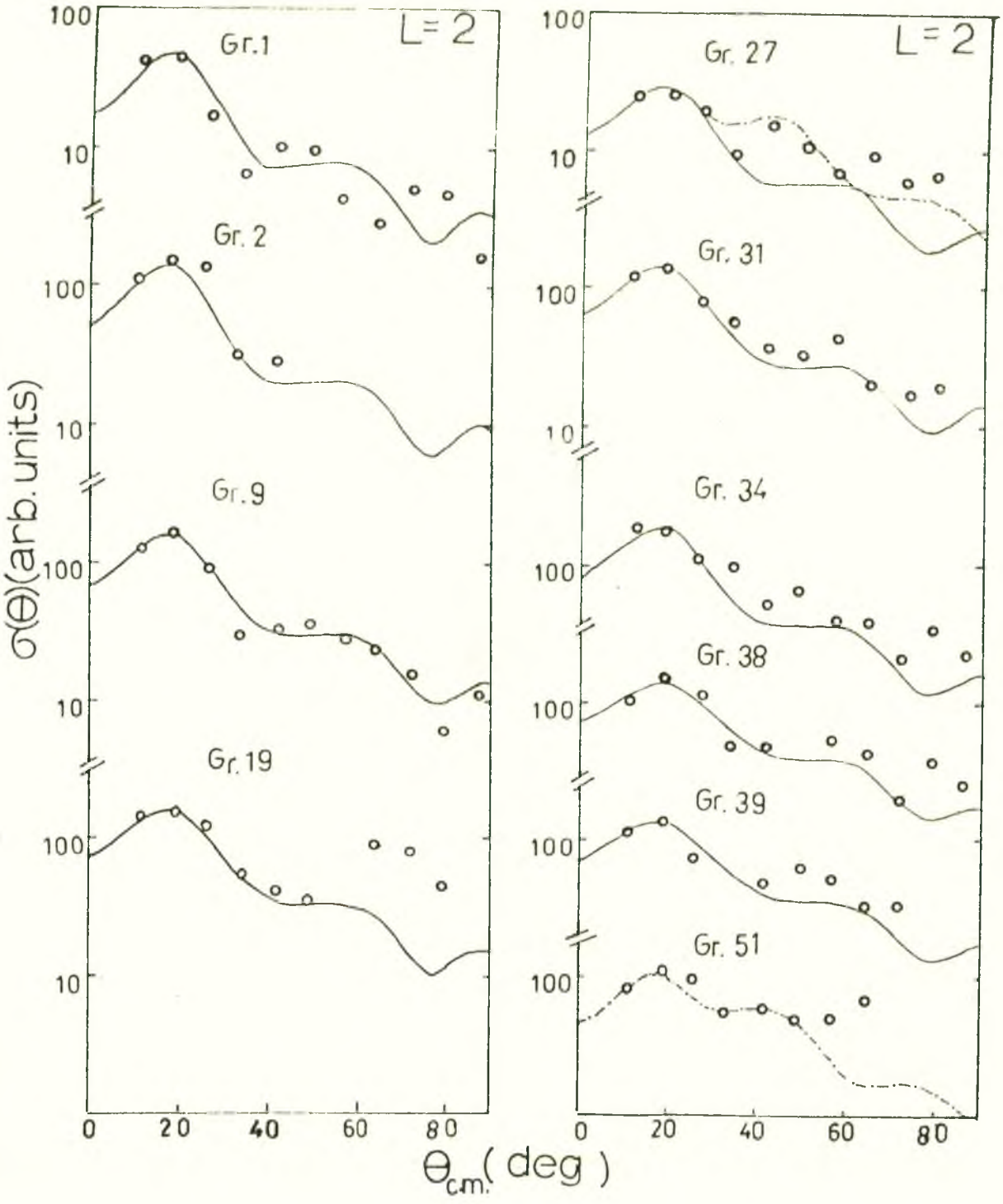

FIG. 7.5. Experimental angular distribution fitted with L=2 DWBA curves

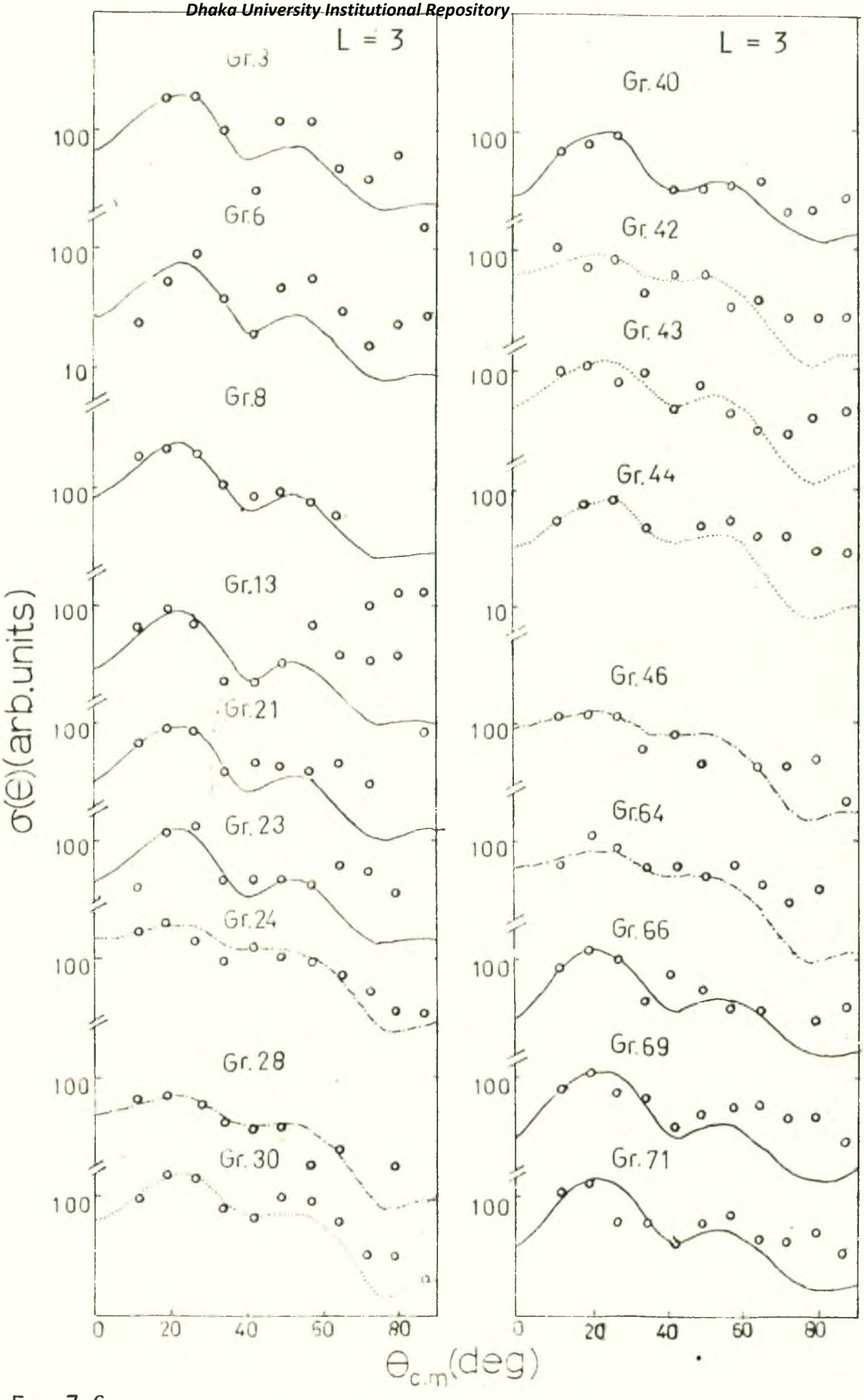

FIG.7.6. Experimental angular distributions fitted with L=3 DWBA curves.

(Mc 68) studies. The levels at 1.979, 2.295 and 3.61 MeV were observed by Pinston et al.(Pi 70) in β- decay work with $J^{\pi}= (1,2)^{+}$, $(2,3)^{+}$ and $(1,2)^{\pm}$ respectively. Sümmerer et al.(Su 78b) observed the levels at 1.979 and 2.285 MeV with $J^{\pi}= 3^{-}$ and 2^{+}. The J^{π} assignment for the level at 1.979 MeV in the present study is in agreement with Sümmerer et al.(Su 78b) and disagreement with that by Pinston et al. The level 2.295 MeV in the present work is observed with $J^{\pi} = 3^{-}$. Its J^{π} value is not in agreement with the J^{π} values of Pinston et al. and Sümmerer et al. Attempts were made to fit the angular distributions for the levels at 2.866, 3.054, 3.766, 3.899 and 4.69 MeV are with set CB. Among these the levels at 3.716 and 3.899 MeV are fitted poorly. The level at 3.716 was observed by Pinston et al. with $J^{\pi} = (1,2)^{\pm}$. On the otherhand the present value is (3^{-}). We tried to fit the angular distributions for the levels at 3.144, 3.780, 3.822 and 4.88 MeV with potential parameter set BB (fig. 7.6). Pinston et al. (Pi 70) identified the 3.780 MeV level as $J^{\pi} = (1,2,3)^{-}$. In the present study the level is assigned a $J^{\pi} = 3^{-}$ which is in agreement with one of the J^{π}- value of Pinston et al.

7.5.4 L = 4 transfer

Nine levels are identified as L = 4 transitions (fig. 7.7)

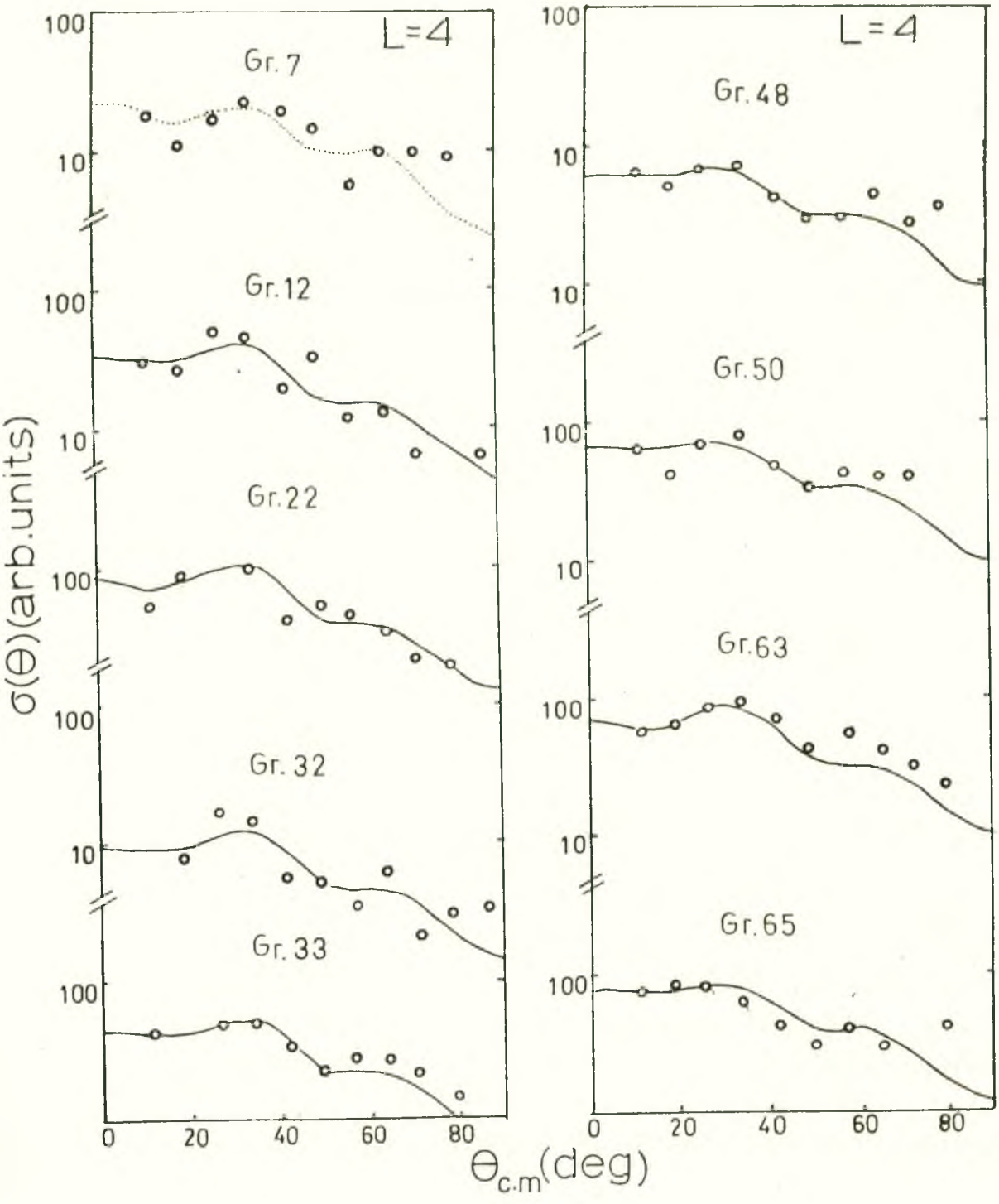

FIG. 7.7. Experimental angular distributions fitted with L=4 DWBA curves.

i.e. with $J^{\pi} = 4^{+}$. The level at 1.88 MeV is reproduced satisfactorily through L = 4 transition with set BB. Pinston et al. (Pi 70) assigned J^{π} of the level at 3.36 MeV as $(1,2)^{\pm}$. The present work on the otherhand assigns $J^{\pi} = 4^{+}$ to this level.

7.5.5 Ambiguous Level

The angular distribution of the level at 2.487 MeV is fitted by DWBA calculation with set AA through L = 4 and with set BB through L = 3 transfers (fig. 7.8). This level is observed with $J^{\pi} = (2,3)^{\pm}$ in the β - decay (Pi 70). Summerer et al. (Su 78b) observed level at 2.282 MeV and assigned it with $J^{\pi} = 3^{-}$. The level at 3.941 MeV is fairly given by both L = 2 and 4 transfers with set AA.

7.5.6 Non-stripping level

There are several levels showing no characteristics of a definite L-transfer. These states may perhaps be considered as being populated by a non-single step process or a compound reaction process.

7.6 Structure of ^{104}Ru

Observing certain regularities in the low-lying levels

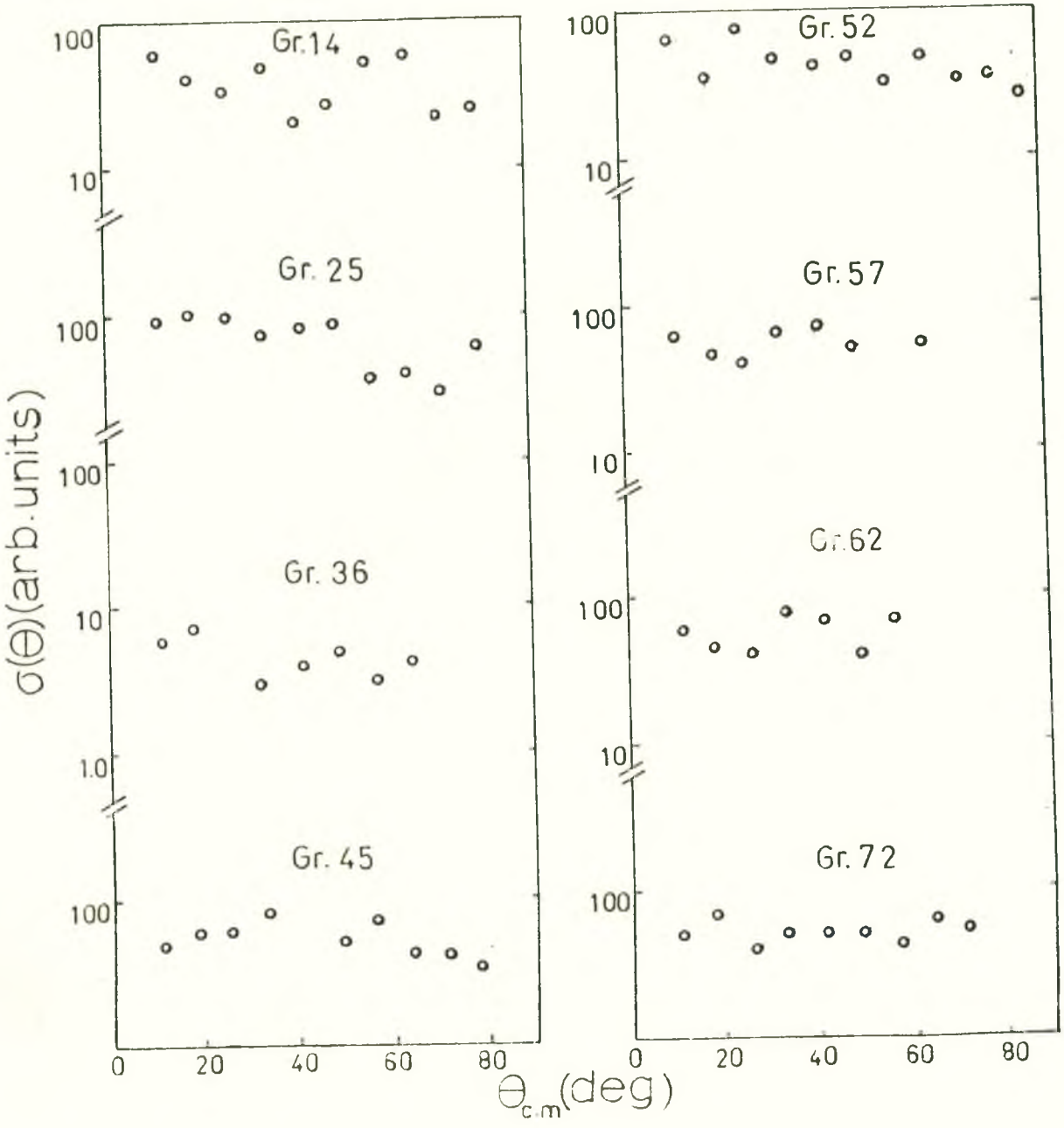

FIG. 7.9. Some of the measured angular distributions displaying a non-stripping character.

of even-even medium weight nuclei from Coulomb excitation Schraff et al. (Sch 55) suggested vibrational model based on Bohr-Mottelson weak to moderate coupling theory. In this model they calculated first and second excited states due to core excitation at $\hbar\omega, 2\hbar\omega$, above the ground state. The $2\hbar\omega$ is a degenerate triplet of character 0^+, 2^+, 4^+ of one phonon. The triplet states are at roughly twice the energy of the first 2^+ state.

There are some other models (Wi 58, Ra 59, Da 58) that were considered to explain the near harmonic spectra observed in the Coulomb excitation. With these models only a few low-lying levels of ^{104}Ru can be explained.

To describe the collective nature of spectra in ^{104}Ru, Summerer et al.(Su 78b) assumed the interacting Boson approximation (IBA)(Ar 76) and triaxial rotor (Da 68) with β-vibration in the vibrational model and also used generalized model (Gn 71) according to the calculation of Sedlmayer et al.(Se 76). In IBA model the level structure was calculated without a detailed knowledge of nuclear motion. The vibrational and rotational limits are obtained by solving analytically.

Besides the limiting cases of vibrator and rotator many

types of plausible nuclei were considered by Gneuss and Greiner (Gr 71) in generalized collective model, from the extreme cases of spherical vibrator and of the strongly deformed rotator. Each nucleus is assumed to have collective potential energy surface as function of collective coordinates to represent the nuclear structure.

In the present study the first and second 2^+ states observed at 0.353 and 0.896 MeV are predicted by all the models (Ar 76, Da 68, Su 78b, Se 76). The 4^+ state at 0.889 MeV observed in β- decay and Coulomb excitation studies, if excited in the present study is not resolved from the level at 0.896 MeV. In present work a level is observed at 0.991 MeV with $J^\pi = (3^-)$, but because of this J-value the level may not be the same as the one predicted by theory at 0.998 MeV with $J^\pi = 0^+$. The level at 1.80 and 2.088 MeV with $J^\pi = 4^+$ and 2^+ respectively observed in the present study are explained by the model of Summerer et al.(Su 78b) and Sedlmayer et al. (Se 76). The predicted positions of these two levels are found to be lower than those observed. The levels at 1.242 MeV ($J^\pi = 3^+$) is well accounted for by the model of Summerer et al. (Su 78b) and of Sedlmayer et al.(Se 76). The agreement between theory and experiment is roughly the same for each of the models discussed (Da 68, Se 76, Ar 76, Su 78b). Summerer et al. (Su 78b)

stresses the need to consider two quasi-particle configurations into the theoretical model to describe the states above the two-phonon triplet.

The other vibrational levels are excited in present (t,p) reaction with $J^{\pi}= 3^{-}$ at 1.81, 1.971, 2.295 MeV etc. and $J^{\pi}= 1^{-}$ at 1.34, 1.504, 2.454, 2.945 MeV etc. The present (t,p) work may be considered to be helpful for a further theoretical study, including levels at high excitation.

CHAPTER 8

Conclusion

The present work is concerned with the studies of (^{3}He,d) reactions on ^{56}Fe and ^{45}Sc, and (t,p) reactions on ^{59}Co and ^{102}Ru. The angular distributions have been measured for most of the levels of ^{57}Co and ^{46}Ti covering an excitation ~7.8 and ~9.9 MeV from (^{3}He,d) reactions and ^{61}Co and ^{104}Ru upto an excitation ~5.23 MeV and ~5.08 MeV from (t,p) reactions.

The level properties were tried to explain on the basis of theoretical calculations as far as possible.

The absolute cross section for the (^{3}He,d) reactions have been measured fairly accurately. More assignments of orbital angular momentum transfers have been made in the present experiment than previous ones, particularly for levels at higher excitation. The ℓ = 1 and 3 strengths are distributed over the entire range of excitation studied. The spectroscopic strengths have been obtained for them level by level.

The spectroscopic strength for 2p and $1f_{7/2}$ transitions for the case of ^{57}Co lies between that given in the previous two measurements (Ro 67, Ha 72), while that for the $1f_{5/2}$ levels given by present work, is the smallest of all (^{3}He,d) and (d,n) values. The summed 2p, $T_<$ strengths obtained in present study and Rosner and Hollrow (Ro 67) are fairly consistent with the shell model limit, whilst those given by Hardie et al.(Ha 72) and Adam et al.(Ad 76) are much smaller than the expected value. The splitting of the measured 2p, $T_<$ strength into $p_{3/2}$ and $p_{1/2}$ components is difficult ; the summed strengths for these components are far from respective single particle limits. The $1f_{7/2}$, $T_<$ transition strength given by Hardie et al.(Ha 72) is only 50% of the expected value, while that given by the present and the remaining experiments are in reasonable agreement with the sum rule limit. The measured $1f_{5/2}$, $T_<$ strengths in the present case and those by Hardie et al. are appreciably smaller than the expected value, while those given by Rosner and Hollrow (Ro 67) and Adam et al.(Ad 76) are in satisfactory agreement with the shell model value. A choice of a different optical model parameter combinations somewhat increases the present $1f_{5/2}$ value, but the change is not sufficient to bring the measured value close to the theoretical limit. It would be interesting to calculate the transition strengths on the pairing theory, which gives a more realistic

picture of the nuclear structure than the simple shell model.

A similar sum rule analysis for the $^{45}Sc(^{3}He,d)^{46}Ti$ reaction is made assuming only the $2p_{3/2}$ and $1f_{7/2}$ shell model states for ℓ = 1 and 3 transitions respectively. The splitting of 2p, $T_<$ strength into $2p_{1/2}$ and $2p_{3/2}$ components and 1f, $T_<$ strengths into $1f_{5/2}$ and $1f_{7/2}$ components are difficult. The $T_<$ components of the total 1f and 2p strength are obtained as 6.3 and 3.7 as against the respective single particle limits 10.5 and 4.5. The spectroscopic strengths for ℓ=3 and ℓ=1 transition increase by about 60% and 20% as found by DWBA calculation when the contribution from $f_{5/2}$ and $p_{1/2}$ strengths are considered and the sum strengths come closer to shell model values for ℓ=3 and further closer for ℓ=1 transition. On the other hand Broman and Pullen (Br 68) obtained the values that are closer to the expected ones assuming all the relevant strength as belonging to the $1f_{7/2}$ and $2p_{3/2}$ shell model states. If one considers the excitation of the $p_{1/2}$ and $f_{5/2}$ shell in ℓ=1 and 3 transition a similar increase in the measured spectroscopic strengths would be observed in their results also and in that case the agreement of the observed values with the single particle limit may not be that good. The positions of only a few low-lying positive parity levels are given by MBZ model. For such levels the transition strengths given by the present

experiment, except for the 0.899 MeV level, are in close agreement with the MBZ model.

Three analogue states for ^{57}Co in agreement with Rosner Holbrow (Ro 67), and four for ^{46}Ti have been identified in the present work ; the relative spacings and the ℓ_p values are consistent with the relative spacings and the J^{π}values of the corresponding parent levels. The Coulomb displacement energy for the isobaric pair of nuclei ^{57}Fe - ^{57}Co comes to be 8.89 MeV for the ground state analogue and 7.63 MeV for the isobaric pair nuclei ^{46}Sc - ^{46}Ti.

Few new levels in ^{61}Co and several in ^{104}Ru have been identified which are not included in the compilation upto 3.365 MeV and 3.776 MeV respectively. Most of the levels in ^{61}Co covering E_x upto 3.74 MeV observed in previous works are excited in the present (t,p) reaction and above E_x=3.976 MeV all levels are new. Hudson et al.(Hu 71) studied the ^{59}Co(t,p) reaction upto 3.976 MeV. Except a few levels most of the levels are populated in the present (t,p) reaction and the excitation energies are in excellent agreement with them. The ^{102}Ru(t, p) reaction populates most of the levels upto E_x=3.776 MeV observed previously in β-decay studies and above this no previous study was made. Several new levels are

observed in the ^{102}Ru (t,p) reaction that have not been identified in the β-decay studies (Pi 70, Ti 75).

In the study of the present $^{59}Co(t,p)$ and $^{102}Ru(t,p)$ reaction the absolute cross sections were not measured and the relative values of angular distributions are obtained. The angular distributions are fitted well by the DWBA calculations. The J^{π}-values/limits are assigned for most of the levels in ^{61}Co and ^{104}Ru upto E_x= 5.23 and 5.08 MeV respectively. The L-assignments in $^{59}Co(t,p)$ reactions in the present study are in agreement with most of L-values measured by Hudson et al. (Hu 71) in (t,p) reaction. Some definite J^{π}- assignments are made for levels having L=0 transfer. Some of the proposed spin limits and parity assignments are found to be consistent with the previously measured values from $^{62}Ni(t,\alpha)$ reaction (Bl 66, Hu 71), β-decay study (Bo 75) and $(p,\alpha\gamma)$ reaction (co 70), as well as the compilation by Mateja et al.(Ma 76) upto an excitation of 3.95 MeV. The present study also gives evidence for the existence of missing high spin states predicted by theoretical calculations.

The only previous information on the J^{π}-values of ^{104} Ru levels is obtained tentatively from β-decay study by Pinston et al.(Pi 70) upto E_x = 3.776 MeV and Summerer et al. (Su 78b)

upto 2.48 MeV. Some of the spin and parity assignments from the present work are consistent with their observed values (Pi 70, Su 78b). The present J^{π}- values for two levels are consistent with those in the compilation by Samuelson et al. (Sa 76).

There have been several calculations to obtain the level scheme, level properties and electromagnetic transition rates of ^{57}Co based on shell model and unified model and of ^{61}Co with unified model. The unified model calculations by Stewart et al. (St 71) satisfactorily reproduce all the observed levels for both the nuclei (^{57}Co and ^{61}Co) upto E_x = 2.3 MeV ; the predicted level density above E_x ~2.3 MeV is less than that observed. The unified model, however, does not calculate the spectroscopic factors relevant to the proton stripping reactions. This seems important in view of the fairly accurate cross sections obtained in the present work. The shell model transition strength calculated by Gómez (Go 72) is not satisfactory except for the ground state.

The level structure of ^{46}Ti has been investigated based on a model of nucleon-nucleon interaction in the ($1f_{7/2}$) shell, outside the ^{40}Ca core and no shell above $1f_{7/2}$ is included.

The simple model may thus be considered to give a reasonable account of only some of the low-lying positive parity levels in ^{46}Ti. At higher excitation the observed level density exceeds that given by the theory and the occurrence of negative parity states and a few 0^+ and 2^+ states at low excitation certainly calls for an extension of the model space so as to include more complicated configurations. One such attempt is the calculations using an augmented basis of 6 particles and 8p-2h configurations, but in a deformed basis rather than difficult full $(fp)^6$, by Skouras. An additional 0^+ states is thereby accounted for.

The theoretical work based on vibrational model, on level scheme of ^{104}Ru is so limited that only a few levels are explained.

REFERENCES

Ad 76 A.Adam, O.Bersillon and S.Joly, Phys.Rev.C14(1976)92

Ar 76 A.Arima and F.Iachello, Ann.of Phys.99(1976)253

At 68 J.Atkinson, L.G.Mann, K.G.Tirsell and S.D.Bloom, Nucl.Phys. A114(1968)143

Au 75 R.L.Auble, Nucl.Data Sheet 16(1975)13

Au 77 R.L.Auble, Nucl.Data Sheet 20(1977)327

Au 78 R.L.Auble, Nucl.Data Sheet 24(1978)1

Ba 66 R.H.Bassel, Phys.Rev. 149(1966)791

Ba 68 R.W.Barnard and G.D.Jones, Nucl.Phys. A111(1968)17

Ba 75 A.Baghdadi, R.Seltz, D.Magnac-Valette, G.Bonneaud and C.Gerardin, Nucl.Phys. A253(1975)20

Be 69 F.D.Becchetti and G.W.Greenlees, Phys.Rev. 182(1969)1190

Bl 66 A.G.Blair and D.D.Armstrong, Phys.Rev. 151(1966)930

Bo 68 N.Bouchard and B.Cujec, Nucl.Phys. 108(1968)529

Br 68 L.Broman and D.C.Pullen, Nucl.Phys. A110(1968)161

Br 71 L.Broman and C.Larsson, Z.Phys. 242(1971)360

Br 75 J.Bron, H.W.Jongsma and H.Verhuel, Phys.Rev.C11(1975)966

Ch 74 J.D.Childs, W.W.Daehnick and M.J.Spisak, Phys.Rev. C10(1974)217

Co 67 J.A.Cookson and D.Dandy, Nucl.Phys. 97(1967)232

Co 69 K.L.Coop, I.G.Graham, J.M.Poate and E.W.Tittarton, Nucl.Phys. A130(1969)223

Co 69 R.G.Couch, Ph.D.Thesis, Northwestern University (1969) unpublished (quoted in ref. Ad 76)

Co 70 K.L.Coop, I.G.Graham and E.W.Tittarton, Nucl.Phys. A150(1970)546

Co 71 A.Covello and V.R.Manfredi, Phys.Letts. 34B(1971)584

Cu 62 B.Cujec, Phys.Rev. 128(1962)2303

Da 58 A.S.Davydov and G.F.Filippov, Nucl.Phys. 8(1958)237

Da 68 A.S.Davydov, Atomic Energy Rev. 6(1968)No.2 and references therein.

Da 71 R.Dayras, M.Toulemonde, B.Cujec, B.Hausch, J.N.Moc and I.M.Szöghy, Nucl.Phys. A173(1971)49

De 73 W.Denhardt, O.C.Kistner, W.Kutschera and H.J.Sann, Phys.Rev. C7(1973)1471

De 75 R.M.DelVecchio, R.A.Naumann, J.R.Duray and H.Hubel, Phys.Rev. C12(1975)69

Di 69 D.L.Dittmer and W.W.Deahnick, Phys.Rev.187(1969)1553

Dr 78 G.D.Dracoulis, D.C.Radford and A.R.Poletti, J.Phys. G4(1978)1323

Es 74 M.T.Esat, J.R.Leslie and W.McLatchie, Nucl.Phys. A232(1974)139

Fa 71 H.Faraggi, M.C.Lemaire, J.M.Loiseaux, M.C.Mermaz, A.Papineau, Phys.Rev. C4(1971)1375

Fl 69 E.R.Flynn, D.D.Armstrong, J.G.Beery and A.G.Blair, Phys.Rev. 182(1969)1113

Fo 76 G.Fortuna, R.B.Hüber, W.Kutschera, M.Morando, H.Morinaga, R.A.Ricci and C.Signorini, Nuovo Cim 34A(1976)321

Ga 69 C.C.Gatrousis, R.A.Mayer, L.G.Mann and J.B.McGrory, Phys.Rev. 810(1969)440

Ga 71 A.Gallmann, G.Guillaume, N.E.Davison, P.Wagner and G.Frank, Nucl.Phys. A166(1971)271

Gl 65 N.K.Glendenning, Phys.Rev. 137(1965)B102

Gn 71 G.Gneuss and W.Greiner, Nucl.Phys.A171(1971)449

Gó 72 J.M.G.Gómez, Phys.Rev. C6(1972)149

Gr 67 H.A.Grench, K.L.Coop and H.O.Menlove,Phys.Rev.161(1967)1118

Gu 67 S.C.Gujrati and S.K.Mukherjee, Phys.Rev.159(1969)909

Ha 67 J.C.Hafele, K.R.Flynn and A.G.Blair, Phys.Rev. 155(1967)1238

Ha 72 G.Hardie, T.H.Braid, L.Meyer-Schützmeister and J.W.Smith, Phys.Rev. C5(1972)1600

Ho 73 H.Horie and K.Ogawa, Nucl.Phys. A216(1973)407

Hu 71 F.M.Hudson and R.N.Glover, Nucl.Phys. A160(1971)480

Ka 64 E.Kashy and T.W.Conlon, Phys.Rev.135(1964)B389

Ko 72 D.H.Kong-A-Siou, F.J.Braundet, J.F.Longequeue, N.Longequeue and B.Vignon, Nucl.Phys.A197(1972)568

Ku 78 W.Kutschera, B.A.Brown and K.Ogawa, Riv.Nuvovo Cim 1(1978)No.12 P.1

Le 68 C.W.Lewis, J.N.Mo, C.F.Monahan, M.I.Thomas and P.J.Twin, Nucl.Phys. 107(1968)273

Le 71 J.R.Leslie, W.McLatchie, C.F.Monahan and J.K.Thrasher Nucl.Phys. A170(1971)115

Le 78 C.M.Lederer and V.S.Shirley, Tables of Isotopes -- ed (1978) (John Willey and Sons Inc.) P.120

Li 67 K.W.A.Lingeman, J.Konizn, F.Diederix and B.J.Meizer, Nucl.Phys. 100(1967)136

Ma 67 J.V.Maher, K.A.Erb, R.W.Miller, Phys.Rev. C7(1967)651

Ma 69 G.Mairle, G.Th.Kaschl, H.Link, H.Mackh, U.Schmidt-Rohr, G.J.Wagner and P.Turek, Nucl.Phys. A134(1969)180

Ma 72 W.Makafske, G.W.Greenlees, H.S.Liers and G.J.Pyle, Phys.Rev. C5(1972)780

Ma 76 J.F.Mateja, J.A.Biezk, J.T.Meek, J.D.Goss, A.A.Rollefson, P.L.Jolivette and C.P.Browne, Phys.Rev. C13(1976)2269

Mc 64 J.D.McCullen, B.F.Bayman and L.Zamick, Phys.Rev. 134(1964)B515

Mc 67 J.B.McGrory, Phys.Rev. 160(1969)915

Mc 68 F.K.McGowan, R.L.Robinson and P.H.Stelson, Nucl.Phys. A113(1968)B515

Mi 62 R.Middelton and S.Hinds, Nucl.Phys.34(1962)404

Mo 66 J.N.Mo, P.J.Twin, J.C.Willmott, Nucl.Phys.89(1966)686

Na 78 H.Nann, E.R.Flynn, D.L.Hunsa and S.Raman, Phys.Rev. C18(1978)2511

O'B70 B.J.O'Brien and G.E.Coote, Nucl.Phys. A153(1970)593

Oh 68 H.Ohmura, T.Ishimatsu, K.Yagi, H.Efri, Y.Nakajima, T.Tohel and T.Nakagawa, J.Phys.Soc.Japan 25(1968)953

Ok 68 V.V.Okorokov, V.M.Serezhin, V.A.Smotryaev, D.L.Tolchenkov, I.S.Trostin and Yu.N.Cheblukov, ITEF Report (1968)598 (quoted in ref. Ad 76)

Pe 63 C.M.Perey and F.G.Perey, Phys.Rev. 132(1963)755

Pe 6 F.G.Perey, Phys.Rev. 131(1965)745

Pe 68 R.J.Peterson, D.M.Perlman, Nucl.Phys. A117(1968)185

Pi 70 J.A.Pinston, J.Blachot and F.Schussler, Nucl.Phys. A157(1970)323

Pi 73 P.Pietrzyk, K.D.Büchs, E.Finckh, W.Fritsch and B.Schrieber, Z.Phys. 262(1973)239

Pr 69 J.R.Priest and J.S.Vincent, Phys.Rev. 182(1969)1121

Ra 59 B.J.Raj, Phys.Rev. A114(1959)1116

Ra 66 J.Rapaport, A.Sperdoto and W.W.Buechner, Phys.Rev. 151(1966)939

Ra 73 J.Rapaport, J.B.Ball and R.L.Auble, Nucl.Phys. A208(1973)37

Ro 66 R.L.Robinson, J.L.Ford, P.H.Stelson and G.R.Stachler, Phys.Rev. 146(1966)816

Ro 67 B.Rosner and C.H.Holbrow, Phys.Rev. 154(1967)1080

Ro 81 J.N.Roy, A.R.Majumder, H.M.Sen Gupta and F.Watt, Private Communications(1981)unpublished

Sa 64 G.R.Satchler, Nucl.Phys.55(1964)1

Sa 68 L.Satpathy and S.C.Gujrathi, Nucl.Phys. A110(1968)400

Sa 75 Saleh-el-Kateb and G.M.Griffiths, Nucl.Phys.A240(1975)120

Sa 76 L.E.Samuelson, W.H.Kelly, R.L.Auble and W.C.McHarris, Nucl.Data Sheet 18(1976)125

Sc 55 G.Scharff-Goldhaber and J.Weneser, Phys.Rev.98(1955)212

Se 76 M.Sedlmayer, Doctoral Dissertation, Univ.Frankfurt. (1976) (quoted in ref. Su 78)

Sk 75 L.D.Skouras, J.Phys. GI(1975)438

Sm 79 J.W.Smits, R.H.Siemsen, S.Y.VanDer Werf and A.VanDer Woude, NuclPhys. A319(1979)29

St 58 P.H.Stelson and F.K.McGowan, Phys.Rev.110(1958)489

St 61 P.H.Stelson and F.K.McGowan, Phys.Rev.121(1961)209

St 66 J.E.Strain and W.J.Ross, J.Inor.Nucl.Chem.28(1966)2075

St 67 R.Stock, B.Bock, P.David, H.H.Duhm and T.Tamura, Nucl.Phys. A104(1967)136

St 71 K.W.C.Stewart, B.Castel and B.P.Singh, Phys.Rev. C4(1971)2131

Su 78a K.Sümmerer, N.Kaffrell and N.Trautmann, Nucl.Phys. A308(1978)1

Su 78b K.Sümmerer, N.Kaffrell, H.Otto, P.Peuser and N.Trautmann, Z.Phys. A287(1978)287

Te 56 G.T.Temmer and N.P.Heydenburg, Phys.Rev.104(1956)967

Ti 75 P.J.Tivin, R.L.Schults and H.W.Taylor, Z.Phys. A273(1975)339

Ve 66 J.Vervier, Nucl.Phys. 78(1966)497

Wi 56 L.Wilets and M.Jean, Phys.Rev. 102(1956)788

Yn 62 J.L.Yntema, Phys.Rev. 127(1962)1959

Za 66 A.R.Zander, P.R.Gray and T.G.Ebrey, Nucl.Phys. 75(1966)209

ACKNOWLEDGEMENT

It is a great pleasure for me to express my sincere and heartfelt gratitude to Professor Hironmay Sen Gupta for his ungrudging help and constant guidance towards the completion of my thesis.

I owe a deep depth of gratitude to Professor Quamrun Nessa Begum, Chairman, Department of Physics, Dacca University, and Professor Harunur Rashid, and Professor Mahtasem Hossain, formerly Chairman of the same Department for their generous suggestions and encouragement as well as providing me all necessary facilities for carrying out my work.

I am indebted to Professor Abdul Matin Patwary, Director, Computer Centre, University of Engineering and Technology, Dacca, for allowing me to use the computer for DWBA calculations as well as the authorities of Atomic Energy Centre, Dacca, for providing me much-needed computer and library facilities.

I wish to express my sincere thanks to my colleagues and friends for their generous assistance and constant encouragements.

I also whole heartedly thank Mrs. Momtaz Begum, Mrs. Salma Yasmin and Mrs. Mahfuza Begum for their readiness and eagerness in some of my scanning works.

I am also indebted to Mr. Md.Mosharraf Hosain for his carefully typing out my thesis.

APENDIX

1.E.1: 2.G

Nuclear Physics **A307** (1978) 106–124; © *North-Holland Publishing Co., Amsterdam*

A STUDY OF THE LEVEL PROPERTIES OF ^{57}Co FROM THE (τ, d) REACTION ON ^{56}Fe

HAMIDA BANU and H. M. SEN GUPTA

Department of Physics, University of Dacca, Dacca, Bangladesh

and

F. WATT

Nuclear Physics Laboratory, Keble Road, Oxford, England

Received 5 May 1978

Abstract: The ^{56}Fe(τ, d)^{57}Co reaction has been studied at E_τ = 18 MeV using the Tandem Van de Graaff accelerator and the multichannel magnetic spectrograph of the Nuclear Physics Laboratory, Oxford. Angular distributions have been measured for most of the levels up to $E_x \approx 7.8$ MeV and are analysed in terms of the DWBA theory of direct reactions. The l_p values and the transition strengths compared with available theories.

E NUCLEAR REACTION ^{56}Fe(τ, d), $E = 18$ MeV; measured $\sigma(E_d, \theta)$. ^{57}Co deduced levels, l, J, π, C^2S. Enriched target.

1. Introduction

The level structure of ^{57}Co has been the subject of a number of experimental investigations through several nuclear reaction processes such as ^{54}Fe(α, p), ^{56}Fe(p, γ), ^{56}Fe(d, n), ^{56}Fe(τ, d), ^{57}Fe(p, n), ^{58}Ni(t, α), ^{60}Ni(α, p) and ^{58}Ni(d, τ), and β-decay studies from ^{57}Ni, as has been summarized recently by Auble [1]. The object of the present investigation is to study the single-particle proton states in ^{57}Co by means of the (τ, d) reaction on ^{56}Fe; such information is a desirable supplement to the existing data.

The ^{56}Fe(τ, d) reaction was previously studied by Rosner and Holbrow [2] at E_τ = 16.5 MeV and later by Hardie *et al.* [3] at E_τ = 22 MeV. The orbital angular momentum transfers in the two experiments, with a few exceptions, are in general in agreement with each other; but there is a systematically large variation in the spectroscopic factors between the two measurements, sometimes by a factor of 3 or more, even for strong transitions. Different conclusions were consequently drawn in the two works. A more recent (τ, d) investigation due to Baghdadi *et al.* [4] at E_τ = 6 MeV was concerned only with the lowest three 2p transitions, two of which carry the major part of the $p_{\frac{3}{2}}$ and $p_{\frac{1}{2}}$ single-particle strengths. The spectroscopic factors were

found to be closer to those by Rosner and Holbrow [2]) than to those by Hardie *et al.* [3]). The ^{56}Fe(d, n) reaction has been recently studied by Adam *et al.* [5]) covering an excitation energy of 4.8 MeV; the spectroscopic factors are close to those given by Rosner and Holbrow for some levels and close to those given by Hardie *et al.* for some others. Earlier (d, n) reactions [6,7]) as quoted in ref. [5]) were concerned with a few low-lying levels. The present work was therefore undertaken to reexamine the level properties of ^{57}Co through the ^{56}Fe(τ, d) reaction at E_τ = 18 MeV and special care was taken for the measurement of the absolute cross section.

2. Experimental procedure

The experiment was carried out with a beam of ^{3}He particles obtained from the Tandem Van de Graaff accelerator of the University of Oxford. The target was prepared by vacuum deposition of Fe_2O_3 (isotopically enriched to 99.5 % of ^{56}Fe) onto a thin carbon backing. The reaction products, after momentum analysis in a magnetic spectrograph, were detected in 25 μm thick Ilford L4 nuclear emulsion placed at the focal plane of the spectrograph. The spectra were taken from 11.25° to 78.75° in steps of 7.5°.

The plates were scanned at Dacca and a typical spectrum at 18.75° is shown in fig. 1. The energy resolution (FWHM) was ≈ 22 keV. Many levels have been identified up to E_x ≈ 7.8 MeV and the angular distributions have been measured for most

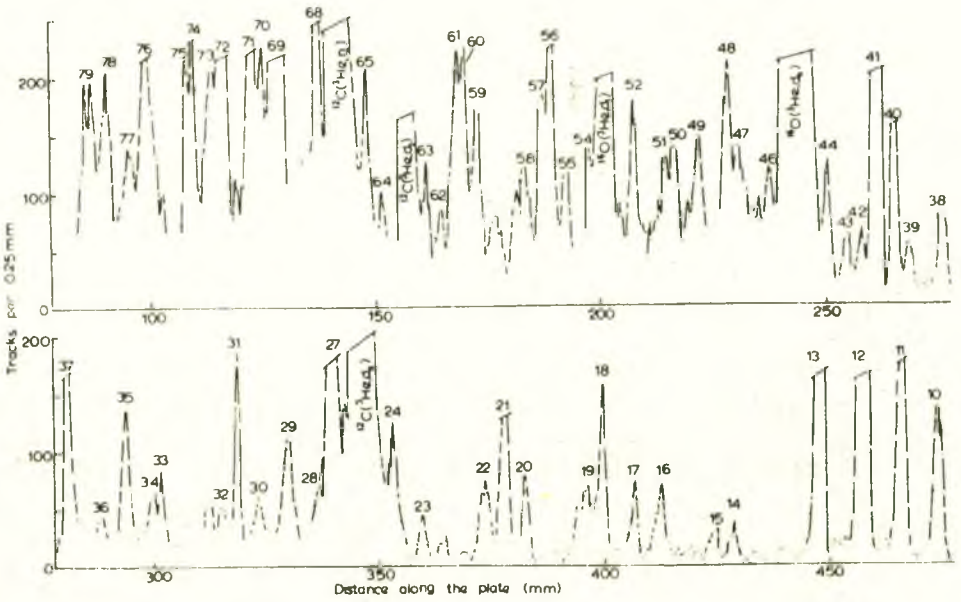

Fig. 1. Part of the energy spectrum of deuterons arising from the ^{56}Fe(τ, d) reaction at 18.75° showing the region of high group density.

of them. Because of the uncertainty in the spectrograph calibration at the high field used ($B \approx 12.8$ kG), an internal calibration was performed by using some of the well-established levels in ^{57}Co. Such levels are shown in italics in table 3.

To measure the target thickness a subsidiary short exposure of 0.0504 μC was taken at a magnetic field of strength ≈ 4.7 kG on the elastic scattering of 6 MeV $^3He^{++}$ particles from the same target. The yields of the elastic group at 26.25° and 33.75° were normalized to the Rutherford cross section and the effective ^{56}Fe target thickness was found to be 93 $\mu g \cdot cm^{-2}$. The total uncertainty in the absolute value of the (τ, d) reaction cross section (resulting mainly from the errors in the target thickness, scanning and background subtraction) is less than 15 %.

3. DWBA analysis

The DWBA cross sections in the local zero range approximation were computed using the code DWUCK due to Kunz. The calculations were carried out by one of the authors (H.M.S.G.) using the IBM 360/195 computer of the Rutherford High Energy Laboratory. The optical model potential was of the standard Woods-Saxon form for the ^{3}He potential and the real part of the deuteron potential, while the Woods-Saxon derivative was used for the imaginary part of the deuteron potential. The optical model parameters [8-12]) are listed in table 1.

The bound-state potential well was taken as the real Woods-Saxon form with the geometrical parameters given by $r_0 = 1.25$ fm and $a = 0.65$ fm, including a Thomas-Fermi spin-orbit term given by

$$\frac{V_0\lambda}{45.2}\frac{1}{r}\frac{d}{dr}f(r, r_0, a)\boldsymbol{l}\cdot\boldsymbol{s},$$

with $\lambda = 25$; $f(r, r_0, a)$ is the Woods-Saxon form factor. The strength of the potential was adjusted so as to give the transferred proton a binding energy $E_B = Q(\tau, d) + 5.49$ MeV.

To start with, the DWBA analysis were carried out for four strong transitions leading to the g.s. and the 1.376, 1.501 and 2.134 MeV levels having $J^\pi = \frac{7}{2}^-, \frac{3}{2}^-, \frac{1}{2}^-$ and $\frac{5}{2}^-$, respectively. The transition strengths are summarized in table 2. Of the different combinations of ^{3}He and deuteron potential parameters, the set τA-dA gives the best fit to the data and also satisfies the condition $V_\tau \approx V_d + V_p$ for the real depths. All the DWBA calculations used in the present work were performed with this set.

4. Results and discussion

The results of the present work are summarized in table 3. The energy levels in column 3 are from the compilation by Auble [1]) up to $E_x \approx 4.3$ MeV; beyond this the levels are taken from the compilation by Hardie *et al.* [3]). Information given by

TABLE 1

Optical model parameters

Particle	Notation	V_0 (MeV)	r_0 (fm)	a (fm)	W_0 (MeV)	$4W_D$ (MeV)	r_I (fm)	a_I (fm)	$V_{s.o}$ (MeV)	$r_{s.o.}$ (fm)	$a_{s.o.}$ (fm)	r_c (fm)	Ref.
τ	A	139.0	1.08	0.80	12.3		1.743	0.721				1.4	[8,9]
	B	165.0	1.43	0.613	30.3		1.50	0.71	8.0	1.43	0.613	1.4	[10]
d	A	94.8	1.12	0.79		61.2	1.32	0.74	6.6	0.90	1.16	1.3	[11]
	B	90.0	1.15	0.81		84.0	1.34	0.68				1.15	[12]
p		[a]	1.25	0.65					$\lambda = 25$			1.3	

Form factors for τ-potential, Woods-Saxon for both the real and imaginary parts; for d-potential, Woods-Saxon for the real part and Woods-Saxon derivative for the imaginary part.

[a]) adjusted to reproduce the binding energy.

the previous (τ, d) and (d, n) studies [2,3,5]) is also included in the table for a comparison. The transition strengths $(2J_f + 1)C^2S$ in the present as well as in the previous (τ, d) works were extracted for the normalization constant $N = 4.42$, relevant to the Gunn-Irving wave function for ^{3}He and Hulthén for the deuteron [12]). For $Q(\tau, d)$ values more negative than -5.5 MeV, corresponding to the breakup of ^{3}He particles, the DWBA cross sections, hence the transition strengths, are not reliable. Such strengths as shown in parenthesis in table 3 are extracted from the extrapolation of the DWBA cross sections to that excitation. The spin-parities in column 13 are from all previous measurements as considered to be the best assignments by the present authors.

Typical examples of the DWBA fits to the measured angular distributions are shown in figs. 2–4. The single-particle strengths are fragmented over levels as displayed in fig. 5 and the results of the sum rule analysis are summarized in table 4; also included are those from previous (τ, d) and (d, n) measurements [2,3,5]) as well as the theoretical limits gives by the single-particle shell model.

The results are discussed below.

TABLE 2

Transition strengths for different combinations of potential parameters

Excitation (MeV)	nl_j	$(2J_f + 1)C^2S$		
		τ_A-d_A	τ_B-d_A	τ_B-d_B
g.s.	$1f_{7/2}$	1.50	1.93	2.07
1.376	$2p_{3/2}$	1.29	1.50	1.59
1.501	$2p_{1/2}$	0.49	0.58	0.61
2.134	$1f_{5/2}$	0.98	1.25	1.21

TABLE 3

Summary of the level properties of ^{57}Co

Group	Excitation (MeV)		$\sigma_{max}(\theta)$ (mb/sr) [a]	l_p transfer				$(2J_t+1)C^2S$				J^π	
	[a]	[b]		[a]	[c]	[d]	[e]	[a]	[c]	[d]	[e]	[f]	[a]
0	*0*	0	0.80	3	3	3	3	1.50	0.89	1.80	1.90	$\frac{7}{2}^-$	[g]
	1.224											$\frac{9}{2}^-$	
1	1.376	1.378	12.75	1	1	1	1	1.29	0.52	1.80	1.07	$\frac{3}{2}^-$	[g]
2	*1.501*	1.505	5.70	1	1	1	1	0.49	0.35	0.72	0.45	$\frac{1}{2}^-$	[g]
		1.689										$\frac{11}{2}^-$	
3	1.758	1.757	2.34	1	1	1	1	0.23	0.13	0.30	0.20	$\frac{3}{2}^-$	[g]
4	1.898	1.897	0.056	n.s.								$\frac{7}{2}^-$	
		1.919										$\frac{5}{2}^-$	
5	*2.134*	2.133	1.05	3	3	3	3	0.98	1.20	2.00	1.18	$\frac{5}{2}^-$	[g]
6	2.314	2.311	0.25	3	3	3	3	0.35	0.20	0.70	0.35	$\frac{7}{2}^-$	[g]
		2.486										$\frac{11}{2}^-$	
		2.524										IV $\frac{13}{2}^-$	
		2.560										IV $\frac{11}{2}^-$	
		2.611										$\frac{7}{2}^-$	
		2.723										$\frac{7}{2}^-$	
		2.731										$\frac{1}{2}^-$, $\frac{5}{2}^-$	
		2.743											
		2.804										$\frac{1}{2}^-$, $\frac{5}{2}^-$	
7	*2.878*	2.879	1.87	1	1	1	1	0.21	0.11	0.39	0.14	$\frac{3}{2}^-$	[g]
8	2.985	2.981	0.13	0	0			0.026				$\frac{1}{2}^+$	[g]
9	3.112	3.108	0.32	1	1		1	0.028, 0.035	0.019		0.09, 0.09	$\frac{1}{2}^-$, $\frac{3}{2}^-$	[g]
		3.121											
		3.165											
10	*3.177*	3.177	0.42	3	3	3	3	0.31	0.55	0.84	0.84	$\frac{5}{2}^-$	[g]
		3.184											
		3.246											
11	3.267	3.262	0.64	3	3	3	3	0.46, 0.71	0.65, 0.44	1.62	0.94, 0.55	$\frac{5}{2}^-$, $\frac{7}{2}^-$	[g]
12	3.355	3.357	3.56	1	1	1	1	0.30, 0.39	0.16	0.56	0.30, 0.27	$\frac{1}{2}^-$, $\frac{3}{2}^-$	[g]
		3.394											
		3.431											
13	*3.459*	3.461	2.84	1	1	1	1	0.26, 0.35	0.14	0.38	0.25, 0.23	$\frac{1}{2}^-$, $\frac{3}{2}^-$	[g]
		3.522											
		3.540										$\frac{3}{2}^+$, $\frac{5}{2}^+$	
		3.553											
		3.622											
		3.665											
14	3.681	3.672	0.091	n.s.								$\frac{7}{2}^-$	
		3.681											
15	3.727	3.720	0.069	4			(0)	0.16			0.02	$(\frac{1}{2}^+)$	$\frac{5}{2}^+$
		3.834											
16	3.862	3.854	0.18	2				0.30					$(\frac{1}{2})$
		3.909										$(\frac{3}{2}^+)$	
17	3.923	3.918	0.38	1			1	0.033, 0.045			0.04, 0.04	$\frac{1}{2}^-$, $\frac{5}{2}^-$	[g]
		3.991										$(\frac{5}{2}^-)$	

TABLE 3 (continued)

Group	Excitation (MeV) [a]	Excitation (MeV) [b]	$\sigma_{max}(\theta)$ (mb/sr) [a]	l_p transfer [a] [c] [d] [e]	$(2J_f+1)C^2S$ [a] [c] [d] [e]	J^π [f] [g]
18	*4.001*	3.999	0.51	(1) (1) 1	0.045, 0.062 / 0.029 / 0.05, 0.05	$\frac{1}{2}^-, \frac{3}{2}^-$ [g]
		4.037				
19	4.067	4.058	0.19	1 (1)	0.019, 0.024 / 0.009	$(\frac{1}{2})\ \frac{1}{2}^-, \frac{3}{2}^-$
		4.111				
20	4.194	4.187	0.38	1 1 1	0.034, 0.044 / 0.024 / 0.06, 0.04	$\frac{1}{2}^-, \frac{3}{2}^-$ [g]
		4.217				
		4.238				
21	4.253	4.251	0.32	3 3 3 3	0.20, 0.31 / 0.26 / 0.70 / 0.56, 0.41	$\frac{5}{2}^-, \frac{7}{2}^-$ [g]
		4.272				
		4.284				
22	4.293	4.297	0.59	1 (1)	0.053, 0.071 / 0.020 / 0.08, 0.07	$\frac{1}{2}^-, \frac{3}{2}^-$ [g]
		4.308				
		4.379		1	0.03, 0.02	$\frac{1}{2}^-, \frac{3}{2}^-$
		4.399				
23	4.455	4.454	0.080	n.s. 1 + 3	0.03, 0.23	
24	4.517	4.500	0.082	n.s.		
25	4.537	4.525	0.54	1 (1)	0.050, 0.064	$(\frac{1}{2}^-, \frac{3}{2}^-)$
26	4.590	4.595	1.53	4 4 2 + 4	2.60 / 4.8 / 0.09, 1.93	$\frac{9}{2}^+$
		4.615				
27	4.677	4.685	2.60	(1) (1) (2) 2	0.26, 0.33 / 0.15 / 1.08, 0.30	$(\frac{1}{2}^-, \frac{3}{2}^-)$
28	4.737	4.730	0.14	n.s.		
29	4.806	4.800	0.32	n.s. 3	0.28, 0.23	$\frac{5}{2}^-, \frac{7}{2}^-$
30	4.886		0.20	n.s.		
31	4.938		0.30	0	0.031	$\frac{1}{2}^+$
32	4.985	4.981	0.25	n.s.		
33	5.138		0.16	n.s.		
34	5.167		0.14	n.s.		
35	*5.228*	5.223	0.34	0 0	0.035 / 0.027	$\frac{1}{2}^+$
36	5.296		0.14	n.s.		
37	5.387	5.370	0.77	1	0.074, 0.086	$\frac{1}{2}^-, \frac{3}{2}^-$
38	5.447	5.425	0.35	1	0.038, 0.041	$\frac{1}{2}^-, \frac{3}{2}^-$
39	5.532	5.528	0.12	n.s.		
40	5.570	5.559	0.73	1	0.086, 0.098	$\frac{1}{2}^-, \frac{3}{2}^-$
41	*5.615*	5.621	3.70	1 1 (1)	0.39, 0.44	$\frac{1}{2}^-, \frac{3}{2}^-$ [g]
42	5.664	5.653	0.076	n.s.		

TABLE 3 (continued)

Group	Excitation (MeV) [a]	Excitation (MeV) [b]	$\sigma_{max}(\theta)$ (mb/sr) [a]	l_p transfer [a]	l_p transfer [c]	l_p transfer [d]	l_p transfer [e]	$(2J_f+1)C^2S$ [a]	$(2J_f+1)C^2S$ [c]	$(2J_f+1)C^2S$ [d]	$(2J_f+1)C^2S$ [e]	J^π [f]	J^π [a]
43	5.699	5.693	0.14	n.s.									
44	5.747	5.743	0.23	1				0.045, 0.050					$\frac{1}{2}^-, \frac{3}{2}^-$
45	5.806	5.799	0.55	n.s.									
46	5.914	5.91	0.14	n.s.									$\frac{3}{2}^+$
47	5.992	5.976	0.39	n.s.									$\frac{3}{2}^+$
48	6.024	6.013	0.75	n.s.									
49	6.098	6.093	0.33	n.s.									
50	6.159	6.153	0.41	1				(0.052, 0.056)					$\frac{1}{2}^-, \frac{3}{2}^-$
51	6.187	6.184	0.45	n.s.									
52	6.278	6.268	0.52	1				(0.068, 0.074)					$\frac{1}{2}^-, \frac{3}{2}^-$
53	6.348	6.344	1.62					(0.14, 0.15)					$\frac{1}{2}^-, \frac{3}{2}^-$
54	6.391		0.41	1				(0.050, 0.052)					$\frac{1}{2}^-, \frac{3}{2}^-$
55	6.472		0.20	n.s.									
56	6.504	6.492	0.49	n.a.	(3)							$(\frac{5}{2}^-, \frac{7}{2}^-)$	
57	6.540		0.28	n.s.									
58	6.589	6.594	0.12	n.a.									
59	6.712	6.699	0.50	n.a.									
60	6.750	6.739	0.46	n.a.									
61	6.785	6.768	0.17	n.a.									
62	6.846	6.848	0.11	n.s.									
63	6.890	6.885	0.34	(1)	(1)			(0.063, 0.059)					$(\frac{1}{2}^-, \frac{3}{2}^-)$
64	7.032	7.020	0.30	(1)	(1)			(0.065, 0.060)					$(\frac{1}{2}^-, \frac{3}{2}^-)$
65	7.066		0.16	n.s.									
66	7.115	7.115	0.41	n.s.	(1)							$(\frac{1}{2}^-, \frac{3}{2}^-)$	
67	7.150	7.162	0.46	1				(0.073, 0.073)					$\frac{1}{2}^-, \frac{3}{2}^-$
68	7.187		0.57	1				(0.084, 0.076)					$\frac{1}{2}^-, \frac{3}{2}^-$
69	7.271	7.265	2.86	1	1	1		(0.34, 0.31)		(0.12)		$\frac{1}{2}^-, \frac{3}{2}^-$ [g]	
		7.281											
70	7.322	7.324	0.35	n.s.									
71	7.370	7.367	0.32	n.s.									
72	7.434	7.432	1.17	3	2, 3	3		(0.52, 0.75)		(0.80)			$\frac{5}{2}^-, \frac{7}{2}^-$
73	7.473	7.480	0.56	n.a.									
74	7.531	7.528	0.42	n.s.									
75	7.559		0.38	n.s.									
		7.610											
		7.626											
		7.634											
		7.648											

TABLE 3 (continued)

Group	Excitation (MeV)		$\sigma_{max}(\theta)$ (mb/sr) [a]	l_p transfer				$(2J_f+1)C^2S$				J^π	
	[a]	[b]		[a]	[c]	[d]	[e]	[a]	[c]	[d]	[e]	[f]	[a]
76	7.665	7.656	0.87	1	1			(0.14, 0.11)		(0.04)		$\frac{1}{2}^-, \frac{3}{2}^-$	[g]
		7.662											
77	7.708		0.27	n.s.									
78	7.809	7.799	0.48	2				(0.047)					$\frac{5}{2}^+$
79	7.839		0.60	2				(0.072)					$\frac{5}{2}^+$

n.s. – non-stripping angular distribution.
n.a. – data not analysed.
[a]) Present work
[b]) Summarized by Auble [1]) up to E_x = 4.308 MeV, beyond which the levels are from the ^{56}Fe(τ, d) work of Hardie *et al.* [3]).
[c]) The (τ, d) reaction at E_τ = 22 MeV (Hardie *et al.* [3]).
[d]) The (τ, d) work of Rosner and Holbrow [2]) at E_τ = 16.5 MeV.
[e]) The (d, n) reaction by Adam *et al.* [5]).
[f]) Previous experiments, summarized by the present authors.
[g]) The J^π values are consistent with the assignment in column 13.

TABLE 4

Results of the sum rule analysis for proton $T_<$ states in ^{57}Co

Single-particle state [a]	$\sum(2J_f+1)C^2S$					E_{nlj} (MeV)			
	theory	[b]	[c]	[d]	[e]	[b]	[c]	[d]	[e]
$1f_{7/2}$	2.00	1.85	1.80	1.09	2.25	0.44	0.0	0.42	0.36
$2p_{3/2}$	3.60	1.73 [f]), 2.49 [g])	2.10	1.06	2.00	1.61	1.43	1.19	2.11
$1f_{5/2}$	4.80	1.95	5.86	2.66	4.32	2.78	2.87	2.83	3.28
$2p_{1/2}$	1.60	2.80 [f]), 2.22 [g])	2.05	0.65	0.69	4.44	2.63	2.39	2.44

[a]) Data for other states being incomplete are not included.
[b]) Present work.
[c]) The ^{56}Fe(τ, d) reaction (Rosner and Holbrow [2])).
[d]) The ^{56}Fe(τ, d) reaction (Hardie *et al.* [3])).
[e]) The ^{56}Fe(d, n) reaction (Adam *et al.* [5])).
[f]) Assuming $J^\pi = \frac{1}{2}^-$ for the levels 3.357, 3459 and 4.067 MeV, as discussed in the text.
[g]) Assuming $J^\pi = \frac{3}{2}^-$ for the levels 3.357, 3.459 and 4.067 MeV, as discussed in the text

4.1. THE ANGULAR DISTRIBUTIONS AND TRANSITION STRENGTHS

4.1.1. The l = 1 transitions. The 2p transition strengths are distributed over a large number of levels (fig. 5). The spectroscopic factor for $l = 1$ transitions, level by level, found in the present work lies between that given by Rosner and Holbrow [2]) and Hardie *et al.* [3]). The higher value of $\sum(2J_f+1)C^2S$ for the 2p states given by the present work than that by Rosner and Holbrow is due to the fact that more $l = 1$

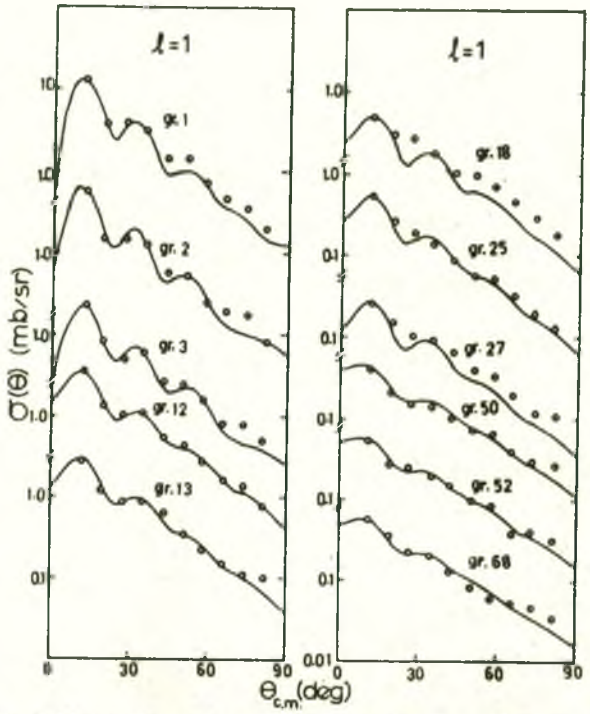

Fig. 2. Measured angular distributions fitted with $l = 1$ DWBA curves.

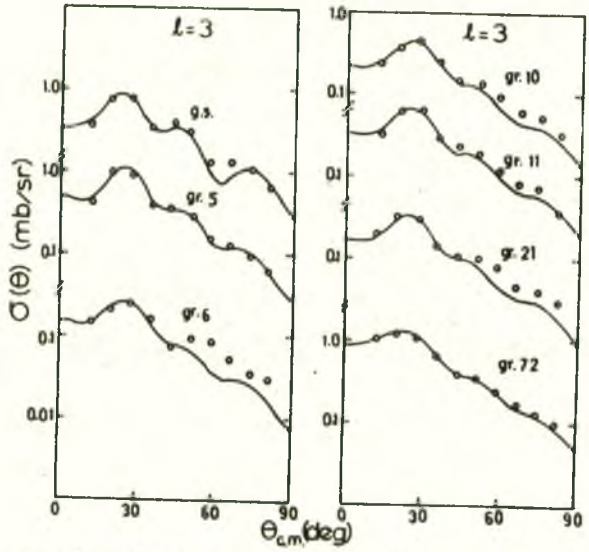

Fig. 3. Measured angular distributions fitted with $l = 3$ DWBA curves.

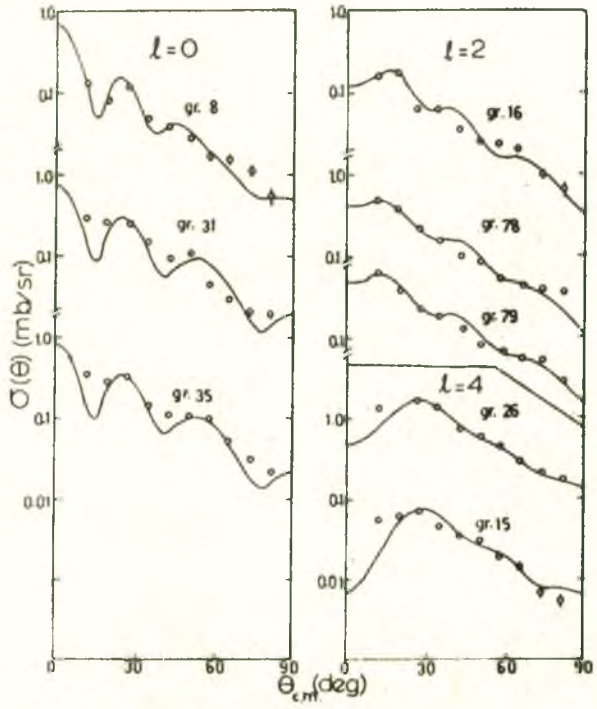

Fig. 4. Measured angular distributions fitted with l = 0, 2 and 4 DWBA curves.

transitions are observed by us than by them. The measured 2p, $T_<$ strength in the present work is 4.53, being almost identical to the expected single-particle value of 5.20 within the limits of uncertainty. The value obtained by Adam *et al.* [5]) from the (d, n) reaction is about 50 % of the expected strength. Splitting of the observed strength into $p_{\frac{3}{2}}$ and $p_{\frac{1}{2}}$ components is difficult, since of all the l = 1 transitions, the J-values are known for only a few low-lying levels (table 3) and further the angular distribution data do not display a J-dependence. The transition strengths of the remaining levels were calculated for both $\frac{3}{2}^-$ and $\frac{1}{2}^-$ states. The known $J^\pi = \frac{3}{2}^-$ levels, namely 1.376, 1.758 and 2.878 MeV, together carry about 50 % of the expected $T_<$ strength (table 4). The levels at 7.271 and 7.655 MeV are considered to be analogues, as discussed in subsect. 4.1.4. The summed transition strength for the remaining levels assumed as $\frac{1}{2}^-$ levels is 2.80 as against the single-particle limit of 1.60. The J^π value of the 3.355, 3.459 and 4.067 MeV levels has been found to be $\frac{3}{2}^-$ by Esat *et al.* [13]) in the ^{56}Fe(p, γ) reaction. With this assignment, the $\sum(2J_f+1)C^2S$ values for the $2p_{\frac{3}{2}}$ and $2p_{\frac{1}{2}}$ states become 2.49 and 2.22, respectively, still far from the single-particle limits. A different choice of the $\tilde{\tau}^L$ and d-potentials increases the values by $\approx$ 20 % (table 2); the $p_{\frac{3}{2}}$ strength thus comes closer to the expected values than above, but at the same time the $p_{\frac{1}{2}}$ value differs further from the shell-model value. Summing up, the observed $2p_{\frac{3}{2}}$, $T_<$ strength is higher than that predicted and the

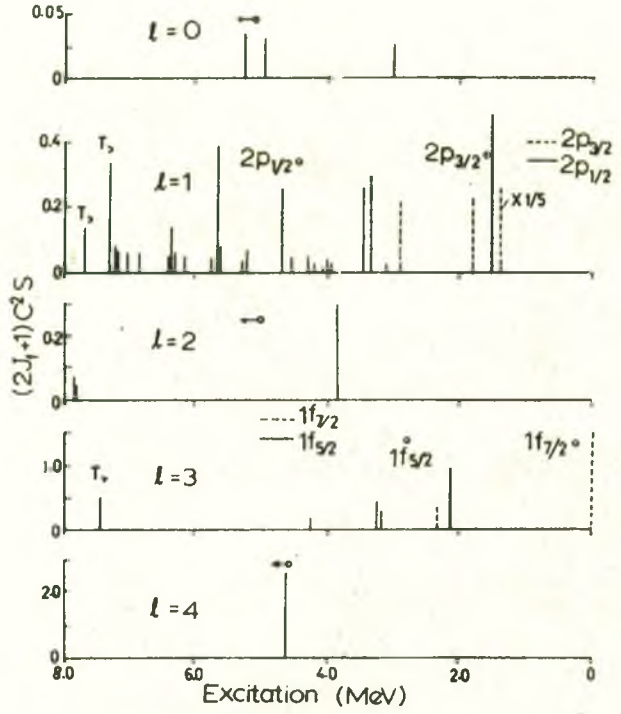

Fig. 5. The spectral distributions of single-particle strengths: the centroids of the different $T_<$ states are also shown.

$2p_{\frac{1}{2}}$, $T_<$ measured value is less than the sum rule limit. It is thus possible that some of the assumed $2p_{\frac{1}{2}}$ levels really belong to the $2p_{\frac{3}{2}}$ state. It is also possible that the $2p_{\frac{1}{2}}$ proton orbit is not completely vacant as assumed in the shell model; the observed $1f_{\frac{7}{2}}$, $T_<$ strength however does not support the latter suggestion. Further comments should await a determination of the J-values of at least the strong $l_p = 1$ transitions.

The angular distribution leading to the 3.355 MeV level is characterized by the $l = 1$ transition (fig. 2) in agreement with previous (τ, d) and (d, n) reactions, but in disagreement with the $l = 3$ assignment in the ^{58}Ni(t, α) reaction (Blair and Armstrong [14]). The transition to the 4.677 MeV level has contradictory l_p assignments in proton stripping reactions (table 3); in agreement with Hardie *et al.* [3]) the present work favours $l_p = 1$ over $l_p = 2$. The present experiment confirms the tentative $l = 1$ assignment made to the levels at 4.067, 4.293 and 4.537 MeV in one or the other (τ, d) reaction (table 3).

4.1.2. The l = 3 transitions. The measured angular distributions are shown in fig. 3. The J-values of the ground state (g.s.) and the lowest three levels (E_x = 2.134, 2.314 and 3.177 MeV) belonging to the $l = 3$ transitions are known (table 3). The g.s. and 2.314 MeV level together exhaust the $1f_{\frac{7}{2}}$, $T_<$ strength (table 4). The 7.434 MeV level is presumably a $\frac{5}{2}^-$, $T_<$ level as discussed later (subsect. 4.1.4). The

remaining transitions together carry about 40 % of the $1f_{\frac{7}{2}}$, $T_<$ strength. The selection of other parameter sets (table 3) increases the $f_{\frac{7}{2}}$ strength by 30–38 % and the $f_{\frac{5}{2}}$ strength by 25–30 % and thus do not much improve the situation. More $J^\pi = \frac{5}{2}^-$ levels thus remain to be identified. Because of the large centrifugal barrier of the $l = 3$ transitions as compared to the $l = 1$ transitions for example, the spreading will be less for $l = 3$ than that for $l = 1$ transitions. Such levels are therefore unlikely to lie above $E_x \approx 7.8$ MeV, the excitation energy covered in the present experiment. The 1f, $T_<$ transition strength is probably overestimated by Rosner and Holbrow [2]); the entire $f_{\frac{7}{2}}$, $T_<$ strength according to them is contained in the g.s. transition. The spectroscopic factor in the present case is smaller than that given by Adam *et al.* [5]). The present values for the $1f_{\frac{7}{2}}$ levels are twice as strong as those obtained by Hardie *et al.* [3]), while for the $1f_{\frac{5}{2}}$ levels the present values are somewhat lower than theirs.

4.1.3. The $l = 0$, 2 and 4 transitions. Three $l = 0$ transitions are observed in the present work ($E_x = 2.985$, 4.938 and 5.228 MeV) and the angular distributions are shown in fig. 4. The 2.985 MeV level is strongly excited in the ^{58}Ni(t, α) reaction [14]) and is probably a 2s hole state. The other two transitions are assumed to belong to the 3s state. A discussion on the $l = 0$ transitions is made in subsect. 4.3.

Three $l = 2$ transitions are identified in this experiment, two of which lie around $E_x = 7.8$ MeV and are likely to belong to the $2d_{\frac{3}{2}}$ particle state. The other level ($E_x = 3.862$ MeV) is assumed to be a $1d_{\frac{3}{2}}$ hole state and is probably identical with the 3.906 MeV level excited with an $l = 2$ character in the ^{58}Ni(t, α) reaction [14]). No $l = 2$ transition was observed by Hardie *et al.* [3]) in the ^{56}Fe(τ, d) reaction. The one tentatively assigned in the ^{56}Fe(τ, d) reaction as $l_p = 2$ by Rosner and Holbrow [2]) at $E_x \approx 4.68$ MeV and later confirmed by Adam *et al.* [5]) in the ^{56}Fe(d, n) reaction in a tentative $l_p = 1$ according to Hardie *et al.* [3]) and the present work.

Two $l = 4$ transitions are observed in the present experiment at $E_x = 3.727$ MeV and the doublet at 4.59 MeV. The former is a tentative $l = 0$ transition and the later a mixture of $l = 2$ and 4 in the ^{56}Fe(d, n) reaction [5]). Both the angular distributions are well fitted by the $l = 4$ DWBA curve (fig. 4).

4.1.4. Isobaric analogue states. The ^{56}Fe(τ, d) reaction can excite both the normal ($T_<$) and analogue ($T_>$) states in ^{57}Co. The $T_<$ states were discussed above. Because of the rather large isotopic spin of ^{56}Fe, not enough strengths are available to the analogue states for them to stand out distinctively from the neighbouring $T_<$ states. It has been suggested by Hardie *et al.* [3]) from a compilation of the available information from the (τ, d) and (p, γ) reactions that there is confusion over the positive identification of the analogue states. In agreement with Rosner and Holbrow [2]) the levels at 7.271, 7.434 and 7.665 MeV were identified in this work as the analogues of the g.s. + 14 (unresolved), 136 and 366 keV levels in ^{57}Fe. The relative level spacings and the l_p values are consistent with the relative level spacings and the J-values of the parent levels. In view of the non-reliability of the DWBA cross sections for the (τ, d) reaction at this excitation, as stated earlier, we refrain from a comparison with the corresponding spectroscopic factors in the ^{56}Fe(d, p) reaction. The Coulomb

displacement energy for the isobaric pair of nuclei ^{57}Fe-^{57}Co comes to be 8.89 MeV for the g.s. analogue.

4.2. NON-STRIPPING LEVELS

Several non-stripping levels are observed in the present work (designated n.s. in table 3), the angular distributions to some of which are shown in fig. 6. The cross sections rise at forward angles, but the distributions are not given by the direct reaction mechanism. The non-stripping levels are usually weakly excited and the cross sections for many of them are an order of magnitude smaller than the average cross sections for the stripping levels. They cannot be described in terms of a single proton coupled to a ^{56}Fe core and some of them arise from a collective mode of excitation.

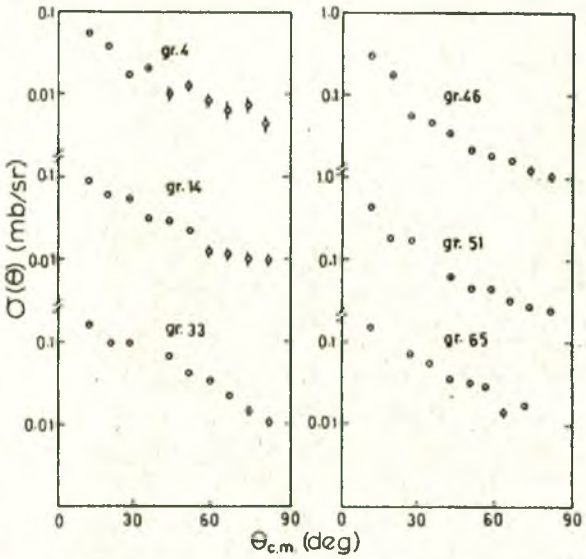

Fig. 6. Some of the measured angular distributions displaying a non-stripping character.

It is interesting to note that the levels with high spin values are either not at all excited in the (τ, d) reaction (levels at 1.224 and 1.689 MeV and the multiplets at ≈ 2.5 MeV, for example) or have angular distributions not characteristic of a direct process (levels at 1.898 and 3.681 MeV for example). Some of the $1d_{\frac{3}{2}}$ hole states (E_x = 5.91 and 5.99 MeV) excited in the ^{58}Ni(t, α) reaction have non-stripping angular distributions.

4.3. THE LEVEL SPECTRUM OF ^{57}Co

Several attempts have been made to calculate the level spectrum of ^{57}Co based on the shell model [15-18]), as well as on the unified model [19-22]). The observed level

spectrum is compared with the predictions of the more important theories in fig. 7.

The shell-model calculation by Vervier [15]) assumes an inert ^{48}Ca core with a proton hole in the $1f_{\frac{7}{2}}$ orbit and the two extra-core neutrons only in the $2p_{\frac{3}{2}}$ orbit; agreement with experiment was poor. The above calculation was then repeated by McGrory [16]) by increasing the model space so as to include also the $2p_{\frac{1}{2}}$ and $1f_{\frac{5}{2}}$ neutron configurations. The residual interaction was taken to give reasonable agreement with other isotonic nuclei. The agreement with experiment, although somewhat improved, is still unsatisfactory. Several well-known levels are not predicted, in particular there are no calculated $J^\pi = \frac{1}{2}^-$ and $\frac{3}{2}^-$ levels below $E_x \approx 2.5$ MeV, whereas such levels have been observed below ≈ 1.5 MeV.

An extended shell-model calculation due to Gatrousis *et al.* [17]) is based on an inert

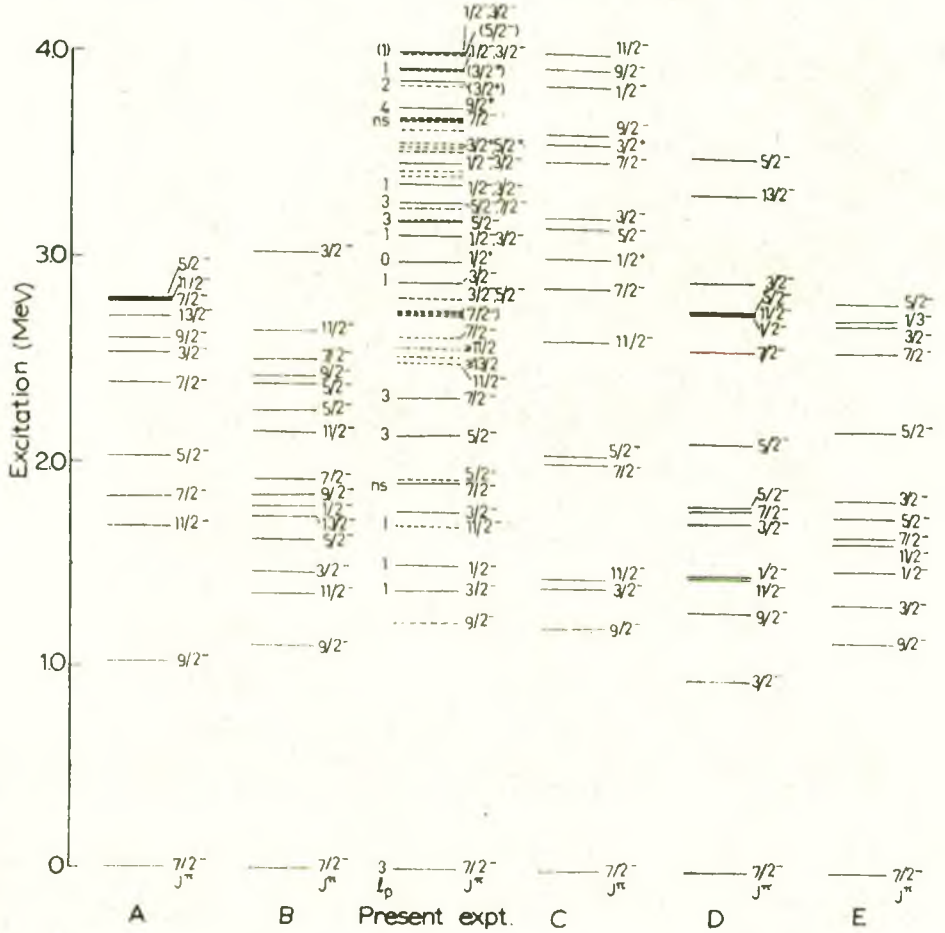

Fig. 7. The experimental level spectrum of ^{57}Co compared with theoretical calculations. The levels not observed in the present experiment are shown by broken lines. A: Ref. [18]). B: Ref. [17]). C: Ref. [19]). D: Ref. [22]). E: Ref. [24]).

^{40}Ca core and includes the neutron configurations $1f_{\frac{7}{2}}$, $1f_{\frac{5}{2}}$, $2p_{\frac{3}{2}}$ and $2p_{\frac{1}{2}}$ and further allows the excitation of protons from the $1f_{\frac{7}{2}}$ shell to the $2p_{\frac{3}{2}}$, $2p_{\frac{1}{2}}$ and $1f_{\frac{5}{2}}$ orbits. The spacings of the single-particle orbits are treated as free parameters and the residual two-body interaction was taken as that given by a free two-nucleon Hamada-Johnston potential. Many more levels are predicted than those by Vervier [15]) and McGrory [16]). A comparison with the experimental level scheme is made in fig. 7. Except for the 1.76 MeV level ($J^\pi = \frac{3}{2}^-$) all the observed levels below $E_x \approx 2$ MeV are reproduced in this calculation, although the sequence and the spacings of the levels are not exact. Some of the high spin states predicted by Gatrousis *et al.* [17]), namely the $J^\pi = \frac{13}{2}^-$ level at ≈ 1.7 MeV and the $J^\pi = \frac{11}{2}^-$ level at ≈ 2.1 and ≈ 2.7 MeV, appear to be strong candidates for some of the high spin states ($E_x = 2.486$ MeV, $J^\pi = \frac{11}{2}^-$; $E_x = 2.523$ MeV, $J \geqq \frac{13}{2}$; $E_x = 2.555$ MeV, $J \geqq \frac{11}{2}$) observed later by Pietrzyk *et al.* [23]) in the ^{57}Fe(p, n) reaction. Two $J^\pi = \frac{9}{2}^-$ levels predicted by this model at ≈ 1.8 and ≈ 2.5 MeV have, however, not been observed in any experiment.

A more recent shell-model calculation by Horie and Ogawa [18]) assumes an inert ^{48}Ca core with a proton hole in the $1f_{\frac{7}{2}}$ shell and the extra-core neutrons in the 2p and $1f_{\frac{5}{2}}$ orbits. Agreement with the observed level scheme is poor (fig. 7). Fewer levels are predicted than observed and the $\frac{1}{2}^-$, $\frac{3}{2}^-$ levels around $E_x = 1.5$ MeV are not reproduced. The predicted $\frac{3}{2}^-_1$ and $\frac{1}{2}^-_1$ levels are, respectively, ≈ 1.1 MeV and ≈ 2.1 MeV higher than observed. The spectroscopic factors for the $J^\pi = \frac{7}{2}^-$, $T_<$ levels populated in the single-proton stripping reaction on ^{56}Fe are also calculated by Horie and Ogawa and almost the entire single-particle strength is predicted to be contained in the g.s. transition (table 5).

Attempts have also been made to obtain the level of spectrum of ^{57}Co on the weak as well as the intermediate coupling versions of the unified model. The low-lying levels of an odd mass nucleus is given in terms of a single particle (or hole) coupled to an excited even core. The levels of ^{57}Co are thus given by the weak coupling of the $1f_{\frac{7}{2}}$ proton hole to the lowest 2^+ vibrational state of ^{58}Ni and a quintet of negative-parity levels with spin $\frac{3}{2}^-$, $\frac{5}{2}^-$, $\frac{7}{2}^-$, $\frac{9}{2}^-$ and $\frac{11}{2}^-$ will be obtained with the centroid at ≈ 1.45 MeV (the energy of the lowest 2^+ state in ^{58}Ni). Such levels may be identified with the observed levels at $E_x = 1.758$, 1.919, 1.898, 1.224 and 1.689 MeV, respectively (Covello and Manfredi [20])). The collective nature of the levels is supported by their much larger B(E2) strengths than the single-particle estimates [24,25]) and the weak excitation in the (τ, d) and (d, n) reactions. The 1.90 MeV level has a non-stripping angular distribution (fig. 7) and the 1.22, 1.69 and 1.92 MeV levels are hardly visible above background. Only the 1.76 MeV level is not weak and the angular distribution leading to this level is of stripping character (fig. 2), which probably arises from a mixing with the single-particle level of the same J-value. The limitation of the weak coupling model is obvious. The observed splitting (≈ 0.7 MeV) of the core multiplet shows that the hole–vibration coupling may not be weak. The centroid of the multiplet is also about 0.2 MeV higher than the energy of the lowest 2^+ state in ^{58}Ni, implying a mixture of states with different numbers of phonons.

TABLE 5

Measured transition strengths from (τ, d) and (d, n) reaction compared with theory

E_x (MeV)	J^π	$(2J_f+1)C^2S$									
		[a]	[b]	[c]	[d]	[e]	[f]	[g]	I [h]	II [h]	[i]
g.s.	$\frac{7}{2}^-$	1.50	0.89	1.80		1.90	1.84	5.20	1.41	1.41	1.98
1.376	$\frac{3}{2}^-$	1.29	0.52	1.80	1.71	1.07	1.11	1.68	1.90	1.60	
1.501	$\frac{1}{2}^-$	0.49	0.35	0.72	0.64	0.45	0.40	0.76	0.75	0.96	
1.758	$\frac{5}{2}^-$	0.23	0.13	0.30	0.35	0.20	0.16		0.86	1.09	
1.898	$\frac{9}{2}^+$								0.44	0.45	0.00
1.920	$\frac{5}{2}^+$								0.04	0.11	
2.134	$\frac{5}{2}^-$	0.98	1.20	2.00		1.18	1.42		3.23	3.58	
2.314	$\frac{7}{2}^-$	0.35	0.20	0.70		0.35			0.95	0.56	0.00
2.611	$\frac{7}{2}^+$								0.04	0.03	
2.731	$\frac{5}{2}^+$								0.29	0.20	
2.804	$\frac{9}{2}^+$								0.47	0.43	
2.878	$\frac{3}{2}^-$	0.21	0.11	0.39		0.14	0.17	0.48	0.43	0.32	

[a]) Present work.
[b]) The ^{56}Fe(τ, d) reaction (Hardie *et al.* [3]).
[c]) The ^{56}Fe(τ, d) reaction (Rosner and Holbrow [2]).
[d]) The ^{56}Fe(τ, d) reaction (Baghdadi *et al.* [4]).
[e]) The ^{56}Fe(d, n) reaction (Adam *et al.* [5]).
[f]) The ^{56}Fe(d, n) reaction (Couch [7]).
[g]) The ^{56}Fe(d, n) reaction (Okorokov *et al.* [6]).
[h]) Shell-model theory (Gómez [22]); I and II denote two different parameter values.
[i]) Shell-model theory (Horie and Ogawa [18]).

The intermediate coupling model as used by Satpathy and Gujrathi [19]) considers up to three phonon states of the core and in addition to the $(1f_{\frac{7}{2}})^{-1}$ proton orbit mentioned above, the $(1d_{\frac{3}{2}})^{-1}$ and $(2s)^{-1}$ proton configurations were also considered. The strength of the coupling was treated as an adjustable parameter. The quintet mentioned above, in particular the doublet nature of the $\frac{5}{2}^-$ and $\frac{7}{2}^-$ levels and of the $\frac{1}{2}^-$ and $\frac{3}{2}^-$ levels, except for a reversal in spin in the latter case, is well reproduced (fig. 7). The $J^\pi = \frac{1}{2}^-$ level at $E_x \approx 2.5$ MeV predicted in this model may correspond to one of the high spin levels observed in the ^{57}Fe(p, n) reaction [23]) mentioned earlier. This model fails to reproduce the $J^\pi = \frac{3}{2}^-$ and $\frac{1}{2}^-$ levels at $E_x \approx 1.5$ MeV and the agreement with experiment is not satisfactory beyond $E_x \approx 2.5$ MeV.

It is, however, possible that some of the observed levels might be accounted for within the framework of the intermediate coupling model by including additional proton configuration like 2p and $1f_{\frac{5}{2}}$. This is done by Gómez [22]) and the spacings between the excited proton configurations were taken from experiment and also from the binding energies. The collective parameters were taken from experimental data. Agreement with the experimental level scheme is considerably improved (fig. 7). The ordering of the low-lying levels is however not correct. The spectroscopic factors for the single-proton stripping reactions leading to ^{57}Co are also calculated by Gómez for some of the strong transitions and the results are summarized in table 5. Excep-

ting the g.s. the agreement with the measured values given by (τ, d) and (d, n) reactions is far from satisfactory† The levels 2.731 and 2.804 MeV predicted to carry reasonable single-particle strengths (table 5) are not at all excited in any proton stripping reaction.

In the above weak and intermediate coupling models the core excitation is assumed to follow a pure harmonic vibration. The intermediate coupling model used by Stewart *et al.*[21]) considers the phonon states built on an anharmonic vibration. The pairing effects are not ignored and the quasi-particle effects have further been introduced. Quite a significant improvement in the level spectrum is thereby achieved (fig. 7); all the levels up to $E_x \approx 2.3$ MeV are reasonably well reproduced.

The above discussions refer to the negative-parity levels. The positive-parity levels are calculated only by Satpathy and Gujrathi [19]) and two $\frac{1}{2}^+$ levels ($E_x = 3.011$ and 5.338 MeV) and four $\frac{3}{2}^+$ levels ($E_x = 3.352, 4.685, 5.448$ and 6.416 MeV) are predicted, arising from the 2s and $1d_{\frac{3}{2}}$ proton-hole states, respectively. The observed $J_\pi = \frac{1}{2}^+$ level at $E_x = 2.99$ MeV is clearly the lowest $\frac{1}{2}^+$ level given by Satpathy and Gujrathi. The difficulty arises with the other $2s_{\frac{1}{2}}$ level. In a previous ^{56}Fe(τ, d) experiment Hardie *et al.*[3]) observed an $l_p = 0$ transition to a level close in energy to this predicted level. Two such levels are identified in the present work with a $l_p = 0$ stripping angular distribution (fig. 4) fairly close to the level under discussion, and the small cross sections are consistent with their identification as 2s hole states. The $\frac{1}{2}^+$ level, however, is not observed in the ^{58}Ni(t, α) reaction [14]), although the spectroscopic factor for this level is calculated to be about half that for the $\frac{1}{2}^+_1$ level (Satpathy and Gujrathi [19])). The identification of the predicted $\frac{1}{2}^+_2$ level thus remains undecided. Five $l_p = 2$ transitions (including two doubtful ones) were observed by Blair and Armstrong [14]) in the ^{58}Ni(t, α) reaction, some of which may correspond to some of the $\frac{3}{2}^+$ levels given by the calculation of Satpathy and Gujrathi.

5. Conclusion

Angular distributions have been measured in the present experiment for most of the levels in ^{57}Co up to $E_x \approx 7.8$ MeV from the ^{56}Fe(τ, d) reaction. A fairly accurate measurement of the absolute cross section has been carried out. The spectroscopic strength obtained in the present work, level by level, for the 2p and $1f_{\frac{7}{2}}$ transitions lies between that given in the previous two measurements [2,3]), while that for the $1f_{\frac{5}{2}}$ levels given by the present work, is the smallest of all (τ, d) and (d, n) values. More assignments of orbital angular momentum transfer have been made in the present experiment than in previous proton stripping studies (table 3). The summed 2p, $T_<$ strength obtained by us and Rosner and Holbrow [2]) is fairly consistent with the shell-model limit, whilst that given by Hardie *et al.* [3]) and Adam *et al.* [5]) is much smaller than the expected value. The splitting of the measured 2p, $T_<$ strength into $p_{\frac{3}{2}}$ and

† The large g.s. transition strength obtained by Okorokov *et al.* [6]) is disturbing.

$p_{\frac{1}{2}}$ components is difficult; the summed strengths for these components are far from the respective single-particle limits. The $1f_{\frac{7}{2}}$, $T_<$ transition strength given by Hardie *et al.*[3]) is only about 50% of the expected value, while that given by the present and the remaining experiments are in reasonable agreement with the sum rule limit. The measured $1f_{\frac{5}{2}}$, $T_<$ strengths in the present case and those by Hardie *et al.* are appreciably smaller than the expected value, while those given by Rosner and Holbrow[2]) and Adam *et al.*[5]) are in satisfactory agreement with the shell-model value. A choice of a different optical model parameter combinations somewhat increases the present $1f_{\frac{7}{2}}$ value, but the change is not sufficient to bring the measured value close to the theoretical limit. It would be interesting to calculate the transition strengths on the pairing theory, which gives a more realistic picture of the nuclear structure than the simple shell model.

In agreement with Rosner and Holbrow[2]) three analogue states have been identified in the present work; the relative spacings and the l_p values are consistent with the relative spacings and the J^π values of the parent levels in ^{57}Fe.

There have been several calculations to obtain the level scheme, level properties and electromagnetic transition rates of ^{57}Co based on the shell model and unified model. The unified model calculations by Stewart *et al.*[21]) satisfactorily reproduce all the observed levels up to $E_x = 2.3$ MeV; the predicted level density above $E_x \approx 2.3$ MeV is less than that observed. The unified model, however, does not calculate the spectroscopic factors relevant to the proton stripping reactions. This seems important in view of the fairly accurate cross sections obtained in the present work. The transition strength calculated by Gómez [22]) on the shell model is not satisfactory except for the g.s.

The authors wish to thank Dr. D. Roaf for invaluable advice in running the magnetic spectrograph and processing the plates and Professor K. W. Allen for his interest in the work. They are thankful to Professor P. D. Kunz for the DWBA code DWUCK and Dr. D. Sinclair for advice on the calculations. The authors would like to thank Mrs. Momtaz Begum for help with some scanning. One of the authors (H.M. S.G.) acknowledges financial support from the Royal Society, London while doing the experiment at Oxford.

References

1) R. L. Auble, Nucl. Data Sheets **20** (1977) 327
2) B. Rosner and C. H. Holbrow, Phys. Rev. **154** (1967) 1080
3) G. Hardie, T. H. Braid, L. Meyer-Schützmeister and J. W. Smith, Phys. Rev. **C5** (1972) 1600
4) A. Baghdadi, R. Seltz, D. Magnac-Valette, G. Bonneaud and C. Gerardin, Nucl. Phys. **A253** (1975) 20
5) A. Adam, O. Bersillon and S. Joly, Phys. Rev. **C14** (1976) 92
6) V. V. Okorokov, V. M. Serezhin, V. A. Smotryaev, D. L. Tolchenkov, I. S. Trostin and Yu. N. Cheblukov, ITEF Report (1968) 598 (quoted in ref. [5]))
7) R. G. Couch, Ph.D. Thesis, Northwestern University (1969), unpublished (quoted in ref. [5]))
8) R. H. Bassel, Phys. Rev. **149** (1966) 791

9) H. Ohmura, T. Ishimatsu, K. Yagi, H. Ejiri, Y. Nakajima, T. Tohei and T. Nakagawa, J. Phys. Soc. Japan **25** (1968) 953
10) R. Stock, B. Bock, P. David, H. H. Duhm and T. Tamura, Nucl. Phys. **A104** (1967) 136
11) J. D. Childs, W. W. Daehnick and M. J. Spisak, Phys. Rev. **C10** (1974) 217
12) C. M. Perey and F. G. Perey, Phys. Rev. **132** (1963) 755
13) M. T. Esat, J. R. Leslie and W. McLatchie, Nucl. Phys. **A232** (1974) 139
14) A. G. Blair and D. D. Armstrong, Phys. Rev. **151** (1966) 930
15) J. Vervier, Nucl. Phys. **78** (1966) 497
16) J. B. McGrory, Phys. Rev. **160** (1967) 915
17) C. Gatrousis, R. A. Meyer, L. G. Mann and J. B. McGrory, Phys. Rev. **180** (1969) 1052
18) H. Horie and K. Ogawa, Nucl. Phys. **A216** (1973) 407
19) L. Satpathy and S. C. Gujrathi, Nucl. Phys. **A110** (1968) 400
20) A. Covello and V. R. Manfredi, Phys. Letts. **34B** (1971) 584
21) K. W. C. Stewart, B. Castel and B. P. Singh, Phys. Rev. **C4** (1971) 2131
22) J. M. G. Gómez, Phys. Rev. **C6** (1972) 149
23) P. Pietrzyk, K. D. Büchs, E. Finckh, W. Fritsch and B. Schrieber, Z. Phys. **262** (1973) 239
24) K. L. Coop, I. G. Graham, J. M. Poate and E. W. Tittarton, Nucl. Phys. **A130** (1969) 223
25) R. Dayras, M. Toulemonde, B. Čujee, B. Hausch, J. N. Moc and I. M. Szöghy, Nucl. Phys. **A173** (1971) 49

Nuclear Physics A378 (1982) 11–28

LEVEL STRUCTURE OF ^{46}Ti FROM THE (τ, d) REACTION ON ^{45}Sc

HAMIDA BANU and H. M. SEN GUPTA [†]

Department of Physics, University of Dacca, Dacca, Bangladesh

and

F. WATT

Nuclear Physics Laboratory, Keble Road, Oxford, England

Received 15 June 1981
(Revised 29 September 1981)

Abstract: The level structure of ^{46}Ti has been studied through the ^{45}Sc(τ, d) reaction at E_τ = 16 MeV using the Van de Graaff accelerator and multi-channel magnetic spectrograph of the Nuclear Physics Laboratory, Oxford. Angular distributions of deuterons are measured up to $E_x \sim 9.9$ MeV and absolute cross sections are measured. The data are analysed in terms of the LZR DWBA theory of the direct stripping reaction. Orbital angular momentum transfers and spectroscopic strengths are obtained.

E | NUCLEAR REACTION ^{45}Sc(^{3}He, d), E = 16 MeV; measured $\sigma(E_d, \theta)$. ^{46}Ti deduced levels, L, π, C^2S. Natural target

1. Introduction

Studies of single-proton transfer reactions have been found to be useful in obtaining information on the ground-state wave function of target nuclei and single-particle/hole states in the final nuclei. In the case of an odd-odd final nucleus such reactions also provide information regarding the residual n-p interaction. The (τ, d) reaction has an obvious advantage over other single-proton stripping reactions from the point of experimental measurements. The present work is concerned with the (τ, d) reaction on ^{45}Sc at E_τ = 16 MeV. This reaction was previously studied by Broman and Pullen [1]) at E_τ = 15 MeV, Barnard and Jones [2]) at E_τ = 38 MeV and Ohmura *et al.* [3]) at E_τ = 24 MeV, covering angular distribution measurements respectively up to $E_x \sim 7.6$, 3.9 and 5.6 MeV. The experiment of Broman and Pullen [1]) was later extended by Broman and Larsson [4]) to include excitation beyond 7.6 MeV using the same set of nuclear plates. There are a few discrepancies in the assignments of the orbital angular momentum transfer in the different measurements (see table 2); more serious is the systematically large difference in the spectroscopic factors, varying

[†] Now at the Department of Physics, University of Birmingham, Birmingham.

by a factor of about two, even for strong transitions, given by Broman and Pullen [1]) on the one hand and Barnard and Jones [2]) and Ohmura *et al.* [3]) on the other, even though the uncertainty in absolute cross section is quoted as less than 40 % in the different measurements. In the ^{45}Sc(α, t) reaction studied by Priest and Vincent [5]), the relative spectroscopic strengths were extracted, while another proton stripping reaction (^{16}O, ^{15}N) by Maher *et al.* [6]) was naturally concerned more with the reaction mechanism itself than with the spectroscopic factors although absolute cross sections were measured.

The present work was therefore undertaken with an energy resolution better than in previous experiments and special care was taken in measuring the absolute cross-section values. Properties of most of the levels in ^{46}Ti up to $E_x \sim 9.9$ MeV are given.

2. Experimental procedure

The experiment was carried out with a beam of 16 MeV ^{3}He particles from the Tandem Van de Graaff accelerator of the Nuclear Physics Laboratory, University of Oxford. The target was natural scandium deposited by vacuum evaporation onto a thin carbon backing. The target was continuously monitored during the experiment

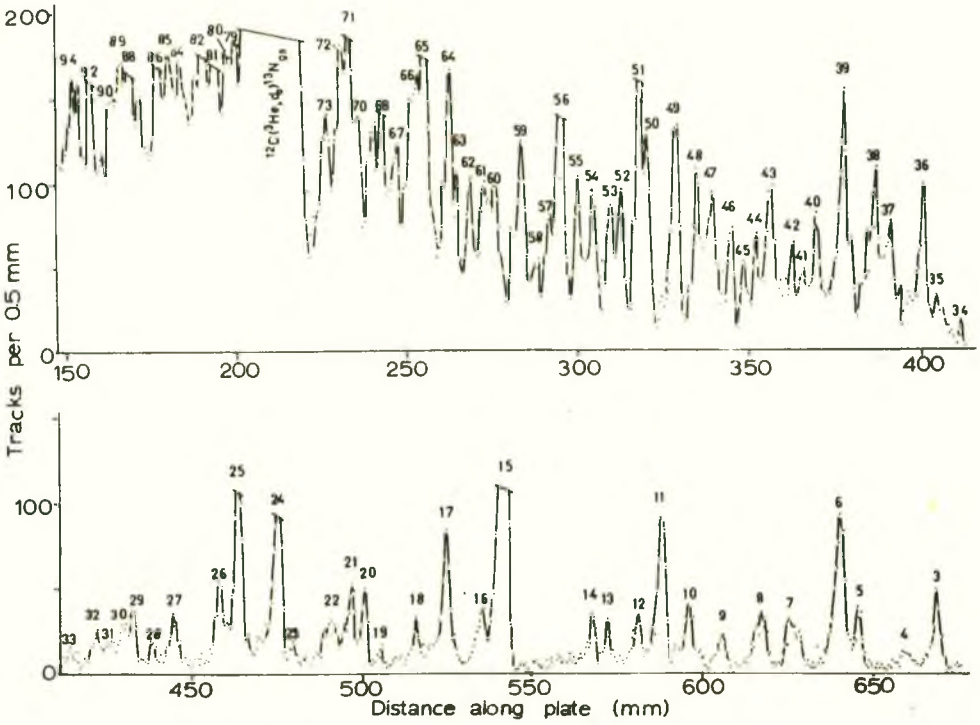

Fig. 1. Part of the energy spectrum of deuterons arising from the ^{45}Sc(τ, d) reaction at 26.25° showing the region of high density.

against any deterioration. The reaction products were magnetically analysed in a multichannel magnetic spectrograph under an applied field of strength ~ 13.57 kG and were recorded in 25 μm thick Ilford L4 emulsion plates simultaneously from 11.25° to 48.75° in steps of 7.5°. The total beam charge was 1885.6 μC. Each plate was marked with six equidistant index lines, designated by A, B, C, etc. immediately after a run. This is for convenience of scanning, as well as for ready determination of the position of a group with respect to the nearest index line.

The plates were scanned at Dacca and the energy spectrum was obtained at each angle. A typical spectrum is shown in fig. 1. The energy levels in ^{46}Ti were obtained as discussed in subsect. 4.1. The energy resolution (FWHM) was ~ 22 keV.

Among other quantities, measurements of solid angle and target thickness are necessary for establishing the absolute cross-section scale. The solid angles were measured both geometrically and using an α-source†. Direct calculations at the magnetic deflection of $\frac{1}{2}\pi$ at the position D+64 scans were made from the width/height of the particle-defining slits and path length from the centre of the spectrograph to the verticle or horizontal slits. Solid angle relative to the value at the $\frac{1}{2}\pi$ position was determined by placing a thin (10 keV) americium α-source (0.5 mm × 2 mm) at the target position and exposing for equal times at six values of the magnetic field so as to cover the scans on the entire nuclear plates, and an absolute value was then obtained by measuring the yield of the α's per solid angle from the americium source in a solid state counter with a pinhole aperture in front. The two methods gave solid angles in agreement to within 5 %. Depending on the position, the solid angle varies by up to ~ 20 % around the mean value of 0.24 msr at the position D+64. Those at the position of interest were obtained by interpolation.

To measure the target thickness, a subsidiary short exposure of 0.92 μC was taken on the elastic scattering of 3 MeV deuterons from the same target as used in the main experiment at a magnetic field of strength ~ 5.48 kG and the yield of the elastic group at 26.25° was normalized to the Rutherford cross section at that angle. The solid angle at the particular position of the elastically scattered deuteron group being known, the effective target thickness was thus found to be 53 $\mu g \cdot cm^{-2}$. The total uncertainty in the absolute value of the (τ, d) cross section, resulting mainly from errors in the target thickness, scanning and background subtraction, was estimated to be less than 15 %.

3. DWBA analysis

The angular distribution data were analysed in terms of the DWBA theory of direct stripping reaction in the local zero-range approximation. The calculations were carried out by one of the authors (H.M.S.G.) at Oxford using the code DWUCK due to Kunz with the IBM 360/195 computer of the Rutherford High Energy Labora-

† We are grateful to Dr. D. Roaf for these measurements.

tory. The optical-model potential was of the standard Woods-Saxon form for the ^{3}He potential and the real part of the deuteron potential, while a Woods-Saxon derivative was used for the imaginary part of the deuteron potential. The bound-state wave function was generated by using the real potential of the form

$$V_0 f(r, r_0, a) + \frac{V_0 \lambda^2}{45.2} \frac{1}{r} \frac{d}{dr} f(r, r_0, a)\, \mathbf{l} \cdot \mathbf{s},$$

where $f(r, r_0, a)$ is the Woods-Saxon form factor and $\lambda = 25$. The strength of the potential was adjusted, with $r_0 = 1.25$ fm, $a = 0.65$ fm and Coulomb radius parameter $r_c = 1.3$ fm, so as to give the correct binding energy of the transferred proton.

TABLE 1

Optical-model parameters

Particle	V_0 (MeV)	r_0 (fm)	a (fm)	W_0 (MeV)	$4W_D$ (MeV)	r_I (fm)	a_I (fm)	$V_{s.o.}$ (MeV)	$r_{s.o.}$ (fm)	$a_{s.o.}$ (fm)	r_C (fm)	Ref.
^{3}He	139.0	1.08	0.80	12.3		1.743	0.721				1.4	[3,7])
d	94.8	1.12	0.79		61.2	1.32	0.74	6.6	0.90	1.16	1.3	[8])
p	[a])	1.25	0.65					$\lambda = 25$			1.3	

[a]) Adjusted to reproduce the binding energy.

The potential parameters used in the DWBA calculation are shown in table 1 [refs. [3,7,8])]. This combination approximately satisfies the condition $V_t \sim V_d + V_p$ for the real depths. The spectroscopic transition strengths $(2J_f + 1)C^2S/(2J_i + 1)$ were obtained by normalising the computed cross section $\sigma_{DW}(\theta)$ to the measured value $\sigma_{exp}(\theta)$ through the relation

$$\sigma_{exp}(\theta) = N \frac{2J_f + 1}{2J_i + 1} C^2S \frac{\sigma_{DW}(\theta)}{2j+1},$$

as suggested in the DWUCK code, where J_i and J_f are respectively the angular momentum of the initial and final nuclear levels and j is the angular momentum of the transferred proton. A normalization constant $N = 4.42$ was used relevant to the Gunn-Irving wave function for ^{3}He and the Hulthén wave function for the deuteron [7]).

4. Results and discussion

4.1. THE ENERGY LEVELS IN ^{46}Ti

The energy levels in ^{46}Ti have been measured from a variety of nuclear reactions and compiled by Lederer and Shirley [9]) and Auble [10]). The excitation energies determined from a previous ^{45}Sc(τ, d) reaction [1]) are systematically larger than those of the compilations and also those given by a recent high resolution γ-ray study [11]) following the (α, n) reaction on ^{43}Ca. It was therefore thought worthwile to redetermine the energy levels in ^{46}Ti so as to make a meaningful comparison with the adopted levels [9,10]), as well as with those levels observed in γ-ray studies [refs. [11-13])].

Because of the uncertainty in the spectrograph calibration at the high magnetic

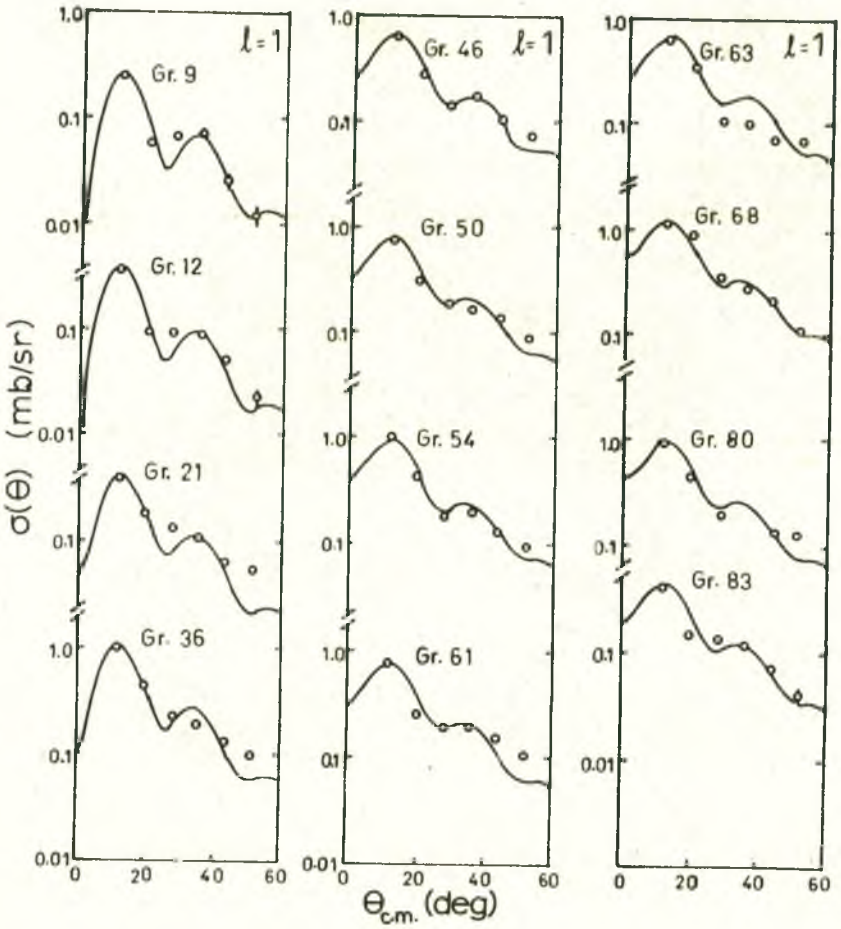

Fig. 2. Measured angular distributions fitted with $l = 1$ DWBA curves.

TABLE 2

Summary of the level properties of ^{46}Ti

Level	E_x (MeV)		$\sigma_{max}(\theta)$ (mb/sr)	l_p transfer				$(2J_f+1)C^2S/(2J_i+1)$			
	[a]	[b]		[a]	[c]	[d]	[e]	[a]	[c]	[d]	[e]
0	0	0	0.11	3	3	3	3	0.26	0.53	0.27	0.17
1	0.890	0.891	0.76	1+3	1+3	1+3	1+3	0.082+0.29	0.25+0.96	0.06+0.28	0.10 +0.34
2	2.011	2.010	0.68	1+3	1+3	1+3	1+3	0.078+0.28	0.20±0.72	0.04+0.22	0.09 +0.25
3	2.960	2.962	0.14	3	3	3	1+3	0.29	0.50	0.22	0.04 +0.06
4	3.060	3.059	0.50	2	2		(1+3)	0.054	0.09		(0.12 +0.09)
5	3.234	3.236	0.081	1+3	1+3	3	(1)	0.012+0.15	0.01+0.24	0.58	(0.07)
6	3.298	3.299	0.29	3	3		3	0.54	0.90		0.64
7	3.441	3.438	0.12	2	2	3	(1+2)	0.11	0.27	0.16	(0.006+0.10)
8	3.573	3.572	0.12	3	1+3		1+3	0.22	0.02+0.36		0.008+0.24
9	3.726	3.724	0.26	1	1		1+(2)	0.024	0.06		0.02+ (0.07)
10	3.842	3.842	0.26	1+3	1+3	1+3	1+2	0.021+0.12	0.06+0.31	0.09+0.36	0.02 +0.22
11	3.930	3.930	0.49	1+3	1+3		(1+3)	0.037+0.28	0.09+0.57		(0.05 +0.36)
12	4.031	4.021	0.38	1	1		1	0.034	0.08		0.04
13	4.136	4.130	0.12	1+3	1+3			0.009+0.037	0.02+0.14		
14	4.199	4.206	0.065	3	3		(0)+3	0.12	0.23		(0.02)+0.20
		4.394			1				0.004		
15	4.526	4.524	0.655	3	3		(0)+3	1.04	2.11		(0.04)+0.84
16	4.617	4.620	0.25	1+3	1			0.022+0.067	0.06		
17	4.719	4.723	0.29	1+3	1+3		(0)+3	0.025+0.28	0.03+0.59		(0.01)+0.39
18	4.845	4.846	0.11	1+3	1+3		1+3	0.008+0.062	0.03+0.08		0.03 +0.05
19	4.966	4.950	0.10	n.s.	1+3				0.01+0.05		
20	5.036	5.045	0.12	0	0			0.028	0.06		
21	5.094	5.098	0.39	1	1		1+3	0.033	0.13		0.08 +0.19
22	5.167	5.187	0.16	1+3	1+3			0.012+0.075	0.02+0.17		
23	5.317	5.326	0.29	1	1			0.25	0.02		
24	5.379	5.383	0.39	1+3	1+3		1+3	0.019+0.31	0.07+0.40		0.09 +0.22
25	5.554	5.557	0.60	1+3	1+3		1+3	0.045+0.21	0.14+0.41		0.08 +0.38
26	5.618	5.610	0.13	1+3	1			0.005+0.12	0.06		
27	5.811	5.816	0.14	0	0			0.030	0.06		
28	5.897	5.899	0.11	1+3	1+3			0.006+0.031	0.02+0.04		
29	5.980	5.982	0.19	1+3	1+3			0.012+0.65	0.02+0.31		
30	6.021	6.029	0.19	1	1			0.015	0.05		
31	6.094	6.088	0.20	n.a.	0				0.03		

32	6.140	6.141	0.35	n.a.	1 + 3		0.01 + 0.08
33	6.217	6.214	0.20	n.a.	0		0.01
34	6.251	6.246	0.23	n.a.			
35	6.337	6.335	0.19	2	1	0.10	0.06
36	6.424	6.427	1.01	1	1	0.070	0.16
37	6.550	6.556	0.76	1	1 + 3	0.059	0.09 + 0.22
38	6.616	6.623	0.60	1	1	0.046	0.03
39	6.742	6.744	0.85	1 + 3	1 + 3	0.052 + 0.25	0.13 + 0.51
40	6.851	6.856	0.14	1 + 3	1 + 3	0.012 + 0.041	0.02 + 0.33
41	6.899	6.897	0.44	1	1	0.030	0.04
42	6.974	6.979	0.16	n.s.	1 + 3		0.02 + 0.14
43	7.041	7.049	0.36	1 + 3	1 + 3	0.031 + 0.18	0.09 + 0.18
44	7.101	7.101	0.36	1	1	0.032	0.08
45	7.147	7.147	0.33	1	1	0.032	0.06
46	7.201	7.204	0.75	1	1 + 3	0.044	0.09 + 0.20
47	7.288	7.294	0.22	1 + 3	1	0.007 + 0.12	0.06
48	7.347	7.349	0.89	1	1	0.066	0.16
49	7.429	7.433	0.92	1	1	0.063	0.25
50	7.558	7.565	0.76	1	1	0.052	0.42
51	7.584		1.38	1		0.096	
52	7.611	7.665	0.57	1		0.040	0.15
53	7.712	7.707	0.56	1	1	0.38	
54	7.780	7.764	1.02	1	1	0.066	0.16
55	7.849	7.849	0.72	1	1	0.045	0.10
56	7.917	7.920	1.30	1		0.094	0.30
57	7.979	7.971	0.41	1	1	0.029	
58	8.038	8.026	0.16	n.s.			
59	8.088	8.090	0.70	1	1	0.052	0.14
60	8.182	8.115	0.92	1		0.063	0.15
61	8.228	8.230	0.78	1	1	0.054	
62	8.293	8.303	0.53	1	1	0.042	0.05
63	8.346		0.64	1		0.044	
64	8.384	8.402	0.51	1 + 3	1	0.024 + 0.18	0.13
65	8.467	8.466	0.76	1 + 3	1	0.044 + 0.17	0.03
66	8.530	8.513	1.77	1		0.12	
67	8.574	8.552	0.54	1 + 3	1	0.033 + 0.062	0.09
68	8.621	8.625	1.14	1	1	0.083	0.06
69	8.662	8.673	0.24	1	1	0.028	0.11
70	8.709		0.19	1		0.026	
71	8.761		1.32	1		0.16	

TABLE 2 (continued)

Level	E_x (MeV)		$\sigma_{max}(\theta)$ (mb/sr)	l_p transfer				$(2J_f+1)C^2S\,(2J_i+1)$			
	[a]	[b]		[a]	[c]	[d]	[e]	[a]	[c]	[d]	[e]
72	8.808	8.797	1.18	1	1			0.10	0.029		
73	8.860	8.884	2.76	1	1			0.21	0.10		
74	8.940	8.945	1.29	1	1			0.10	0.09		
75	9.984	9.019	1.52	1				0.13			
76	9.070	9.053	0.68	1	1			0.055	0.12		
77	9.111	9.124	1.37	1 + 3	1			0.10 + 0.18	0.06		
78	9.141		0.31	n.s.							
79	9.176	9.197	0.35	3				0.28			
80	9.205	9.242	0.94	1	3			0.064	1.07		
81	9.253		1.00	1				0.082			
82	9.304		0.82	1				0.066			
83	9.345		0.40	1				0.030			
84	9.385	9.418	0.50	1	1			0.041	0.11		
85	9.426		0.34	3				0.29			
86	9.474	9.472	1.23	1	1			0.085	0.11		
87	9.519		0.30	2				0.20			
88	9.572	9.608	0.41	3				0.28			
89	9.618		0.43	1				0.040			
90	9.649	9.670	0.52	1				0.049			
91	9.682		0.21	n.s.							
92	9.718	9.741	0.58	2				0.058			
93	9.761		0.41	n.a.							
94	9.790	9.816	0.38	n.a.							
		9.847									
95	9.864	9.887	0.42	n.a.							

n.s. Non stripping angular distribution.
n.a. Data not analysed.
[a]) Present work.
[b]) Refs. [9-11]).
[c]) The (τ, d) reaction at E_τ = 15 MeV [ref. [1])]; the l-values and transition strengths above E_x = 7.6 MeV are from ref. [4]).
[d]) The (τ, d) reaction at E_τ = 37.7 MeV [ref. [2])].
[e]) The (τ, d) reaction at E_τ = 24.3 MeV [ref. [3])].

field used in the present experiment ($B \sim 13.57$ kG), an internal calibration was made using least squares parabolic fits to several well-known levels in ^{46}Ti (shown underlined in table 2) and the ground state of the ^{12}C(τ, d)^{13}N reaction. The latter provided a useful calibration point in a region of the plates where the density of the levels is high. The criteria used for the identification of the levels were that the excitation energies of levels in ^{46}Ti obtained at different angles were consistent to within 10 keV and that the deuteron groups at different angles belonging to the same levels had similar widths.

4.2. THE ANGULAR DISTRIBUTIONS AND TRANSITION STRENGTHS

A large number of levels, including a few analogues, have been observed up to $E_x \sim 9.9$ MeV. The angular distributions have been measured for all the groups

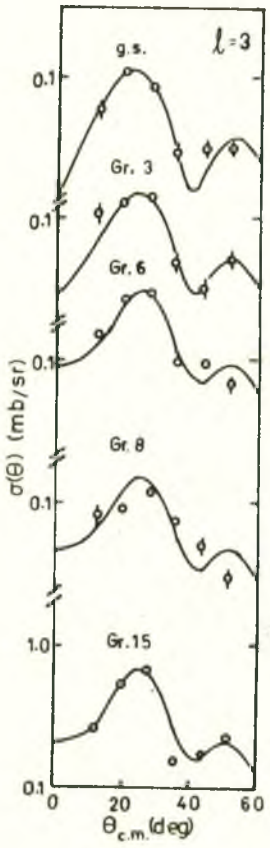

Fig. 3. Measured angular distributions fitted with $l = 3$ DWBA curves.

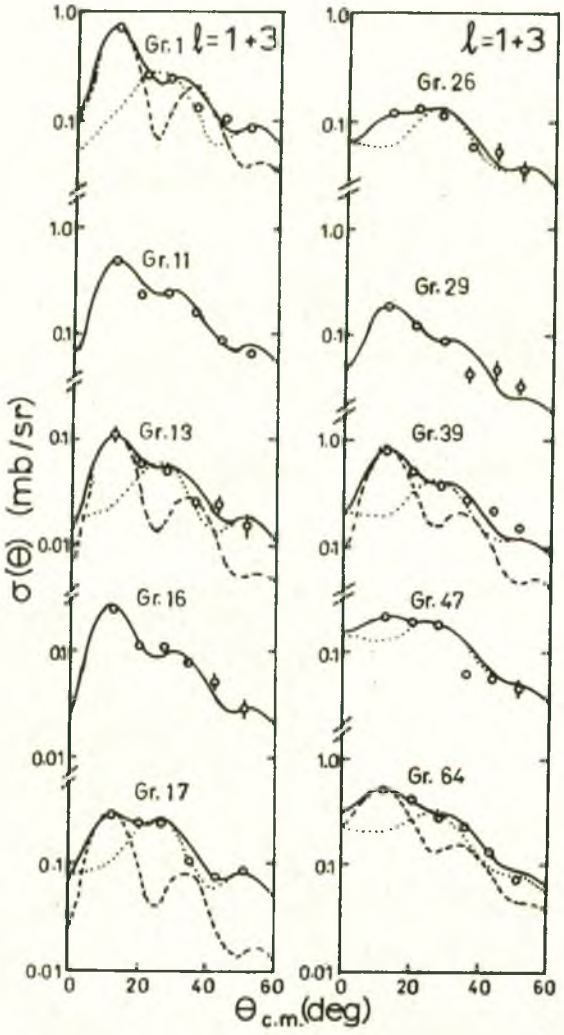

Fig. 4. Measured angular distributions fitted with $l = 1 + 3$ DWBA curves: solid line, $l = 1 + 3$; broken line, $l = 1$; dotted line, $l = 3$.

and transition strengths extracted for many of them. The results are summarized in table 2.

Typical examples of the DWBA fits to the measured angular distributions are shown in figs. 2-7. The levels for which the cross sections at the first two forward angles are missing, either due to the presence of a contaminant or to an emulsion disturbance, are excluded from the DWBA analysis; these are marked n.a. in table 2. A few levels do not have angular distribution characteristics of a direct stripping process. Such levels are denoted by n.s. in the table. Also included in the table for

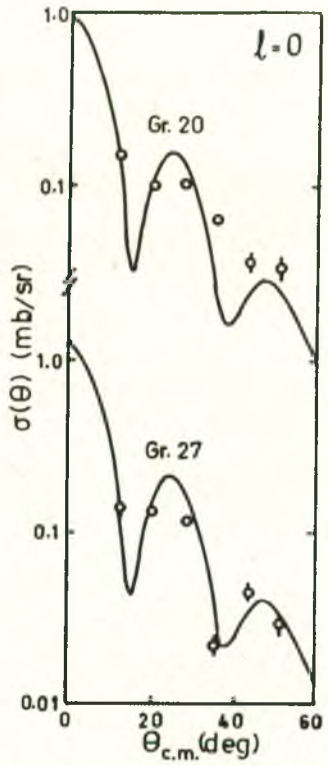

Fig. 5. Measured angular distributions fitted with $l = 0$ DWBA curves.

comparison are the results from previous (τ, d) reactions on ^{45}Sc [refs. [1-3])]. The transition strengths in all these studies as well as in the present work are extracted using the same normalization constant ($N = 4.42$) and should therefore be directly comparable (columns 9-12).

The (τ, d) reaction excites both normal ($T_<$) and analogue ($T_>$) states and the summed transition strengths according to the simple shell model $G_j (= (2J_i + 1) C^2S/(2J_i + 1))$ are related to the shell vacancies as given by

$$\sum G_j = \begin{cases} \langle \text{neutron holes} \rangle / (N - Z + 1), & T_> \text{ state} \\ \langle \text{proton holes} \rangle - \langle \text{neutron holes} \rangle / (N - Z + 1), & T_< \text{ state,} \end{cases}$$

where N and Z are the neutron and proton numbers of the target nucleus.

4.2.1. The $l = 1$ and 3 transitions. The 1f and 2p single-particle strengths are heavily fragmented and the 2p strength is more or less evenly distributed over the entire range of excitation energy studied, while a large proportion of the 1f shell-model strength is carried by a few low-lying levels (table 2). A number of angular distributions required a mixture of $l = 1$ and 3 transfers, signifying a high degree of mixing

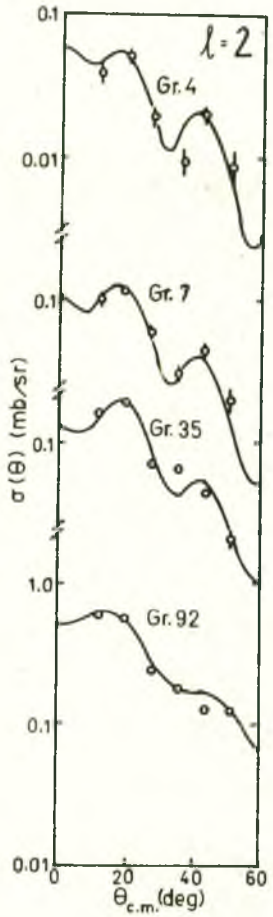

Fig. 6. Measured angular distribution fitted with $l = 2$ DWBA curves.

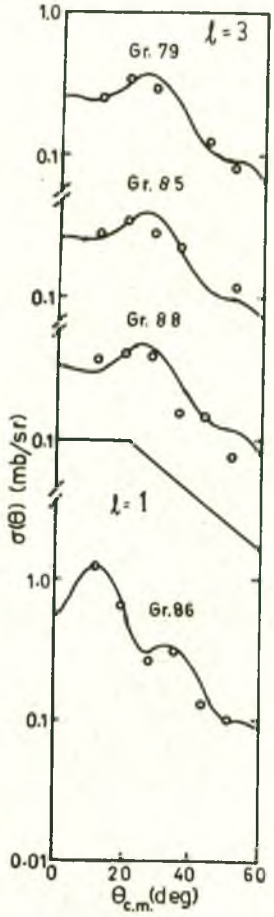

Fig. 7. Measured angular distribution for analogue states.

of the 1f and 2p shell-model configurations. Such a mixture was considered during the DWBA analysis only when the quality of a fit was thereby improved significantly and the $l = 3$ component had an appreciable contribution. A few examples are given in fig. 4 where fits from individual l-values are also shown in some cases.

The transition strengths in table 2 were deduced by assuming that all $l = 1$ and 3 transitions populate respectively the $2p_{\frac{3}{2}}$ and $1f_{\frac{7}{2}}$ shell-model states. The summed transition strengths so obtained are shown in table 3 for a comparison with the shell-model values. The $T_<$ component of the total 1f strength thus comes to be 6.3, as against the single-particle limit 10.5 for $1f_{\frac{7}{2}} + 1f_{\frac{5}{2}}$ shells. Likewise the observed strength for 2p transitions is 3.7 being fairly close to the expected $T_<$ component of the total $2p_{\frac{3}{2}} + 2p_{\frac{1}{2}}$ strength of 4.5. It could then be assumed that most of the $T_<$ component

TABLE 3

Results of the sum-rule analysis for the proton $T_<$ states in ^{46}Ti

Single-particle state	$\sum(2J_f+1)C^2S/(2J_i+1)$			
	shell-model limit		[a]	[b]
$1f_{7/2}$	6	10.5	6.3	11.3
$1f_{5/2}$	4.5			
$2p_{3/2}$	3	4.5	3.7	4.9
$2p_{1/2}$	1.5			

The strengths are deduced by assuming that all $l_p = 1$ and 3 transitions belong to the $2p_{3/2}$ and $1f_{7/2}$ shell respectively; the possibility of excitation of $1f_{5/2}$ and $2p_{1/2}$ shells increases the strengths.

[a]) Present work.

[b]) Ref. [1]).

TABLE 4

Summary of the results on the isobaric analogue states in ^{46}Ti

^{45}Sc(τ, d)^{46}Ti [a]				^{45}Sc(d, p)^{46}Sc						
E_x^A (MeV)	E_x [b]) (MeV)	l_p	$(2J_f+1)C^2S$	E_x^p (MeV)	l_n		$(2J_f+1)C^2S$		J^π	ΔE_c (MeV)
					[c])	[d])	[c])	[d])		
9.176	0	3	2.24	0	3	3	4.64	2.88	4^+	7.591
9.426	0.250	3	2.32	0.228	3	3	4.96	2.86	3^+	7.613
9.474	0.298	1	0.68	0.279	(1)	1+3	(0.80)	0.44 [e])	5^+	7.610
9.572	0.396	3	2.24	0.444	3	3	2.48	1.60	2^+	7.643

[a]) Present work.

[b]) Excitation in "^{46}Sc" obtained with the 9.176 MeV level as the ground-state analogue.

[c]) Ref. [14]).

[d]) Ref. [15]).

[e]) The strengths of the $l_n = 1$ component.

of the 1f and 2p shell-model strengths has been reached within the excitation ($E_x \sim$ 10 MeV) covered in the present work.

A few low-lying levels in ^{46}Sc are fairly strongly excited in the (d, p) reaction on ^{45}Sc and it would be expected that the corresponding analogues in ^{46}Ti lie above $E_x \sim 9$ MeV. On the basis of relative level spacings and the consistency between the l_p transfer in the (τ, d) reaction and l_n transfer in the (d, p) reaction, four levels, namely 9.176, 9.426, 9.474 and 9.572 MeV, have been identified as analogues. The results are summarized in table 4 for a comparison with the levels in the ^{45}Sc(d, p) reaction [refs. [14, 15])]. There is a reasonable resemblance between the transition strength given by the present (τ, d) work and the (d, p) work of ref. [15]). It may be mentioned that the level at 9.205 MeV was previously identified as the analogue of the first

excited level of ^{46}Sc [ref. [4])]. The level in the present experiment is populated with an angular distribution typical of an $l_p = 1$ transfer (fig. 2), rather than $l_p = 3$ as expected from the corresponding (d, p) reaction. Even though the background in the region of the plate where the group lies is relatively high, repeated scans yielded a consistent set of cross-section data, never differing by more than 10 % for different scans. It is surprising then that the analogue of a very strong group, found in a previous (τ, d) work [4]), is missing in the present experiment. There is no evidence of an $l_p = 1 + 3$ mixture in this angular distribution as found in many other distributions (fig. 7 and table 2).

4.2.2. The $l = 0$ and 2 transitions. A few levels were observed with angular distributions characteristics of $l = 0$ and 2 transfers (figs. 5 and 6). The transitions to the negative-parity states are a result of the $(2s_{\frac{1}{2}})^{-2}(1f_{\frac{7}{2}})$ and $(1d_{\frac{3}{2}})^{-2}(1f_{\frac{7}{2}})$ configurations in ^{45}Sc, i.e. the negative-parity states arise from the $(2s_{\frac{1}{2}})^{-1}(1f_{\frac{7}{2}})$ and $(1d_{\frac{3}{2}})^{-1}(1f_{\frac{7}{2}})$ two-proton configurations in ^{46}Ti†. The negative-parity states thus have the characteristics of a deformed rotational band and based on the energy spacings, the characteristic cascade and crossover transitions and an enhanced E2 transition, the levels at $E_x = 3.059$, 3.442, 3.853, 4.663, 5.198 and 6.150 MeV with respective $J^\pi = 3^-, 4^-, (5^-), (6^-), (7^-)$ and (8^-) have been identified in the ^{43}Ca(α, nγ) reaction [11]) as the members of a rotational band. It is therefore possible that the negative-parity levels populated in the (τ, d) reaction have a contribution from a non-single-step process. In fact the measured angular distributions for $l = 0$ transitions (fig. 5) do not follow the detailed shape of the single-step DWBA curve and thus in view of the limited data in the present experiment the contribution from a multi-step process cannot be ruled out.

The levels at 3.059 and 3.44 MeV have a contradictory l_p assignment in previous ^{45}Sc(τ, d) experiments (table 2). The present experiment in agreement with Broman and Pullen [1]) assigns $l_p = 2$ to both these levels. This l_p value is consistent with the negative parity of these levels clearly given by the lifetime measurements in the ^{43}Ca (α, nγ) and ^{32}S(^{16}O, 2pγ) reactions [11, 12]). These levels as mentioned above are the lowest two members of the negative-parity band in ^{46}Ti. No other member of the band is populated in the (τ, d) reaction.

4.3. LEVEL SPECTRUM OF ^{46}Ti

The level spectrum of ^{46}Ti has been calculated by several authors [3, 5, 16]) on the basis of the McCullen-Bayman-Zamick (MBZ) model [17]). The spectroscopic strengths relevant to the $l_p = 3$ transitions in the ^{45}Sc(τ, d)^{46}Ti reaction have also been calculated [3, 5]) within the framework of the model.

The MBZ model starts with a closed ^{40}Ca core and the states are built on the pure $(1f_{\frac{7}{2}})^n$ configurations. Furthermore the two-body residual interaction is assumed

† The authors are grateful to the referee for pointing it out.

to be independent of the number of particles in the $f_{\frac{7}{2}}$ orbit. The different calculations differ from one another only in the details of the interaction.

The levels in ^{46}Ti up to $E_x = 5$ MeV which are excited in the present investigation with $l_p = 3$ character (table 2) are shown by solid lines in fig. 8 for a comparison with the predictions of the MBZ model [5, 16]; also included by dotted lines are the

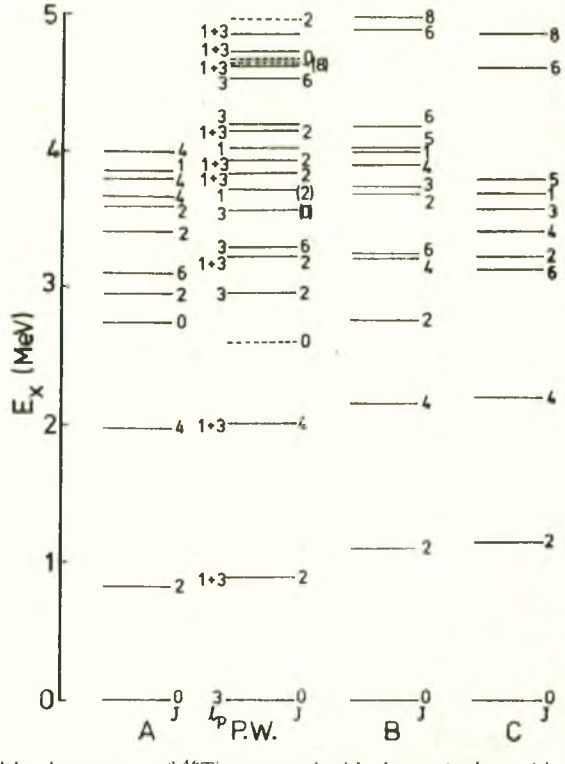

Fig. 8. Experimental level spectrum of ^{46}Ti compared with theory (only positive-parity levels shown). P.W.: Present work [levels with $l_p = 3$ character are shown by solid lines and other positive-parity levels are shown by broken lines; the J-values are from refs. [9-11])]. (A) ref. [18]), (B) ref. [5]), (C) ref. [16]).

other positive-parity levels that are known to exist in this excitation region. The J^π values of most of the low-lying levels in ^{46}Ti are established on a firm basis [see a discussion by Dracoulis *et al.* [11])], but a definite correspondence between theory and experiment can be made for only a few of them. A comparison of the transition strengths for such levels given by theory [5]) and all (τ, d) experiments [present work and refs. [1-3])] is made in fig. 9. It is observed that the strengths given by the present experiment are in excellent agreement with the MBZ theory (fig. 9) for all but the first excited level (2_1^+); the strength for the latter group given by the present work is much smaller than that predicted. The strength given by Broman and Pullen [1]) on the other hand agrees with theory only for this 2_1^+ level. Several low-lying 2^+

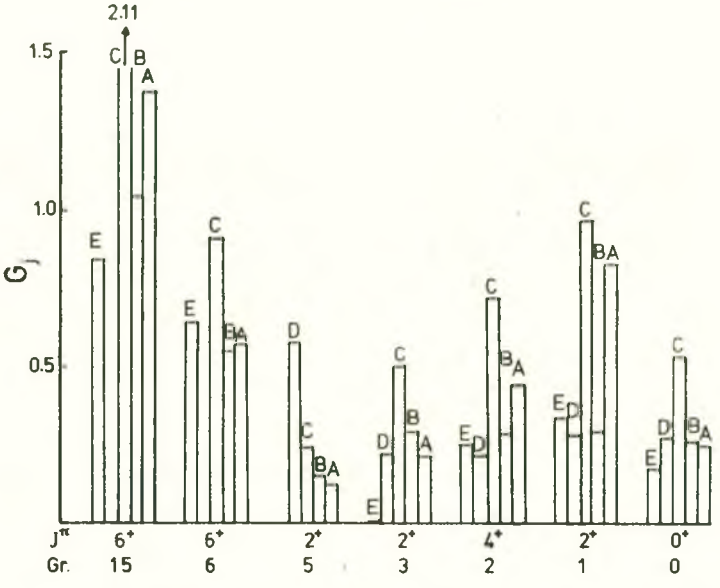

Fig. 9. Measured spectroscopic strengths compared with theory. (A) MBZ theory [5]. (B) present work. (C) ref. [1]. (D) ref. [2]. (E) ref. [3].

states are observed in the (τ, d) experiments, only three of which are given by the MBZ model (figs. 8 and 9). It is, however, interesting to note that the summed strength 1.13 measured in the present experiment for all the 2^+ states up to $E_x \sim 4$ MeV, namely groups 1, 3, 5, 10 and 11 (group 9 is excluded for not having an $l = 3$ component) is indeed in excellent agreement with the summed strength 1.16 given by given by the theory [5]) for the 2_1^+, 2_2^+ and 2_3^+ states and one may be tempted to account for the difference in strength between theory and experiment for the 2_1^+ state in terms of this fragmentation.

A 4^+ level at $E_x = 3.90$ MeV is predicted [5]) to be strongly populated in the (τ, d) reaction [†] (predicted strength = 1.01), but no single level is found in the experiment that may be a possible candidate. Whether or not the predicted strength is distributed over several of the levels with undetermined J^π values excited with $l_p = 1 + 3$ character (table 2) is difficult to say.

A detailed comparison with the (τ, d) experiment thus shows the inadequacy of the MBZ model; a satisfactory description of only a few low-lying levels in ^{46}Ti is given by the simple $(1f_{\frac{7}{2}})^n$ configuration. Further indications of the existence of more complicated configurations come from the excitation of low-lying negative-parity states and several states excited with $l = 1$ character in the (τ, d) reaction and also from the existence of two low-lying 0^+ states [9,10]) other than the ground state. An

[†] Another 4^+ state at 3.22 MeV is predicted to have a small strength.

augmented basis of 6 particles and 8p-2h configurations employed later by Skouras [ref. [18])] is a step in that direction. Since it is extremely difficult to perform such a shell-model calculation on the full $(fp)^6$ basis, a deformed scheme was adopted. Other than reproducing the 0_2^+ state the improvement is however not significant.

A passing mention may be made here on the band structure of ^{46}Ti. From γ-ray studies following the (α, n) reaction on ^{43}Ca, a ground-state band has been proposed [ref. [11])] comprising of the levels at E_x = 0, 0.889, 2.010, 3.299, 4.897 and 6.244 MeV with respective $J^\pi = 0^+, 2^+, 4^+, (6^+), (8^+)$ and (10^+) values. This is slightly different from the band suggested by Fortuna *et al.* [13]) from the ^{40}Ca(^{12}C, α2pγ) reaction, namely levels at E_x = 0, 0.889, 2.010, 3.299, 4.643, 6.244 and 6.519 MeV with respective $J^\pi = 0^+, 2^+, 4^+, 6^+ (8^+), (10^+)$ and $(11^+, 12^+)$ values. The difference is probably due to the uncertainty in the spin assignments to higher members of the proposed band. Only the lowest four members of the band (and not the high-spin levels) are populated in the (τ, d) reaction. The E2 transition strengths were derived by Dracoulis *et al.* [11]) from the lifetime measurements and it is interesting to note that the enhancements of these transitions are approximately given by the MBZ model [16]), as well as by the more detailed calculations of Skouras [18]).

A second positive-parity band with the 2.613 keV level ($J^\pi = 0^+$) has also been tentatively proposed by Dracoulis *et al.* [11]). The excitation energies of the levels at E_x = 2.613, 2.962, 3.827, 4.416, 5.280 and 6.027 MeV, with $J^\pi = 0^+, 2^+, (4), (5^-)$, (6) and (7) respectively, are remarkably linear against $J(J+1)$ and it is thus possible that some of the levels (obviously all of these cannot be members of the even-J band) really belong to the same band. Only one member, namely the one at E_x = 2.962 MeV, is populated in the (τ, d) reaction, and only weakly so.

5. Conclusion

Angular distributions of deuterons arising from the ^{45}Sc(τ, d) reaction have been measured for all the levels up to $E_x \sim 9.9$ MeV, and most of them were analysed in terms of the DWBA theory of the stripping reaction. More assignments of orbital angular momentum transfer have been made in the present work than previous ones, particularly for levels at high excitation. The l = 1 and 3 strengths are distributed over the entire range of excitation and a sum rule analysis gives the $T_<$ components of the respective 2p and 1f total spectroscopic strength which within errors are fairly close to the single-particle limits, in particular for the 2p shells.

The positions of only a few low-lying postive-parity levels are given by the MBZ model. For such levels the transition strengths given by the present experiment, except for the 0.89 MeV level, are in close agreement with the MBZ model. The simple model may thus be considered to give a reasonable account of only some of the low-lying positive-parity levels in ^{46}Ti. At higher excitation the observed level density exceeds that given by the theory and the occurrence of negative-parity states and a

few 0^+ and 2^+ states at low excitation certainly calls for an extension of the model space so as to include more complicated configurations. One such attempt is the calculation by Skouras using an augmented basis of 6 particles and 8p-2h configurations, but in a deformed basis rather than the difficult full $(fp)^6$. An additional 0^+ state is thereby accounted for. Whether or not it also accounts for the $^{45}Sc(\tau, d)$ transitions strengths remains to be seen. The present experiment provides accurate cross-section data for such a future calculation.

The authors wish to thank Dr. D. Roaf for advice in running the multichannel magnetic spectrograph at Oxford. They are thankful to Professor P. D. Kunz for the code DWUCK, and Professor G. C. Morrison, Professor K. W. Allen and Dr. J. B. A. England for their interest in the work. One of the authors (H.M.S.G.) appreciates support from the Royal Society, London.

References

1) L. Broman and D. C. Pullen, Nucl. Phys. **A110** (1968) 161
2) R. W. Barnard and G. D. Jones, Nucl. Phys. **A111** (1968) 17
3) H. Ohmura, T. Ishimatsu, K. Yagi, H. Ejiri, Y. Nakajima, T. Tohei and T. Nakagawa, J. Phys. Soc. Japan **25** (1968) 953
4) L. Broman and C. Larsson, Z. Phys. **242** (1971) 360
5) J. R. Priest and J. S. Vincent, Phys. Rev. **182** (1969) 1121
6) J. V. Maher, K. A. Erb and R. W. Miller, Phys. Rev. **C7** (1973) 651
7) R. H. Bassel, Phys. Rev. **149** (1966) 791
8) J. D. Childs, W. W. Daehnick and M. T. Spisak, Phys. Rev. **C10** (1974) 217
9) Tables of Isotopes, ed. C. M. Lederer and V. S. Shirley (Wiley, NY, 1978) p. 120
10) R. L. Auble, Nuclear Data Sheets **24** (1978) 1
11) G. D. Dracoulis, D. C. Radford and A. R. Poletti, J. of Phys. **G4** (1978) 1323
12) W. Denhardt, O. C. Kistner, W. Kutschera and H. J. Sann, Phys. Rev. **C7** (1973) 1471
13) G. Fortuna, R. B. Hüber, W. Kutschera, M. Morando, H. Morinaga, R. A. Ricci and C. Signorini, Nuovo Cim. **34A** (1976) 321
14) J. Rapaport, A. Sperduto and W. W. Buechner, Phys. Rev. **151** (1966) 939
15) J. N. Roy, A. R. Majumder, H. M. Sen Gupta and F. Watt, unpublished (1981)
16) W. Kutschera, B. A. Brown and K. Ogawa, Riv. Nuvovo Cim. **1** (1978) no. 12, p. 1
17) J. D. McCullen, B. F. Bayman and L. Zamick, Phys. Rev. **134** (1964) B515
18) L. D. Skouras, J. of Phys. **G1** (1975) 438